Doctoral Dissertation

Application of Nearshore Sand Dredging and Nourishment for Shore Protection

Chu Duc Thang

July 2016

Graduate School of Engineering,

Osaka University

Acknowledgements

I challenged myself to move to a new discipline, coastal engineering for research. There were so many topics to select from and it was difficult to decide how to narrow them to something achievable. I narrowed down my research aims early by reading academic papers and seeking the academic and technical advices from my supervisors. There are many things that I learnt from the dissertation process, such as time management, critical review and analysis, how to work independently and the most important thing is how to deal with the people who working with me. During the dissertation process, I received a lot of support and encouragement from my professors, family and friends. Words can never express how truly grateful I am to you.

I am deeply indebted to my supervisor, Prof. Shinichi Aoki, who advised me from the bottom of his heart. He not only gave technical advice but also help the difficulties I face in daily life in Japan. He showed me the basic knowledge in details and always encouraged me to think independently, which helped me self-confident on the research. I owe my gratitude to Assoc. Prof. Susumu Araki. He is a gentle and kind person, I know that he contributed to my experiments and gave me many valuable advices in my research. I would like to acknowledge Dr. Bui Trong Vinh for his guidance. Although he is very busy with his works in Vietnam, but he always gave me many helpful advises. I am indebted to Emeritus Prof. Ichiro Deguchi for his thoughtful comments on the numerical simulation in my research.

I gratefully acknowledge the members of my doctoral committee for their time and valuable feedback on preliminary process of this dissertation. I would like to deliver special thanks to Prof. Shuzo Nishida and Assoc. Prof. Masayasu Irie for their valuable time in assessing my dissertation and giving many comprehensive advises and comments.

This dissertation would not be possible without my colleagues Mr. Gen Himori, Mr. Yuki Saito, Mr. Muhajjir Ajir who cooperated and worked hard with me in conducting experiments for the research. Mr. Akalanka Silva, Mr. Joaquin Ferrer, Ms. Mei Shen help me to check my dissertation. I will always be grateful to my friends in Land Development and Management Engineering laboratory for the wonderful times that we have shared. Special thanks to Mr. Naoyuki Kinda and Mr. Akihiro Usui who helped me in learning Japanese and teaching me so many things about the Japanese culture since I entered the laboratory. I appreciate everything all of you has done for me. You are always in my heart.

I cannot thank my financial sponsor enough, Japan International Cooperation Agency (JICA). They fully supported the financial expenses for three years of my research. I owe my gratitude to two kind coordinators Ms. Kayuzo Takeda and Ms. Eriko Miyashita who helped me complete my studies in Osaka University.

I am deeply thankful to my family for their love, support, and sacrifices. Without them, this dissertation would never be done. This last word of acknowledgment I have saved, is for my dear wife

Ms. Ngo Thi Ngoc Han who has been by my side all these years and always supported and encouraged me in many ways. I love you all.

And many others people who helped me complete my dissertation. Regrettably, I cannot acknowledge them by name.

Thank you my God!

Chu Duc Thang

Osaka, Japan

July, 2016

To my loving parents,
and my lovely wife Ngo for their love, support and sacrifices.

Abstracts

One of the effects of global climate change on the coastal management is increment of amount of offshore sediment transport which causes unbalance in on/offshore sediment transport rate, hence coastal erosion. On the other hand, shore protection work by coastal structures such as detached breakwaters and groins has recently shown some limitations causing various environmental problems. To answer the question whether we could propose a new concept of shore protection in the management of on/offshore sediment transport, this study investigates, through a number of laboratory experiments, practical countermeasures for shore protection under severe storm conditions preserving the features of natural beaches.

Chapter One illustrates the effects of global climate change on beach erosion and outlines the limitations of the coastal structures in shore protection and environmental problems caused by the protection work. Synthesizing the results of previous studies on post-storm beach recovery, the effects of global climate change, such as sea level rise and high storm waves, on sediment transport are summarized.

In this study, two practical countermeasures for shore protection are investigated. The first one is “shore-face nourishment” which is based on a new idea that we utilize the sand at an offshore bar that was transported offshore during a storm. In this method, some amount of sand is dredged at the offshore bar and filled back at the shore-face, which may accelerate recovery of the beach under post-storm calm wave condition. This method includes two parts i.e. the sand dredging at the bar and the beach nourishment at the shore-face. These two parts of the method are studied in Chapter Two and Chapter Three, respectively. The other countermeasure investigated in Chapter Four is “perched beach nourishment”. In this method, beach is nourished by sand on the onshore side of a submerged breakwater. From the viewpoint of sediment management, the sand volume lost over a submerged breakwater as well as beach deformation is discussed based on the experimental results.

In Chapter Two, the effects of sand dredging at an offshore bar on the shoreline change are investigated through a series of 2D and 3D hydraulic experiments and numerical simulations. Sand dredging under the erosive wave condition causes quick retreat of the shoreline almost proportionally to the dredged volume. The shoreline retreat caused by the sand dredging is quantified with a simple relationship between the volume of sand dredging and the shoreline position of the equilibrium profile. In addition, it is found that the speed of shoreline retreat can be delayed by periodic sand dredging in the calm wave seasons.

In Chapter Three, the effectiveness of the shore-face nourishment is studied based on a series of hydraulic experiments in which various methods of sand dredging are tested under different conditions of waves and sea levels. The results show that the shore-face nourishment under the accretive

wave condition is able to accelerate beach recovery by enhancing onshore sediment transport rate. It is found that the sand volume of nourishment, the wave condition and the sea level are predominant parameters in the post-storm beach recovery. In addition, the location of the nourishment is also a factor affects to the recovery.

In Chapter Four, the effectiveness of the perched beach nourishment is investigated through a series of hydraulic experiments. The results are discussed in terms of beach deformation and sediment volume that is lost offshore over a submerged breakwater under storm waves. The effects of irregularity of the waves are also highlighted comparing between regular and irregular wave cases. Under irregular storm waves, both the beach deformation and the volume loss are insignificant, which indicates the perched beach nourishment has high potential for shore protection. Regarding the effects of irregularity, the deformation of the beach profile and volume loss under regular waves are always greater than those under irregular waves in the case of equivalent wave height.

In Chapter Five, major findings and conclusions obtained in this study are summarized.

Table of Contents

Acknowledgements ..... **i**

Abstracts ..... **iv**

Table of Contents ..... **vi**

List of Figures ..... **viii**

List of Tables ..... **xiv**

Chapter 1 Introduction **1**

1.1 Background 1

1.2 Methodology of Study 11

1.3 Goals, Scopes and Objectives of Study 12

1.4 Structure of Dissertation 13

References 15

Chapter 2 Nearshore Sand Dredging **18**

2.1 Introduction 18

2.2 Quantification of Shoreline Retreat 19

2.2.1 Theoretical analysis 19

2.2.2 Physical and numerical modelling 21

2.2.2.1 Physical modeling 21

2.2.2.2 Numerical modelling 23

2.3 Position of Shoreline Change Caused by Near Shore Sand Dredging 30

2.4 Infill Rate of Dredged Hole 35

2.5 Discussions 37

2.6 Conclusions 38

References 39

Chapter 3 Shore-face Nourishment **41**

3.1 Introduction 41

3.2 Shore-face Nourishment in Regular Waves 42

3.2.1 Effectiveness of Shore-face Nourishment on Beach Recovery 42
3.2.2 Beach Recovery Rate under Different Shore-face Nourishment Conditions 52
3.2.2.1 Shore-face Nourishment Position 52
3.2.2.2 Post-storm Accretive Wave Condition 58
3.2.2.3 Shore-face Nourished Volume of Sediment 63
3.2.2.4 Water Level after Storm 68
3.2.2.5 Method of Shore-face Nourishment 72
3.3 Shore-face Nourishment in Irregular Waves 76
3.3.1 Effect of Shore-Face Nourishment on Beach Recovery in Irregular Waves 76
3.3.2 The Differences of Shore-face Nourishment in Regular and Irregular Waves 82
3.4 Discussions 86
3.5 Conclusions 87
References 88
Chapter 4 Perched Beach Nourishment 89
4.1 Introduction 89
4.2 Equivalent Wave Height of Regular and Irregular Waves 91
4.2.1 Effect of Wave Conditions on Response of Perched Beach Profile 93
4.2.2 Effect of Water Levels on Response of Perched Beach Profile 101
4.3 Equivalent Wave Energy of Regular and Irregular Waves 106
4.4 Discussions 112
4.5 Conclusions 113
References 114
Chapter 5 Conclusions 115

List of Figures

Chapter 1 Introduction

Fig. 1.1 The world's cities by size class of urban settlement, 1990, 2014 and 2030. 2

Fig. 1.2 Estimated trends (cm per decade) in the height of a 50-year since 1970 event in extreme sea level from total elevation after removal of annual medians. Only trends significant at the 95% confidence level are shown (data are from Menéndez and Woodworth). 3

Fig. 1.3 Simplified model of landward coastal retreat under sea level rise (regarding to the Bruun Rule). 4

Fig. 1.4 General consensus assessment of the numerical experiments. All values represent expected percent change in the average over period 2081–2100 relative to 2000–2019. Four metrics were considered: the percent change in (I) the total annual frequency of tropical storms, (II) the annual frequency of Category 4 and 5 storms, (III) the maximum intensity achieved during a storm's lifetime (LMI) and (IV) the precipitation rate within 200 km of storm center at the time of LMI (denoted 'insf. d.' is insufficient data). 5

Fig. 1.5 Number of days $>30^0$C (left) and rainfall >100 mm/day (right) for Japan predicted by MIROC-hi. 5

Fig. 1.6 Projected heights of waves in Japan's surrounding waters with annual exceedance probabilities of 1 in 50 year (current climate corresponds to 1979-2003; future climate corresponds to 2075-2099). 6

Fig. 1.7 The increment of growth ratio of coastal structures in Japan. 7

Fig. 1.8 Changes in shoreline of Ghotsu coast, Shimane prefecture, Japan 7

Fig. 1.9 Turtle in Enshu-Nada coast, Toyohashi, Aichi Prefecture, Japan (by Tanaka Y., Omotehama Network). 8

Fig. 1.10 Cumulative recovery of West Beach. Calveston Island, expressed as a percent of total sand eroded by Hurricane Alicia. 9

Fig. 1.11 Activities of human and nature on littoral zone in coastal area. 10

Fig. 1.12 Possible zones for nourishments, (a) dune nourishment, (b) beach nourishment, (c) shore-face nourishment. 11

Chapter 2 Nearshore Sand Dredging

Fig. 2.1 Definition sketch for response of profile due to nearshore sand dredging. 20

Fig. 2.2 Isolines of dimensionless shoreline change, $\Delta y/W_*$, vs dimensionless sand dredging volume in nearshore zone, $V_d/(BW_*)$, dimensionless breaking depth, h_*/B. 21

Fig. 2.3 Physical modelling for nearshore sand dredging in 2D wave flume. 22

Fig. 2.4 Sand grain size distribution. 23

Fig. 2.5 Definition sketch for four principal zones of cross-shore sand transport (*BP*: break point, *PP*: plunge point). 25

Fig. 2.6 Beach profiles of cases with different sand dredging volumes. 26

Fig. 2.7 Shoreline retreat after dredging different volumes of sand. 27

Fig. 2.8 Average absolute sediment transport rate of physical experiments. 27

Fig. 2.9 Final shoreline retreat after near shore bar sand dredging (h^*/B=2.2). 28

Fig. 2.10 Beach profiles of cases with different methods and times of sand dredging. 29

Fig. 2.11 Shoreline retreat with different methods and times of sand dredging. 30

Fig. 2.12 Final shoreline retreat with different methods and times of sand dredging. 30

Fig. 2.13 Physical modelling for nearshore sand dredging in 3D wave basin (W: wave gauge No.). 31

Fig. 2.14 Shoreline at 240mins of wave generation from initial beach. 32

Fig. 2.15 Shoreline change of experiment E2D1 during 120 minutes after sand dredging..... 33

Fig. 2.16 Shoreline change of experiment E2D2 during 120 minutes after sand dredging..... 34

Fig. 2.17 Breaking wave height and location of wave breaking point in middle of beach slope (line A-B in Fig. 2.14). 34

Fig. 2.18 Sketch of wave refraction induced by nearshore bar sand dredging results in shoreline change. 35

Fig. 2.19 Infill rate of dredged hole after sand dredging. 36

Fig. 2.20 Cross-shore beach profile in the middle of dredged hole x = 1.585 m (case E2D2)..... 36

Fig. 2.21 Longshore beach profile in the middle of dredged hole y = 2.75 m (case E2D2)..... 37

Chapter 3 Shore-face Nourishment

Fig. 3.1 Accretive and erosive profile in littoral zone (mhw: mean high water level; mlw: mean low water level). 41

Fig. 3.2 Physical modelling of shore-face nourishment in 2D wave flume. 43

Fig. 3.3 Beach profiles of cases with/without (W/WO) shore-face nourishment. 46

Fig. 3.4 Post-storm shoreline recovery of cases with/without (W/WO) shore-face nourishment. 47

Fig. 3.5 Post-storm berm volume of cases with/without (W/WO) shore-face nourishment. 48

Fig. 3.6 Cross-shore sediment transport rate of the cases with/without (W/WO) shore-face nourishment in 30mins. 49

Fig. 3.7 Cross-shore sediment transport rate of the cases with/without (W/WO) shore-face nourishment in 60mins. 50

Fig. 3.8 Cross-shore sediment transport rate of the cases with/without (W/WO) shore-face nourishment in 120mins. 51

Fig. 3.9 Cross-shore profiles and wave height distribution of shore-face nourishment cases in different nourished positions d_{sh}. 53

Fig. 3.10 Cross-shore sediment transport rate of shore-face nourishment cases in different positions of shore-face nourishment d_{sh}. 54

Fig. 3.11 Post-storm berm volume of shore-face nourishment cases in different shore-face nourishment positions d_{sh}. 55

Fig. 3.12 Post-storm shoreline recovery of shore-face nourishment cases in different shore-face nourishment positions d_{sh}. 55

Fig. 3.13 Change of topography at the nourishment area in the first 30 minutes after shore-face nourishment in different shore-face nourishment positions d_{sh}. 57

Fig. 3.14 Net sediment transport in cross-shore section. 58

Fig. 3.15 Beach profiles of shore-face nourishment cases in different accretive wave conditions. 59

Fig. 3.16 Cross-shore sediment transport rate of shore-face nourishment cases in different accretive wave conditions. 60

Fig. 3.17 Shoreline recovery of shore-face nourishment cases in different accretive wave conditions. 61

Fig. 3.18 Post-storm berm volume of shore-face nourishment cases in different accretive wave conditions. 62

Fig. 3.19 Criterion of regular accretive wave condition for shore-face nourishment. 63

Fig. 3.20 Beach profiles of shore-face nourishment cases in different nourished volumes. 64

Fig. 3.21 Cross-shore sediment transport rate of shore-face nourishment cases in different nourished volumes. 65

Fig. 3.22 Post-storm shoreline recovery of shore-face nourishment cases in different nourishment volumes. 66

Fig. 3.23 Post-storm shoreline recovery of shore-face nourishment cases in different nourished sand volume. 67

Fig. 3.24 Post-storm berm volume of shore-face nourishment cases in different nourished sand volume. 67

Fig. 3.25 Beach profiles of shore-face nourishment cases in different water levels after shore-face nourishment. 69

Fig. 3.26 Cross-shore sediment transport rate of shore-face nourishment cases in different water levels after storm. 70

Fig. 3.27 Post-storm shoreline recovery of shore-face nourishment cases in different water levels after storm. 71

Fig. 3.28 Post-storm berm volume of shore-face nourishment cases in different water levels. 72

Fig. 3.29 Beach profiles of shore-face nourishment cases in different nourishment methods. 73

Fig. 3.30 Cross-shore sediment transport rate of shore-face nourishment cases in different nourishment methods (V_n=0.03 m^3/m) 74

Fig. 3.31 Post-storm shoreline recovery of shore-face nourishment cases in different nourishment methods. 75

Fig. 3.32 Post-storm berm volume of shore-face nourishment cases in different nourishment methods. 76

Fig. 3.33 Beach profiles of shore-face nourishment cases in different irregular wave after with/without (W/WO) shore-face nourishment. 78

Fig. 3.34 Cross-shore sediment transport rate of shore-face nourishment cases in different irregular wave conditions. 80

Fig. 3.35 Post-storm shoreline recovery of shore-face nourishment cases in different irregular wave conditions. 81

Fig. 3.36 Post-storm berm volume of with/without (W/WO) shore-face nourishment cases in different irregular wave conditions. 81

Fig. 3.37 Beach profiles of shore-face nourishment cases in different regular/irregular waves after shore-face nourishment. 83

Fig. 3.38 Wave spectrum of irregular waves at wave gauge No. 3. 84

Fig. 3.39 Post-storm berm volume of shore-face nourishment cases in different regular/irregular waves conditions. 85

Fig. 3.40 Post-storm shoreline recovery of shore-face nourishment cases in different regular/irregular wave conditions. 85

Chapter 4 Perched Beach Nourishment

Fig. 4.1 Physical modelling of perched beach nourishment in 2D wave flume. 91

Fig. 4.2 Wave energy density of regular and irregular waves. 93

Fig. 4.3 Spectrums of irregular waves at the offshore-wave gauge No.1. 94

Fig. 4.4 Beach profile in irregular waves at low water level (LWL) after 60mins of wave generation. 95

Fig. 4.5 Beach profile in regular waves at low water level (LWL) after 60mins of wave generation and wave height distribution just after perched nourishment. 95

Fig. 4.6 Beach profile in irregular waves at mean water level (MWL) after 60mins of wave generation. 96

Fig. 4.7 Beach profile in regular waves at mean water level (MWL) after 60mins of wave generation and wave height distribution just after perched nourishment. 96

Fig. 4.8 Scour depth in different wave height at low/mean water level (LWL/MWL) after 60mins of wave generation. 97

Fig. 4.9 Wave energy distribution along the beach profile of regular and irregular waves at mean water level. 98

Fig. 4.10 Net volume loss for different wave conditions and water levels after 60mins of wave generation. 99

Fig. 4.11 Wave spectrum of the irregular wave cases at wave gauge 4th in low and mean water levels. 100

Fig. 4.12 Beach profile in irregular waves at different water levels after 60mins of wave generation..... 101

Fig. 4.13 Wave spectrum of the same irregular wave conditions over the submerge breakwater (the wave gauge 4th) in different water levels. 102

Fig. 4.14 Beach profile in regular waves at different water levels after 60mins of wave generation..... 103

Fig. 4.15 Scour depth in different water levels after 60mins of erosive wave generation. 103

Fig. 4.16 wave energy distribution along the beach profile of regular and irregular waves in different water levels. 105

Fig. 4.17 Net volume in different water levels after 60mins of erosive wave generation..... 106

Fig. 4.18 Beach profiles in the same wave energy of irregular/regular erosive wave condition 3 and 6 after 60mins of wave generation, respectively. 107

Fig. 4.19 Beach profiles in the same wave energy of irregular/regular erosive wave condition 5 and 6 after 60mins of wave generation, respectively. 108

Fig. 4.20 Scour depth of the cases in similar wave energy after 60mins of wave generation..... 109

Fig. 4.21 Net volume of the cases in similar wave energy after 60mins of wave generation. 109

Fig. 4.22 Wave energy distribution along the beach profile of regular and irregular waves with similar wave energy. 110

Fig. 4.23 Criterion for distinguishing profile type of irregular waves regarding to experimental data..... 112

List of Tables

Chapter 2 Nearshore Sand Dredging

Table 2.1 Experimental conditions in 2D wave flume. 23

Table 2.2 Experimental conditions in 3D wave basin. 32

Chapter 3 Shore-face Nourishment

Table 3.1. Cases of physical modelling of shore-face nourishment in regular waves. 45

Table 3.2 Cases of physical modelling of shore-face nourishment in irregular waves. 77

Table 3.3 Cases of physical modelling of shore-face nourishment in regular and irregular accretive waves. 82

Chapter 4 Perched Beach Nourishment

Table 4.1 Cases of physical modelling of perched beach nourishment. 90

Chapter 1 Introduction

1.1 Background

The world population has approximately reached 7.4 billion in 2016. The United Nations recently announced that the world population would increase to between 9.6 billion and 12.3 billion in 2100[1)]. Many of large cities in the world are located in coastal zones[2)] and more than 75% of people are expected to live within 100 km from coast by 2025[3)]. The number of megacities that the population is over ten million increases rapidly since last two decades (Fig. 1.1)[4)]. Rapid urbanization has many consequences such as enlargement of natural coastal inlets and dredging of waterways for navigation, port facilities, and pipelines exacerbate saltwater intrusion into surface and ground waters[2)]. In addition, some of human economic activities affect sediment supply to the coasts. By constructing dams for flooding control, hydroelectric power etc. upstream, the amount of sediment discharge to downstream significantly decreases[5)]. Coastal zone may suffer cumulative burden from the urbanization and the economic activities. These issues pose potential risks of coastal damage.

Evidence shows that global sea level has been rising because of the global warming over the last several decades. Menéndez and Woodworth[6)] studied a change in extreme high water levels and showed that in the Southeast United States, the Western Pacific, Southeast Asia and a few locations in Northern Europe, the water level had a change in amplitude of more than 5 mm/year after removal of annual medians water level (Fig. 1.2)[7)]. The Fourth Assessment Report of Intergovernmental Panel on Climate Change concluded that the highest water levels have been increasing since the 1950s in most regions of the world, caused mainly by increasing mean sea level. Since then, there are many published studies continuously support this conclusion[8) 9) 10) 11)].

Unnikrishnan et al. used Regional Climate Model (RCM) simulations to force a storm surge model for the Bay of Bengal and found that a combined effect of mean sea level of 4 mm/year and RCM projections for the A2 scenario (2071-2100) gave an increase in total levels of the sea in 100 years between 0.4 to 0.67 m along the northern part of the east coast of India[12)]. The coastal systems and low lying areas will experience the extreme sea levels and their adverse impacts. The sea level rise causes unsteady changes of beach profile. The sediment is now underwater level and only natural way the beach can reach a new balance conditions is to erode (Fig. 1.3)[13) 14)]. There are also many studies by observations of coastal erosion due to the sea level rise[15) 16) 17) 18)].

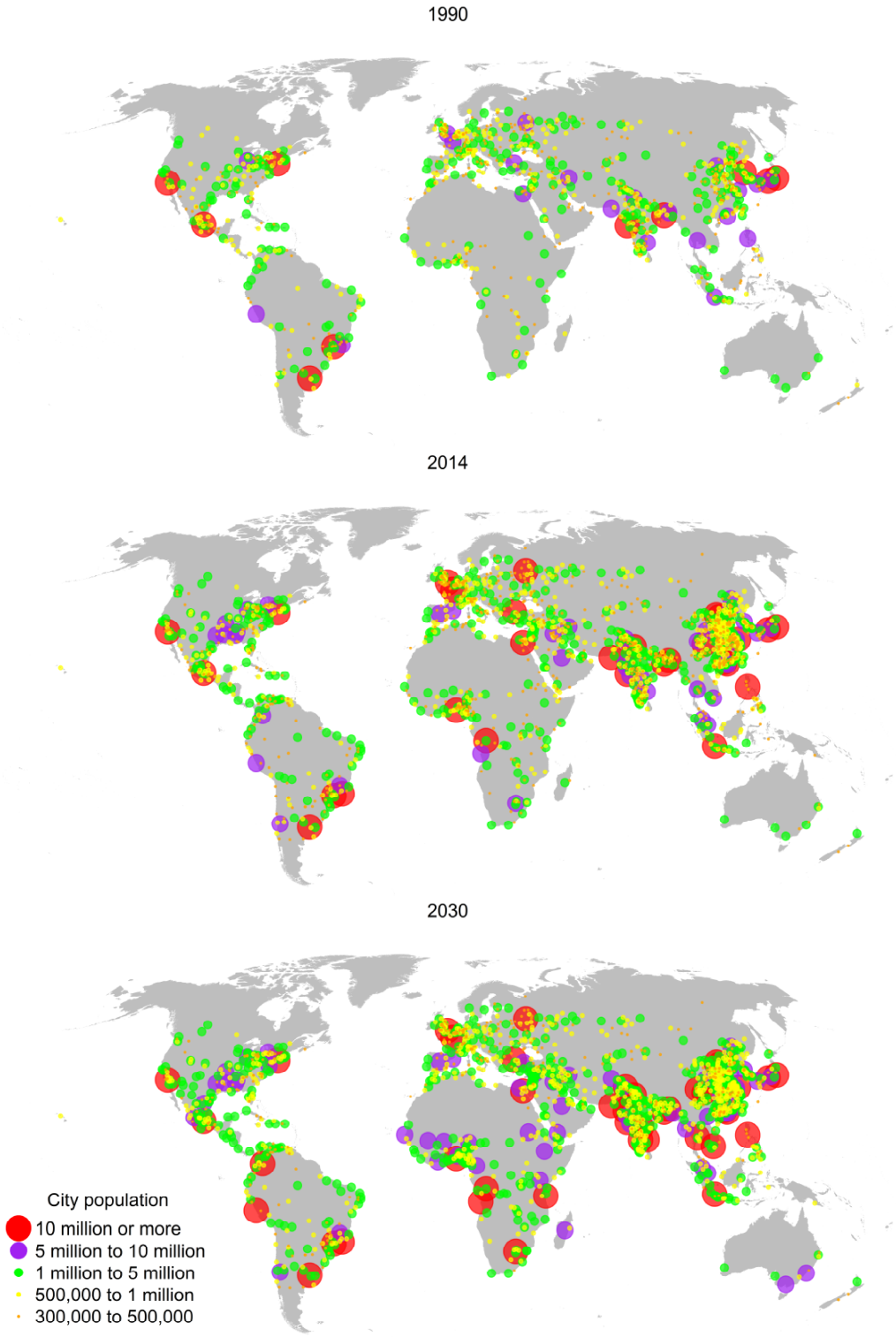

Fig. 1.1 The world's cities by size class of urban settlement, 1990, 2014 and 2030[4)].

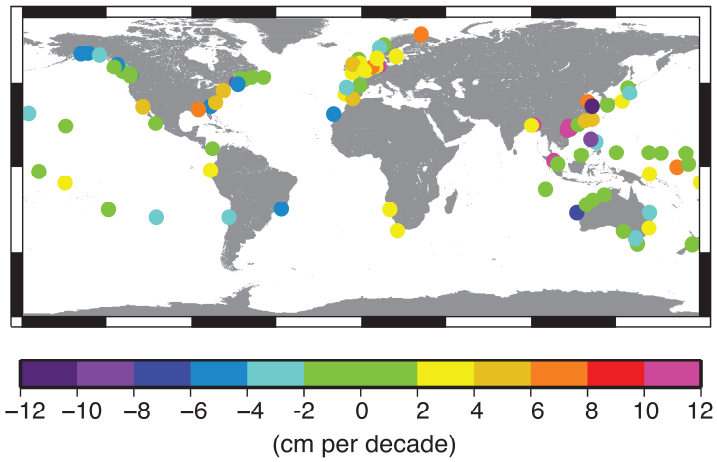

Fig. 1.2 Estimated trends (cm per decade) in the height of a 50-year since 1970 event in extreme sea level from total elevation after removal of annual medians. Only trends significant at the 95% confidence level are shown (data are from Menéndez and Woodworth[6)])[7)].

The global climate change also affects wind velocity and cyclone increment. There is increasing evidence for a strengthening wind stress field in the Southern Ocean since the early 1980s from atmospheric reanalysis, satellite observations, and island station data[7)]. Ocean waves are generated by the wind systems. Thus, the extreme change in wind velocity causes high wave formation. The data of in situ and satellite altimeter observations, and wave model showed that significant wave heights have increased in regions of the North Pacific and the North Atlantic over the past half century, also, in the Southern Ocean since the mid-1980s[19)]. Besides that, the positive trends of wave height have been detected in the Southern Ocean between 1985 and 2008 regarding satellite data[7)]. Ocean waves are main driving forces of coastal erosion, thus as the wave height increases, wave energy dissipation in nearshore area increases, resulting in elevated coastal sea levels through wave set-up, run-up and hence the beach erosion. In addition, the wave directions and periods vary by wind conditions which influence shoaling and refraction[20)]. According to the change in wave condition, the beach is adjusted to equilibrium by on/offshore sediment transport. Under steep erosive waves, the sediments are dragged offshore to the wave breaking point where sand bars are formed, steepened the beach face. Rate of shoreline erosion from the water level and the wave action is related to both the rise in the sea level and the shape of the beach slope[21) 22)]. Globally, beaches and dunes have undergone the erosion over the past century or longer[23)]. Along the coastline of the United States of America, Mid-Atlantic and New England coasts, the long term rate of erosion is 0.5 ± 0.09 m/year[24)].

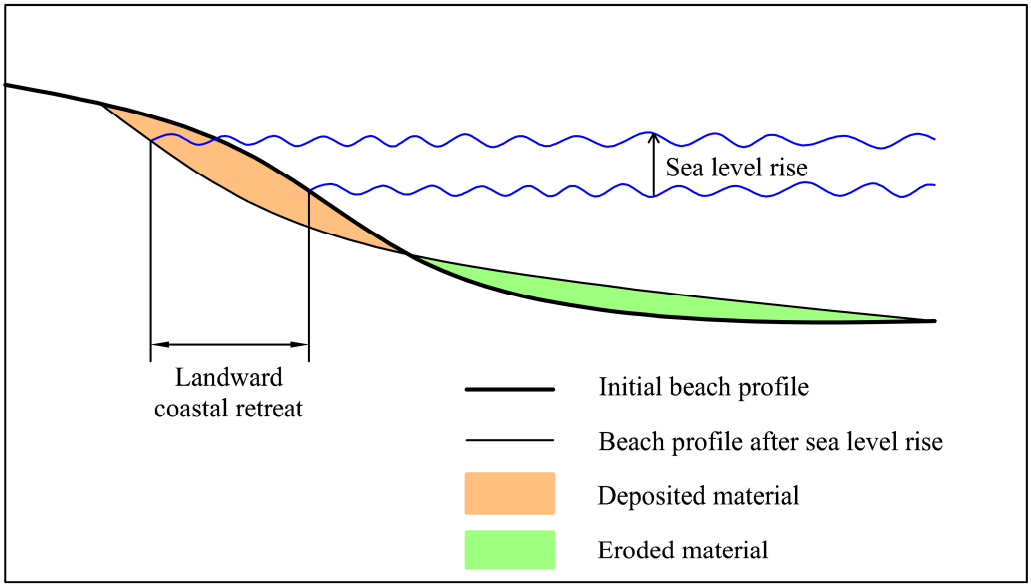

Fig. 1.3 Simplified model of landward coastal retreat under sea level rise (regarding to the Bruun Rule[21])[14].

In the last decade, the severe erosion of the coasts at the Gulf of Mexico were caused by many powerful hurricane including Charley (2004), Ivan (2004), Katrina (2005), Rita (2005), and Ike (2008)[25]. Extreme storms can erode and completely remove dunes, degrading land elevations and exposing them to inundation and the worse cases of incomplete recovery before the next storm[26]. A number of experiments that are able to simulate intense tropical cyclones project increasing the frequency of the storms in some regions. However, there are limited studies and insufficient data to assess for most regions (Fig. 1.4). The confidence is higher in the North Atlantic and Western North Pacific basins where an increase in the frequency of the strongest storms is projected[7]. The projections of global warming under the 21st century indicate that, the global frequency of tropical cyclone will either decrease or remain essentially unchanged, however, an increase is likely to occur in both global mean tropical cyclone maximum wind speed and rainfall rates[7]. Thus, factors may affect the coastal erosion caused by climate change are sea level rise, increase of wave height; in some regions, the intense storm may increase in frequency, rainfall rate, and maximum wind speed.

In the Asia-Pacific regions, the global climate models show increasing the confidence with which projections of future changes in extreme climatic events, such as heat waves, heavy rainfall and typhoons. For instance, the frequencies of extreme high temperatures and heavy rainfall events in Japan are expected to increase during the present century (Fig. 1.5)[27]. Mori et al.[28] based on MRI (Meteorological Research Institute) Global Climate Model and SRES (The Special Report on Emissions Scenarios) Scenarios A1B[29], projected wave height in Japan's surrounding water and concluded that

the extreme wave heights of future climate will be increased significantly in tropical cyclone areas (Fig. 1.6). The increment of wave height may be from +2.34 to +8.49 m.

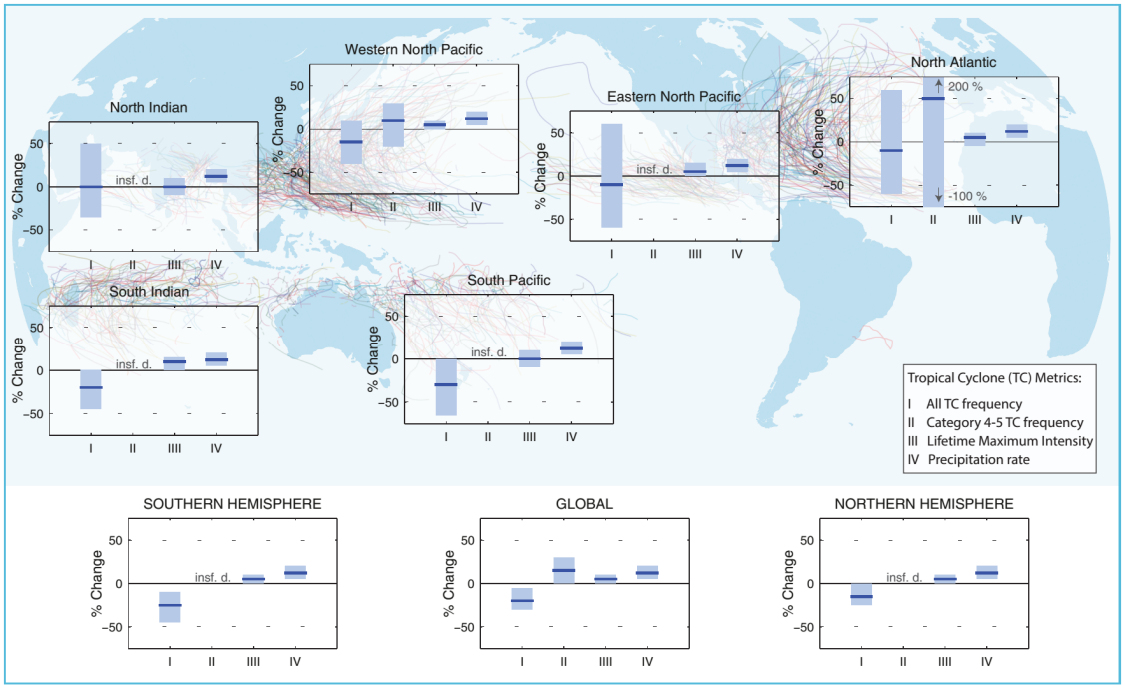

Fig. 1.4 General consensus assessment of the numerical experiments. All values represent expected percent change in the average over period 2081–2100 relative to 2000–2019. Four metrics were considered: the percent change in (I) the total annual frequency of tropical storms, (II) the annual frequency of Category 4 and 5 storms, (III) the maximum intensity achieved during a storm's lifetime (LMI) and (IV) the precipitation rate within 200 km of storm center at the time of LMI (denoted 'insf. d.' is insufficient data)[20].

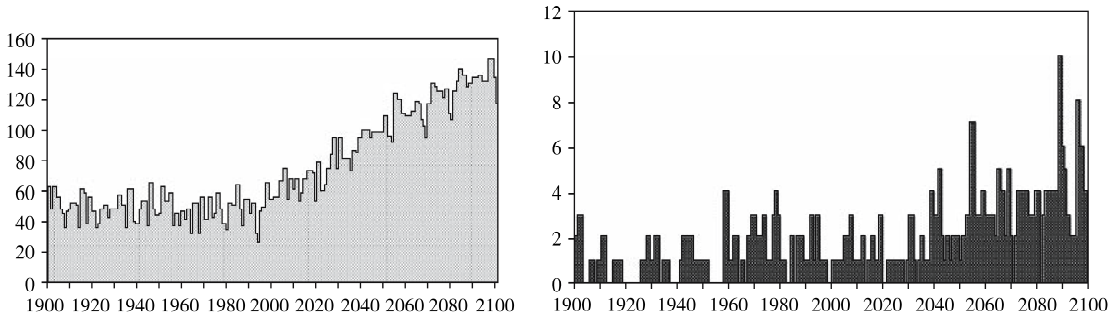

Fig. 1.5 Number of days >30^{0}C (left) and rainfall >100 mm/day (right) for Japan predicted by MIROC-hi[28].

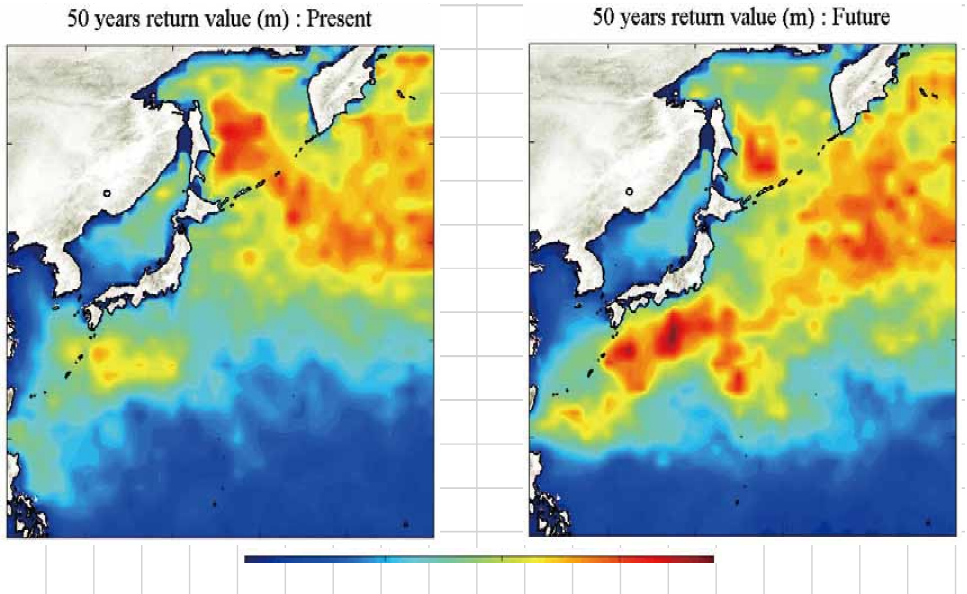

Fig. 1.6 Projected heights of waves in Japan's surrounding waters with annual exceedance probabilities of 1 in 50 year (current climate corresponds to 1979-2003; future climate corresponds to 2075-2099)[28].

There is little room for doubt that the coastal zone has faced severe geohazard phenomena such as storm, landslide/cliff collapse and erosion due to the global climate change. The erosion of sandy beaches and low-lying land are in great effects from floods, sea level rise, storm. Furthermore, together with the growth of the world's population, the coastal zones are affected not only by the natural hazards but also by the anthropogenic hazards. This issue is likely to increase during the next decades.

On the other hand, shore protection works by coastal structures such as detached breakwaters and groins has recently shown some limitations causing various environmental problems. The beach erosion in Japan has been occurring significantly since 1960s. In this time, a number of coastal structures such as detached breakwater, sea dike, jetty, seawall, groin have been constructed (Fig. 1.7)[30]. The number of detached breakwater is remarkable. Uda[31] studied the causes of erosion in Japan and classified it in seven types of beach erosion in which four reasons are related to the shore protection works by coastal structures. On a coast with predominant longshore sediment transport, a breakwater, jetty, detached breakwater or groin can obstruct or slow down the longshore sediment transport at the upcoast and the erosion occurs at the downcoast causes an unbalance of sediment budget between up/down coasts. Fig. 1.8 shows the shoreline changes caused by the construction of detached breakwaters at Ghotsu coast, Shimane prefecture, Japan. If the sediment budget is not balanced, beach erosion will occur at some other places although coastal structures may solve the problem locally. In addition, the coastal structures may cause other environmental problems such as loss of natural beach landscape, altering the natural hydraulic processes, damage to ecosystem, etc. Fig. 1.9 showed the

effects of coastal structures on breeding of turtle at Enshu-Nada coast, Toyohashi, Aichi Prefecture, Japan.

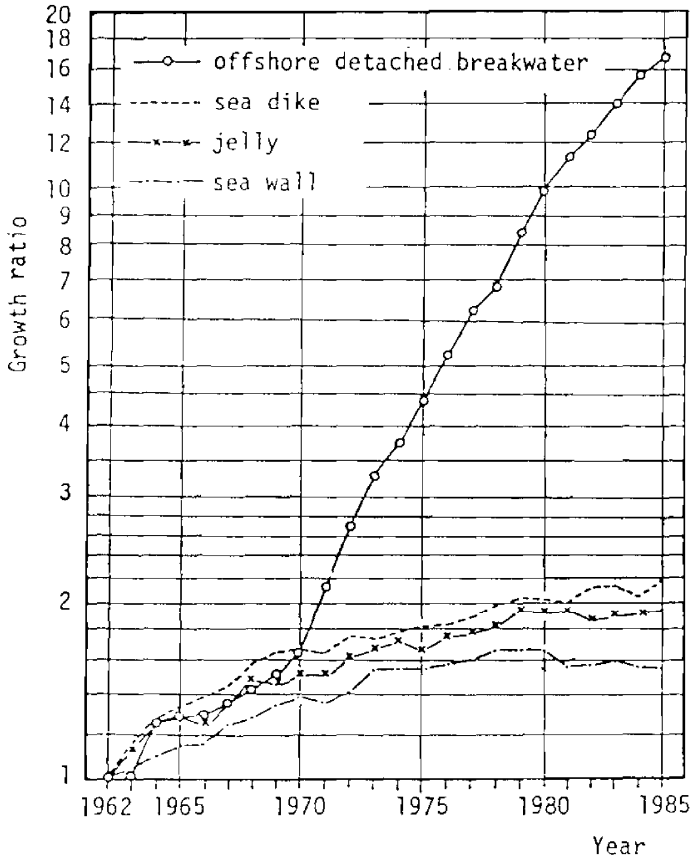

Fig. 1.7 The increment of growth ratio of coastal structures in Japan[30].

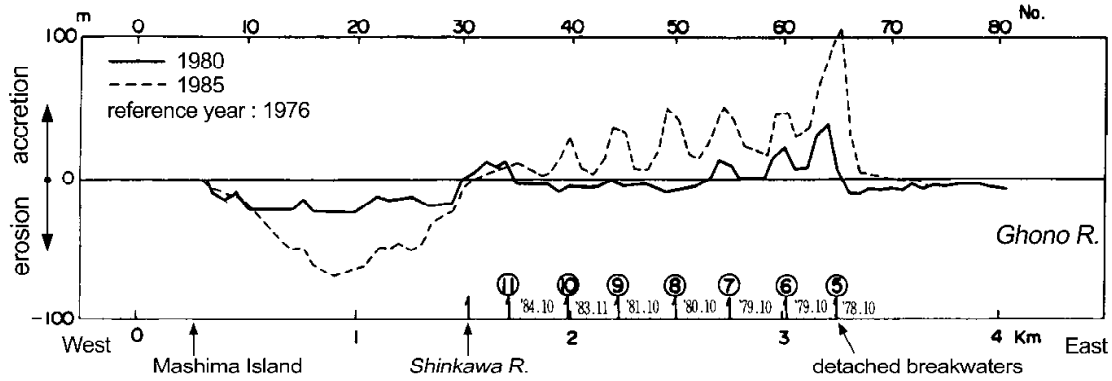

Fig. 1.8 Changes in shoreline of Ghotsu coast, Shimane prefecture, Japan[31].

Fig. 1.9 Turtle in Enshu-Nada coast, Toyohashi, Aichi Prefecture, Japan (by Tanaka Y., Omotehama Network).

In storm season, the offshore sediment transport is dominant. Sediments of the foreshore area are dragged far away from the shoreline by magnificent or successive storm waves, retreated shoreline may result. Whereas, in calm season, the onshore sediment transport becomes dominant in turn. Sediments are moved onshore by accretive waves; hence the shoreline is recovered. The beach is completely recovered in the case that the amount of offshore sediment transport is balanced with the amount of offshore sediment transport. There were studies that investigated the recovery of post-storm beach and showed that the post-storm beach recovery occurred at larger time scales in some post-storm wave conditions[32) 33)]. Beaches of southeastern Texas, the United State of America after the Hurricane Alicia is one instance of the partial recovery and subsequent erosion as observed (Fig. 1.10). The most significant period of recovery was the first post-storm year when about 40% of the eroded sand returned to the entire beach. Recovery during the next three years was much slower where the recovery is about 10%. However, even ten years after the storm, the beach had not been completely recovered. In some areas, the beaches are attacked by other storms during the recovery period[34)]. In that areas, the amount of offshore sediment transport is higher than the amount of onshore sediment transport in a certain period post-storm. Therefore, the rate post-storm beach recovery is very slow. Under the global climate change, the frequency of tremendous storms increases as well as precipitation intensity and maximum wind speed. The less recovery of post-storm beaches commonly occurs in the next decades. To some extent, under the global climate change, a concept of shore protection in sustainable development of coastal zone has been changed. In the case that sediment volume inside the littoral cell is preserved i.e.

the amount of sediment moved out is balance with the amount of sediment moved in, stable shoreline is observed (Fig. 1.11). In this study, the concept of shore protection under the global climate change should be management of the on/offshore sediment transport in littoral cell.

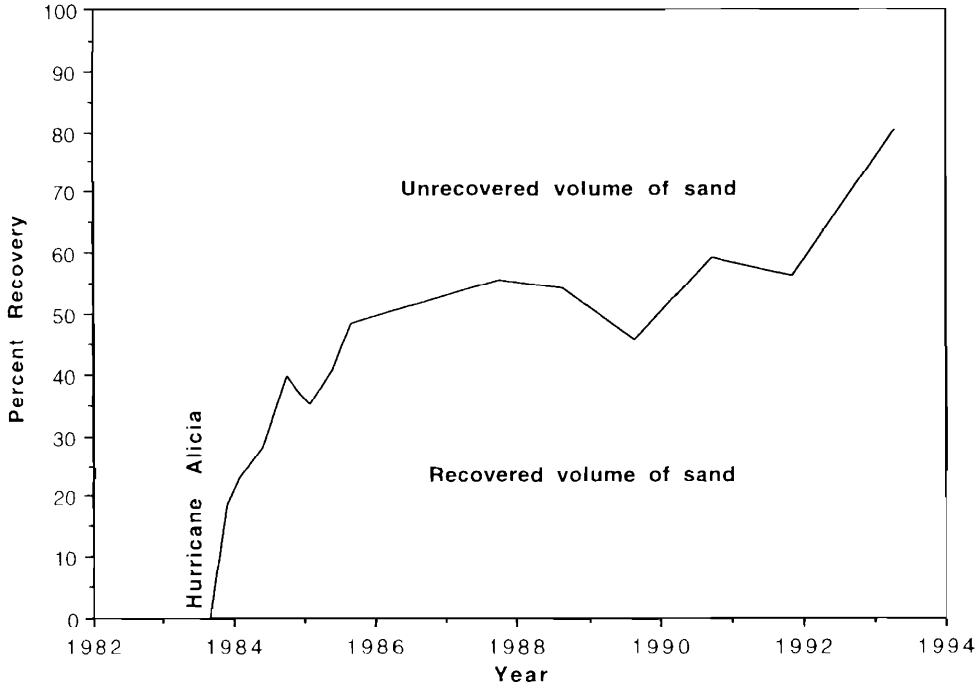

Fig. 1.10 Cumulative recovery of West Beach. Calveston Island, expressed as a percent of total sand eroded by Hurricane Alicia[33)].

Along with the increment of natural hazards and the limitations of shore protection works by coastal structures such as detached breakwaters and groins causing various environmental problems, the population in coastal area are rapidly increased, thus demand for tourism and other leisure activities on beaches apparently grow. Therefore, developing some practical countermeasures to protect the coasts under severe storms while retain some features of the natural shorelines are essential for the coastal conservation. Beach nourishment is one of solutions fulfill the requirements. Beach nourishment comprises the placement of large quantities of good quality sand within the nearshore system[35)]. In general, nourishment activity is placing a volume of sediment taken from other places outside the littoral cell on the shore zone (Fig. 1.12). Thus, enormous amount of sediment is required for the nourishment, however, sources of material for replenishment is gradually becoming exhausted and costly. Therefore, reduction of the amount of materials for replenishment is one of the solutions to cost reduction in beach nourishment projects. In this study, two recommendation methods were tested and proposed for the issue.

First, perched beach nourishment aims at not only advancing the shoreline but also decreasing the amount of nourished sediment, which consists of placing a submerged breakwater at proper location

on beach and nourishing material for replenishment onshore side. The submerged breakwater has two main roles which are dissipating wave energy and restraining volume of the nourished sediment lost offshore. Chatham[36] studied the response of perched beach profile by conducting physical experiments in regular storm waves. The regular storm waves were generated for 3 to 12 hours continuously until the perched beach profile reached equilibrium condition. Sorensen and Beil[37] conducted experiments to investigate the response of perched beach profile under 42 hours of irregular storm waves generation. The results showed that scour depth and volume loss of the perched beach of these studies are comparatively high. In real time scale, storm attacks beach only for several hours. Thus, the time scale of experiments in researches of Chatham[36] and Sorensen and Beil[37] were not realistic as the storm waves of these experiments were generated for very long time. In this study, the gaps of compatibility between experimental time scale and real time scale are fulfilled. A hypothesis that the perched beach nourishment method is an effective engineering method for coastal protection. The relationship between scour depth of the perched beach, volume lost over submerged breakwater and intensity of storm was tested. It was hypothesized that under some storm wave conditions, the submerged breakwater of the perched beach could dissipate the wave energy, and the scour depth and volume loss are insignificant.

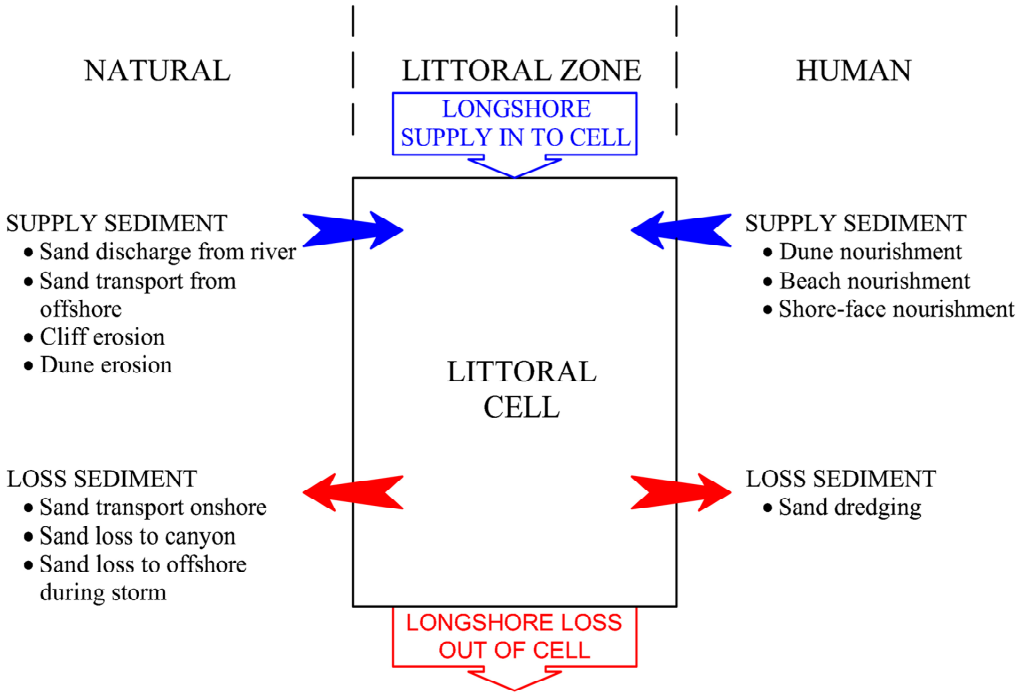

Fig. 1.11 Activities of human and nature on littoral zone in coastal area.

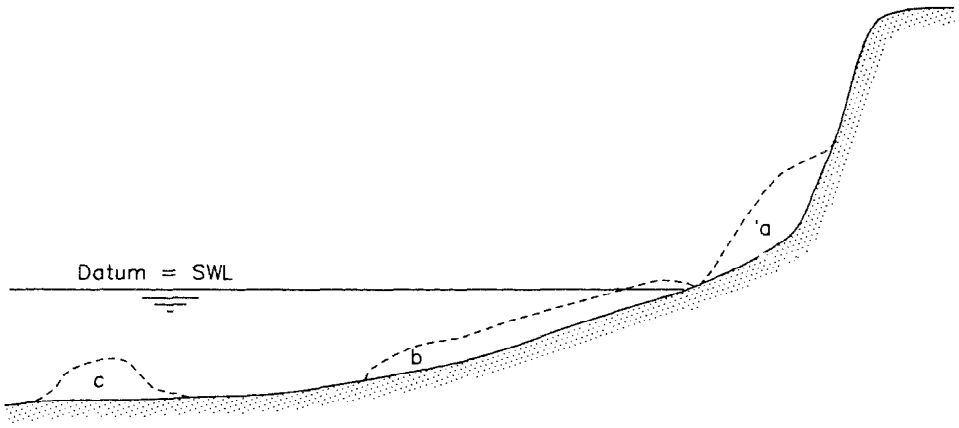

Fig. 1.12 Possible zones for nourishments, (a) dune nourishment, (b) beach nourishment, (c) shore-face nourishment[38].

Second, shore-face nourishment is defined as nearshore berms or mounds constructed from dredged material as a feeder berm in shallow water at the seaward flank of the most offshore bar or as a reef berm in deeper water acting as filters for storm waves[38]. In this definition, the replenishing sediment is taken from other littoral cells. In this study, however, "shore-face nourishment" is looked in another perspective i.e. the replenishing sediment is dredged from offshore bar in which was formed during the storm and nourished on the shore-face of the beach. The time of shore-face nourishment is in calm season. The waves of this season is almost accretive waves move the nourished sediment onshore. Thus, the onshore sediment transport rate is accelerated. Therefore, the balance of the rate of on/offshore sediment transport during and after storm is assured. In addition, the method can save a big amount of sediment for nourishment. Regarding this issue, a hypothesis such that the shore-face nourishment is an effective engineering method to accelerate post-storm beach recovery rate is proposed. The hypotheses regarding the relationship between the post-storm beach recovery rate of shoreline and berm volume in cases of with and without shore-face nourishment is tested. It is hypothesized that under the case of shore-face nourishment, the post-storm beach recovery rate is accelerated.

1.2 Methodology of Study

To evaluate feasibility of the shore-face nourishment method on acceleration of post-storm beach recovery, and assess the effectiveness of perched beach method in the shore protection under storm, physical experiments are conducted in 2D wave flume and 3D wave basin. The shore-face nourishment includes two processes. A volume of sand is dredged from the offshore bar; thereafter, it is nourished on the shore-face of the beach. In the prior process, the sediment is taken out of the littoral cell, thus it may give some negative effects on the beach erosion. Therefore, the effects of nearshore bar sand dredging on the beach erosion are firstly quantified.

In the shore-face nourishment method, first, the effects of nearshore sand dredging on the shoreline changes were examined. Volumes of sand dredging directly affected the intensity of shoreline retreat, thus quantification of the impacts of sand dredging volume on the intensity of shoreline retreat is studied by using theoretical analysis. The results are verified by physical experiments in 2D wave flume and numerical simulation model SBEACH. Other impact parameters on the shoreline retreat such as dredging time and dredging method are also discussed by conducting physical experiment in 2D wave flume. Sand is dredged under erosive and accretive waves to illustrate that which is the proper time for sand dredging with less effect on the beach erosion. Sand is also dredged by one-time or periodic dredging method. To determine positions of retreated shoreline as well as erosion rate of the shoreline after nearshore sand dredging, physical experiments are conducted in 3D wave basin.

To examine the feasibility of the shore-face nourishment on acceleration of post-storm beach recovery, a series of experiments with various experimental conditions such as post-storm wave conditions, water levels, nourished sand volume, method of nourishing sand are carried out in 2D wave flume. The feasibility of shore-face nourishment on post-storm beach recovery is tested by using shoreline recovery rate and recovered berm volume. The experiments are also conducted in irregular waves, in order to assess the applicability of the shore-face nourishment to real wave conditions.

To examine the response of perched beach on regular and irregular storm waves, a series of experiments is conducted in 2D wave flume. In each pair cases of the regular and irregular waves, the waves were generated in same conditions. The wave conditions of regular and irregular waves are discussed in term of equivalent wave height and equivalent wave energy. The scour depth and volume loss are used for evaluate the effectiveness of the perched beach in the shore protection.

1.3 Goals, Scopes and Objectives of Study

The goals of this study are to assess the coastal development and management in the next several decades; to develop a new concept of shore protection in sustainable development and management of coastal zone. The beach nourishment is the most effective method of shore protection while retain the natural features of beaches. However, the sediment budget for beach nourishment is more and more exhausted. In this study, two methods are proposed to reduce the nourished sediment. Whereas, the perched beach nourishment method uses less nourished sediment than the conventional beach nourishment, the shore-face nourishment method does not use any volume of additional nourished sediment.

Previously, we introduced the effects of climate change on the coastal erosion in which storm is a tremendous natural hazard causes severely beach erosion by dragging sediment offshore. In the storm and post-storm, the cross shore sediment transport is dominant, thus it is taken into account for evaluation of shore protection in this study. To accomplish the goals under the scopes of the study in

which using less of nourished sediment and dominant of cross shore sediment transport, the objectives of the research are as follows:

To quantify the impacts of sand dredging at the nearshore zone on shoreline change.

To evaluate the feasibility of the combination between nearshore sand dredging and shore-face nourishment in terms of acceleration of post-storm beach recovery.

To identify the effectiveness of the perched beach on the shore protection under storm waves.

1.4 Structure of Dissertation

The dissertation is composed of five chapters, each of them deals with different subjects.

Chapter One introduces the research issue and defines the goals, scopes, as well as objectives of the study. Chapter One consists of three main parts. Part 1.1 describes the evolution of coastal development and management. By identifying the impacts of the world population growth, economic development, the limitations of coastal structure on shore protection and the global climate change on the beach erosion. The world population growth and economic development make burdens on the coastal zones. Thus, the coastal zones may be exposed to increasing risks of erosion. Coastal structures locally protect the shore in this place, however, causes erosion in other places. In addition, coastal structures also cause many other environmental problems. The global climate change causes increasing of sea level, height of waves, and frequency of big storms. Thus, coastal erosion issue has been getting seriously. A new concept of shore protection was proposed that is balancing the on/offshore sediment transport or constraining the sediment from offshore transport in the littoral cell. Therefore, two countermeasures of beach erosion were suggested for the study. Part 1.2 describes the methodology of research. In this part, the components of research strategy were briefly stated. Part 1.3 explains goals, scopes and objectives of the study.

Under storm condition, the combination of nearshore sand dredging and shore-face nourishment were taken into account for shore protection. However, nearshore sand dredging is an activity that removes the sediment out of the littoral cell, thus it may cause shoreline retreat. Therefore, Chapter Two studies the effects of nearshore sand dredging on shoreline retreat. Chapter Two consists of four main parts. Part 2.2 illustrated the quantification of shoreline retreat under various sand dredging volumes. The results showed that the nearshore sand dredging causes rapidly retreat of shoreline. The retreat of shoreline is proportional to the volume of sand dredging. The other factors that affect the shoreline retreat such as time of dredging, method of dredging were also discussed. Sand dredging in calm season and periodic sand dredging can delay the shoreline retreat. However, magnitude of the final shoreline retreat was not different. Part 2.3 examined the positions of shoreline retreat after the nearshore sand dredging. The shoreline retreat area is located at the lee of dredged hole and flanks by two accreted areas. Part 2.4 assessed infill rate of nearshore dredged hole after sand dredging. The

dredged hole was quickly filled by the sand that was transported from the foreshore area, hence the shoreline. Finally, in order to minimize the effects of nearshore sand dredging on the shoreline retreat, the suggestions are shown in part 2.5.

Chapter Three examines the applicability of the shore-face nourishment method to artificial acceleration of post-storm beach recovery in regular and irregular waves. This chapter consists of three main parts. Part 3.2 illustrates the feasibility of the shore-face nourishment on acceleration of post-storm beach recovery. The recovery of post-storm beach is evaluated by two parameters: the shoreline recovery rate and the volume of berm in the foreshore area. The results of experiments showed the quick recovery of post-storm beach in the cases of shore-face nourishment comparatively with the cases of without shore-face nourishment. Part 3.3 investigated the other parameters that affect the post-storm beach recovery rate in the cases of shore-face nourishment such as accretive wave conditions, nourished volumes, positions of nourished areas, water levels, methods of nourishment. Part 3.4 addresses the issue of feasibility of the shore-face nourishment on post-storm beach recovery rate in irregular waves. In irregular waves, the post-storm beach recovery rate also increases. The comparison of the results of shore-face nourishment in regular and irregular waves is also discussed in this part. In the irregular waves, the artificial acceleration of post-storm beach recovery rate is smaller than that in regular waves.

Chapter Four examines the effectiveness of perched beach nourishment on shore protection. Part 4.2 illustrates the response of perched beach profile in regular and irregular waves under equivalent wave height. Under the normal waves, the response of the perched beach profile between these two waves are similar. Under erosive waves, however, the scour depth and volume loss of irregular waves are insignificant and much less than those of regular waves. Part 4.3 looked into the issue with other perspective. This part investigates the response of perched beach profile in regular and irregular waves under equivalent wave energy. The results showed that the response of perched beach under regular and irregular waves are similar except for the scour depth intensity. Finally, the classification criterion for the type of perched beach profile in irregular waves was proposed regarding the results of this study and empirical results of Larson and Kraus[39].

Conclusions were summarized in Chapter Five. The main aim of the dissertation that proves the initial hypotheses has been reached. The study concluded that the cross shore sediment transport management is one of important key concepts for shore protection under global climate change. The shore-face nourishment and perched beach nourishment are two effective methods for coastal conservation in the next few decades. Finally, the limitations of the research and the recommendations for the future research were discussed regarding the results of study, consequences of experiment conditions, insufficient data and lack of field data.

References

1) Gerland P, Raftery AE, Sevcikova H, Li N, Gu D, Spoorenberg T, et al. World population stabilization unlikely this century. Science. 2014 Sep. 346(6206): 234–237.

2) Timmerman P, White R. Egahydropolis: coastal cities in the context of global environmental change. Global Environmental Change. 1997. 7: 205–234.

3) EEA. The changing faces of Europe's coastal areas. Luxembourg: Office for Official Publications of the European Communities. 2006 Jun.

4) United Nations. World urbanization prospects. Department of Economic and Social Affairs, Population Division. 2014.

5) Walling DE. Human impact on land-ocean sediment transfer by the world's rivers. Geomorphology. 2006. 79: 192–216.

6) Menéndez M, Woodworth PL. Changes in extreme high water levels based on a quasi-global tide-gauge data set. Journal of Geophysical Research: Oceans. 2010 Oct. 115.

7) WGI_AR5. Climate Change 2013: The Physical Science Basis. Contribution of Working Group I to the Fifth Assessment Report of the Intergovernmental. e [Stocker TF., Qin D, Plattner GK, Tignor M, Allen SK, Boschung J, Nauels A, Xia Y, Bex V, Midgley PM, Cambridge, United Kingdom and New York, NY, USA: Cambridge University Press. 2013. 1535.

8) AR4. Climate change 2007: the synthesis report. contribution of working groups I, II and III to the fourth assessment report of the intergovernmental panel on climate change. Cambridge, United Kingdom and New York, NY, USA: Cambridge University Press. 2007.

9) Abeysirigunawardena DS, Walker IJ. Sea level responses to climatic variability and change in Northern British Columbia. Atmosphere Ocean. 2008. 46: 277-296.

10) Haigh I, Nicholls R, Wells N. Assessing changes in extreme sea levels: Application to the English Channel, 1900–2006. Continental Shelf Research. 2010. 30: 1042-1055.

11) Park J, Obeysekera J, Irizarry M, Barnes J, Trimble P, Park-Said W. Storm surge projections and implications for water management in South Florida. Climate Change. 2011. 107: 109-128.

12) Unnikrishnan AS, Kumar MRR, Sindhu B. Tropical cyclones in the Bay of Bengal and extreme sea-level projections along the east coast of India in a future climate scenario. Current Science. 2011. 101: 327–331.

13) USACE (US Army Corps of Engineers). Coastal engineering manual. Washington, DC: US Army Corps of Engineers, Coastal and Hydraulics Lab. 2002.

14) Matthew ML, Robert JN. Technologies for climate change adaptation coastal erosion and flooding. Roskilde: UNEP Risø Centre on Energy, Climate and Sustainable Development. 2010.

15) Leatherman S, Zhang K, Douglas B. Sea level rise shown to drive coastal erosion. EOS Transactions of the American Geophysical Union. 2000a. 81(6): 55-57.

16) Leatherman S, Zhang K, Douglas B. Sea level rise shown to drive coastal erosion: a reply. EOS Transactions of the American Geophysical Union. 2000b. 81(38): 437-441.

17) Sallenger A, Morton R, Fletcher C, Thierler ER, Howd P. Discussion of "Sea level rise shown to drive coastal erosion" by Leatherman et al. (2000). EOS, Transactions of the American Geophysical Union. 2000. 81(38): 436.

18) Zhang X, Zwiers FW, Li G. Monte Carlo experiments on the detection of trends in extreme values. Journal of Climate. 2004. 17: 1945-1952.

19) Seneviratne SI, Nicholls N, Easterling D, Goodess CM, Kanae S, Kossin J, Luo Y. Changes in climate extremes and their impacts on the natural physical environment. In: Managing the Risks of Extreme Events and Disasters to Advance Climate Change Adaptation. Cambridge, UK, and New York, NY, USA: Cambridge University Press. 2012. Vols. [Field CB, Barros V, Stocker TF, Qin D, Dokken DJ, Ebi KL, Mastrandrea MD, Mach KJ, Plattner GK, Allen SK, Tignor M, Midgley PM (eds.)].

20) WGII_AR5. Climate Change 2014: impacts, adaptation, and vulnerability. Cambridge, United Kingdom and New York, NY, USA: Cambridge University Press. 2014.

21) Bruun P. Coast erosion and the development of beach profiles. Beach Erosion Board. 1954.

22) Bruun P. Sea-level rise as a cause of shore erosion. Journal of Waterways and Harbour Division. 1962. 88: 117-130.

23) Bird ECF. Coastal geomorphology: an introduction. Chichester, UK and Hoboken, NJ, USA: John Wiley & Sons. 2000.

24) Hapke C, Himmelstoss E, Kratzmann M, List J, Thierler ER. National assessment of shoreline: historical shoreline changes along the new England and Mid-Atlantic coasts. Reston, VA, USA: United States Geological Survey (USGS) Open-File Report. 2011. 2010-1118, USGS.

25) Hilary FS, Kara JD, David MT, Kristin LS, Nathaniel GP, Asbury HS. National assessment of hurricane induced coastal erosion hazards: Gulf of Mexico. Virginia: U.S. Geological Survey, Reston. 2012.

26) Plant N, Stockdon H, Sallenger A, Turco M, East J, Taylor A, Shaffer W. Forecasting hurricane impact on coastal topography. EOS, Transactions of the American Geophysical Union. 2010.

91(7): 65-72.

27) Hay J, Mimura N. Supporting climate change vulnerability and adaptation assessments in the Asia-Pacific region: an example of sustainability science. Sustainable Science. 2006. 1: 23-35.

28) Mori N, Yoshimura T, Yasuda T, Mase H. Projection of extreme waves under a global warming scenario. Journal of Japan Society of Civil Engineers, Ser. B2 (Coastal Engineering). 2010. 66(1). (In Japanese).

29) IPCC. Contribution of working group I to the fourth assessment report of the intergovernmental panel on climate change, chapter 5. Cambridge Univ. Press. 2007. 387-429.

30) Toyoshima 0. Shore protection works. Lecture notes on practical design of coastal structures, The Ministry of Construction. 1986. (In Japanese).

31) Uda T. Japan's beach erosion (Advanced series on ocean engineering). World Scientific. 2010. 31.

32) Maspataud A, Ruz MH, Hequette A. Spatial variability in post-storm beach recovery along a macrotidal barred beach, Southern North Sea. Journal of Coastal Research. 2009. 56: 88-92.

33) Morton RA, Gibeaut JH, Paine JG. Stages and durations of post-storm beach recovery, Southeastern Texascoast, U.S.A. Journal of Coastal Research. 1994. 10: 884-908.

34) Corbella S, Stretch DD. Shoreline recovery from storms on the east coast of Southern Africa. Natural Harzards and Earth System Sciences. 2012. 12: 11-22.

35) Dean GR. Beach nourishment: theory and practice (Advanced series on ocean engineering). World Scientific. 2003. 18

36) Chatham CE. Movable bed model studies of perched beach concept." Proc. 13th International Conference on Coastal Engineering. 1972. 1197-1215.

37) Sorensen R, Beil N. Perched beach profile response to wave action. Proceedings 21st Coastal Engineering Conference, ASCE. 1988. 1. 482-492.

38) Van de Graaff J, Niemeyer HD, Van Overeem J. Beach nourishment, philosophy and coastal protection policy. Coastal Engineering. 1991. 16: 3-22.

39) Larson M, Kraus NC. Sbeach: Numerical model for simulating storm-induced beach change. Report 1: Empirical foundation and model development. Coastal Engineering Research Center, Waterways Experiment Station, Corps of Engineers. 1989. 129-137.

Chapter 2 Nearshore Sand Dredging

2.1 Introduction

In some developing countries, sand dredging in nearshore zone is very common. However, the sediment management in coastal area is in infancy. In Japan, however, to enhance sediment management in coastal area, sand is sometimes dredged at the nearshore zone in the deposited areas and then nourished to the eroded areas. Sediment management in terms of nearshore sand dredging is important for beach nourishment, sand bypassing and sand recycling. However, the sand dredging in the nearshore zone may cause negative effects to the shoreline erosion. In this chapter, the shoreline changes because of the nearshore sand dredging as well as the evolution of dredged hole after sand dredging were taken into account to evaluate and quantify the effects of nearshore sand dredging.

Price et al.[1)] studied the existing dredging area in south of England and shown that the sand dredging area close to the shore can have significant negative impacts, causing severe erosion of the foreshore. A study in the Genkai Sea, Japan found that dredged holes in an area where the water depth is less than 30 m refilled with sand that was mainly transported from the onshore side[2)]. On the western Black Sea coast of Turkey where sand dredging is planned at the near-shore zone for construction, the most critical problem is whether the project results in significant negative impacts or changes in physical or biological processes[3)]. These studies qualitatively evaluated the negative impacts of sand dredging to the shoreline by field observations. Quantitative evaluation, however, is required for sediment management.

The impacts of dredged hole that located very offshore on the shoreline change have been investigated in many studies, however, varied results of shoreline change were showed, i.e. along the shoreline, both accretion and erosion were found behind the dredge hole in different conditions. Horikawa et al.[4)] conducted experiments in wave basin and assessed the impact of offshore dredged hole to the shoreline change using the refraction model, in which accretion was observed at the lee of the dredged hole. Motyka and Willis[5)] used a wave refraction model for the offshore dredged hole and the results give the reverse of that observed by Horikawa et al.[4)]. Bender[6)] modeled the shoreline change by combined wave refraction and diffraction, and found that the changes of shoreline could alter with specifications of wave conditions and unchanged dredged hole. Work et al.[7)] studied the impacts on shoreline due to the sand dredging outside the surf zone. The results showed that the sediment was accumulated at the lee of dredged hole and wave diffraction was neglected in wave model. McDougal et al.[8)] studied the wave diffraction caused by dredged hole under long wave condition and showed that the appropriate selection of dredged hole dimension and placement may lead to significant reduction in wave height in the lee of dredged hole. The accretion in the lee of the dredged hole can occur if the

width of dredged hole is large enough. To some extent, the impacts of the dredged hole that located in the nearshore zone on the shoreline changes may differ.

In the study of evolution of dredged hole after sand dredging, Gonzalez et al.[9] developed a numerical model for predicting the morphodynamic evolution of offshore dredged hole (dredged area depth h_o > 20 m). The simple model provides an estimation of the infill rate and migration velocities of the offshore dredged holes on the scale of years. Dolah et al.[10] studied infill rate in sand borrow areas at the offshore sites used for beach nourishment projects in South Carolina, the result showed that the infill rate is inversely proportional to the distance of dredged hole from the shore.

To evaluate quantitatively the shoreline retreat caused by nearshore sand dredging, a combination of theoretical, numerical and physical methods was used. The experimental and numerical methods were used for verifying the theoretical analysis of the shoreline retreat in difference of sand dredging volumes. The experiments were conducted in 2D wave flume and 3D wave basin, and the SBEACH model was used for numerical simulation. The results showed that after nearshore sand dredging, the shoreline rapidly retreated at the lee of dredged hole and then the dredged hole is speedily filled up.

2.2 Quantification of Shoreline Retreat

2.2.1 Theoretical analysis

Bruun[11] suggested the simple relationship for equilibrium beach profile as

$$h(y) = Ay^{2/3} \tag{2.1}$$

in which h is the water depth at a distance y from the shoreline, A is a profile scale parameter.

A definition sketch of the profile before and after sand dredging in the nearshore zone is presented in Fig. 2.1. It is common to assume that the profile retreats uniformly at all active elevations as long as the beach maintain its shape across the profile. In addition, it will be assumed that within the surf zone wave height is proportional to the local water depth with the proportionality factor, κ, i.e. $H=\kappa h$ (κ=0.78). At the breaking point, wave breaking height $H_b = \kappa h_*$, where h_* is closure depth. Referring to Fig. 2.1, sand dredging volume, V_d, is equal to the eroded volume, V_e

$$V_d = V_e \tag{2.2}$$

When Equation 2.1 and 2.2 are combined the following implicit equation for the maximum shoreline change, Δy, is obtained

$$\frac{V_d}{BW_*} = -\frac{\Delta y}{W_*} + \frac{3}{5}\frac{h_*}{B}\left(1-\frac{\Delta y}{W_*}\right)^{5/3} - \frac{3}{5}\frac{h_*}{B} \tag{2.3}$$

in which W_* is the seaward limit of active profile (m), B is the berm height (m).

$$W_* = \left(\frac{H_b}{\kappa A} \right)^{3/2} \tag{2.4}$$

In this case the shoreline is in recession thus, $\Delta y < 0$. Equation 2.3 can be expressed in non-dimensional form as

$$V_d' = -\Delta y' - \frac{3}{5} h_*' \left(1 - \left(1 - \Delta y' \right)^{5/3} \right) \tag{2.5}$$

in which the non-dimensional variables are

$$\Delta y' = \frac{\Delta y}{W_*}; h_*' = \frac{h_*}{B}; V_d' = \frac{V_d}{B W_*} \tag{2.6}$$

The Equation 2.5 is plotted in Fig. 2.2. This figure showed the non-linear relationship between shoreline retreat Δy and sand dredged volume V_d. For small values of V_d, Equation 2.5 can be approximated as

$$\Delta y = -\frac{V_d}{B + h_*} \tag{2.7}$$

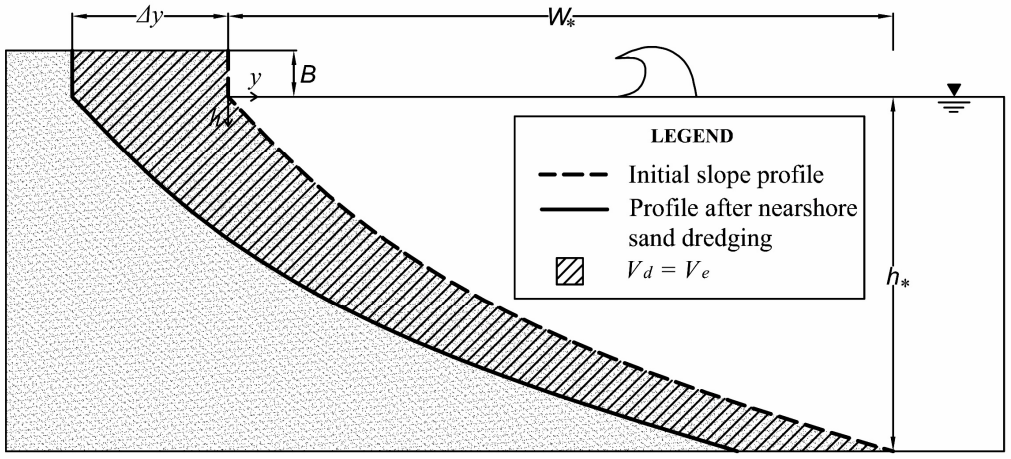

Fig. 2.1 Definition sketch for response of profile due to nearshore sand dredging[12].

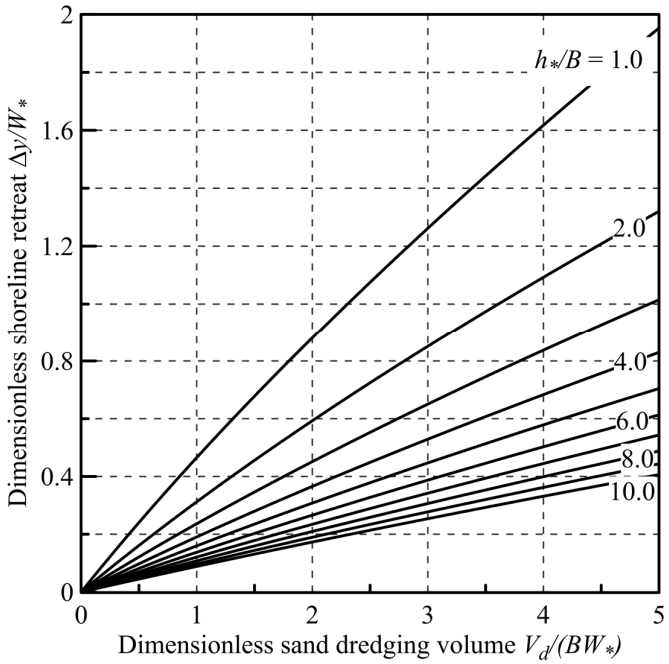

Fig. 2.2 Isolines of dimensionless shoreline change, $\Delta y/W_*$, vs dimensionless sand dredging volume in nearshore zone, $V_d/(BW_*)$, dimensionless breaking depth, h_*/B[12].

2.2.2 Physical and numerical modelling

2.2.2.1 Physical modeling

The experimental study of the sand dredging in the near shore zone was carried out at the Hydraulic Laboratory of Osaka University. The experiments were conducted in a 2D wave flume of 30 m long, 0.7 m wide and 0.7 m deep. To evaluate the influences of volumes, times and methods of sand dredging on the intensity of the shoreline retreat, seven cases of the experiments were conducted (Table 2.1). The experiment was set up as shown in Fig. 2.3. Median grain size of sediment d_{50} is 0.22 mm. The sediment grain size distribution is shown in Fig. 2.4. The median grain size of sediment is larger enough to eliminate the viscous and surface tension effects. This sediment is used for all of physical experiments in this study. To create barred type profile from the initial slope, regular erosive waves were generated for 60 minutes with incident wave height H = 0.14 m and wave period T = 1 s[13]. Thereafter, a volume of sand was dredged only one-time in all the cases except for experiment E2D where sand was dredged at the bar every 60 minutes during a 300 minutes wave generation period and the total dredged volume was 0.066 m^3/m. After the sand dredging, the same wave condition was generated again for 300 minutes in all the cases except for case E5D. In the case E5D, to dredge sand in accretive wave condition, waves were shifted to accretive wave condition with incident wave height H = 0.05 m and wave period T = 2 s[13] and generated for 300 minutes after sand dredging. Thereafter, waves were shifted back to erosive waves with wave height H = 0.14 m and wave period T = 1 s and generated for 300 minutes. The beach profile was measured at 2-cm intervals by an optical bottom

profiler and the wave height was measured at 50-cm intervals along the profile by the first wave gauge. The measuring instruments were placed on a trolley car. At each position, the wave height was measured for 10 s before moving to the next position. The second wave gauge, which measured the offshore wave height, was set 7.3 m from the end of the slope.

Even in the case without sand dredging (case E1), the shoreline still gradually retreated after 60 minutes of erosive waves generation. Thus, the additional shoreline retreat caused by sand dredging was defined as the difference between the measured retreat and that of case E1.

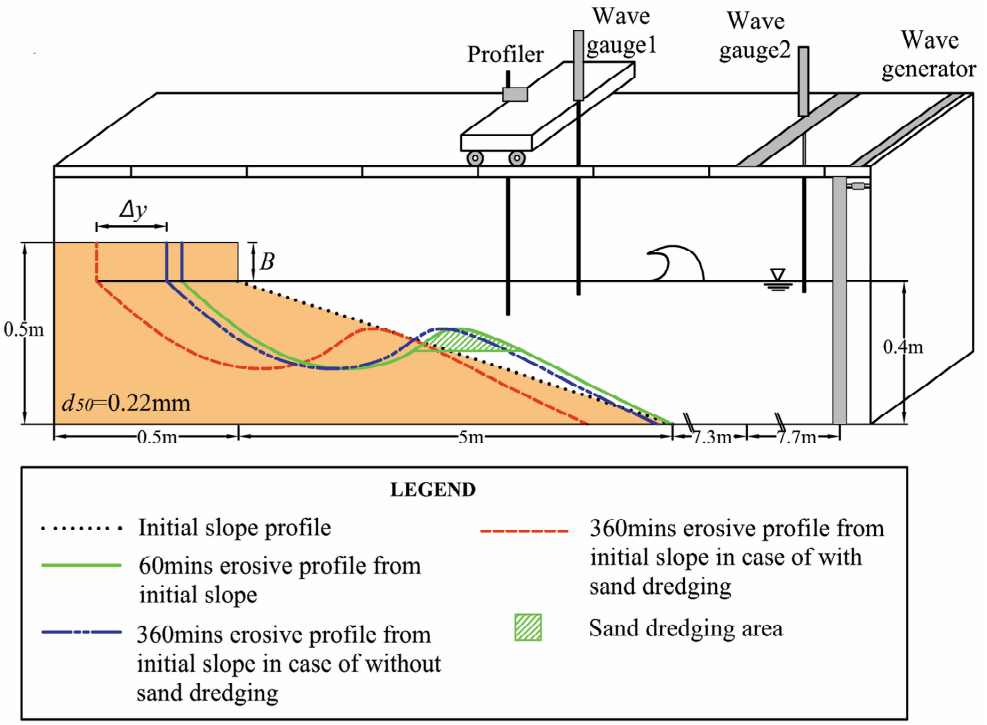

Fig. 2.3 Physical modelling for nearshore sand dredging in 2D wave flume.

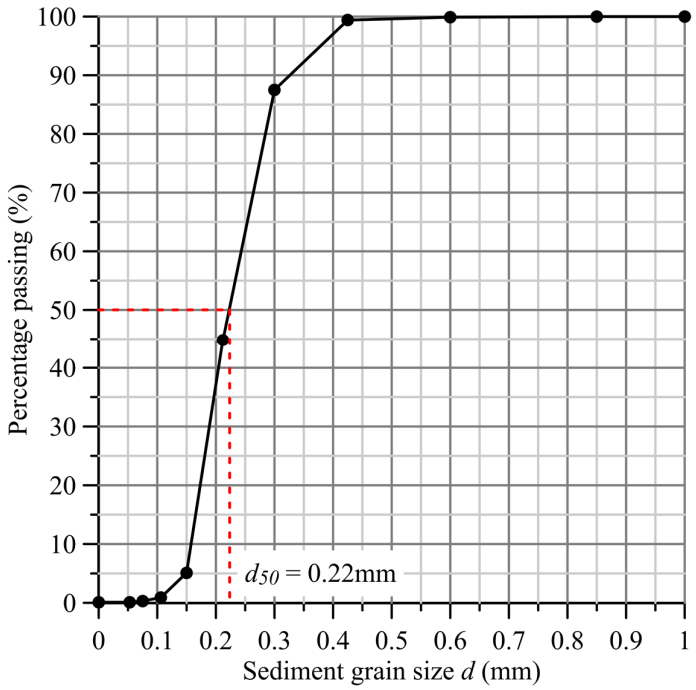

Fig. 2.4 Sand grain size distribution.

Table 2.1 Experimental conditions in 2D wave flume[14].

Case No.	Dredging method	Wave condition (*H*/*T*)	Dredging volume V_d (m^3/m)	Type of wave
E1	Without dredging	0.14/1.0	0.000	Erosive wave
E3D1	One-time dredging	0.14/1.0	0.020	Erosive wave
E3D2	One-time dredging	0.14/1.0	0.040	Erosive wave
E3D3	One-time dredging	0.14/1.0	0.060	Erosive wave
E3D4	One-time dredging	0.14/1.0	0.080	Erosive wave
E2D	Periodic dredging	0.14/1.0	0.066	Erosive wave
E5D	One-time dredging	0.05/2.0 - 0.14/1.0	0.060	Accretive wave-erosive wave

2.2.2.2 Numerical modelling

In the numerical modelling, SBEACH program was used for simulating the changes of beach profile cause by the nearshore sand dredging. SBEACH was developed to simulate storm induced beach change, which has been validated and used extensively for erosive conditions[15]. The model was slightly modified for the experimental approximation. Sediment transport zone is divided in 4 zones as in Fig.

2.5. As the wave height distribution is calculated across-shore for a given time step, location of the boundaries between the different sand transport zones is determined. Sediment transport is calculated from zone I to zone IV by following equations, respectively:

$$q = q_b e^{-\lambda_1 (y - y_b)} \qquad y_b < y \tag{2.8}$$

$$q = q_p e^{-\lambda_2 (y - y_p)} \qquad y_p < y \le y_b \tag{2.9}$$

$$q = \begin{cases} K\left(D - D_{eq} + \dfrac{\varepsilon}{K}\dfrac{dh}{dy} \right) & D > D_{eq} - \dfrac{\varepsilon}{K}\dfrac{dh}{dy} \\ 0 & D < D_{eq} - \dfrac{\varepsilon}{K}\dfrac{dh}{dy} \end{cases} \tag{2.10}$$

$$q = q_z \left(\frac{y - y_r}{y_z - y_r} \right) \qquad y_r < y < y_z \tag{2.11}$$

in which

q = net cross-shore sand transport rate, m^3/m-sec

$\lambda_{1,2}$ = spatial decay coefficients in Zones I and II, 1/m

y = cross-shore coordinate directed positive offshore, m

K = sand transport rate coefficient, m^4/N

D = wave energy dissipation per unit water volume, N-m/m^3-sec

D_{eq} = equilibrium wave energy dissipation per unit water volume, N-m/m^3-sec

ε = slope-related sand transport rate coefficient, m^2/sec

h = still-water depth, m

Subscripts *b*, *p*, *z* and *r* stand for quantities evaluated at the break point (*BP*), plunge point (*PP*), end of the surf zone and run-up limit, respectively. Equation of mass conservation is written as

$$\frac{\partial q}{\partial y} = \frac{\partial h}{\partial t} \tag{2.12}$$

The undistorted geometric scale used to construct model was 1:20 with respect to the experiment. Froude similarity was used for the simulation of the wave motion, whereas the sediment grain size has been imposed preserving in the model the value of settling velocity parameter[16]. Four cases of sand dredging N3D1, N3D2, N3D3 and N3D4 were simulated using SBEACH model in which the dredged volume were similar to the four experimental cases E3D1, E3D2, E3D3, E3D4, respectively.

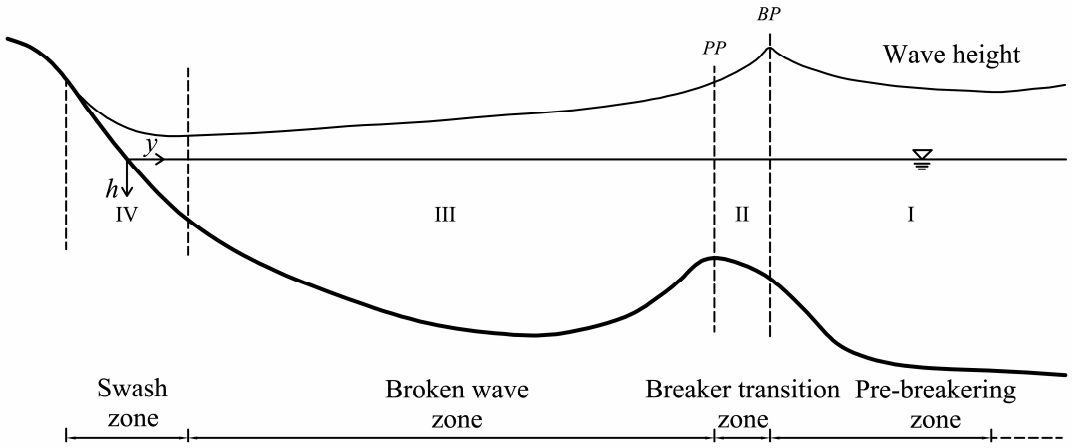

Fig. 2.5 Definition sketch for four principal zones of cross-shore sand transport (*BP*: break point, *PP*: plunge point)[15].

Shoreline retreat and volume of sand dredging

In the experiments E3D1 to E3D4, the four different volumes of sand were dredged one-time after 60 minutes of erosive wave generation. Change of beach profiles after sand dredging was shown in Fig. 2.6. Just after dredging of sand bar, the sediment of the foreshore area is quickly transported offshore causes shoreline retreat. The amount of the sediment was deposited at the place in which a new bar was formed. After 300 minutes of wave generation, the position of the new bar of cases with sand dredging E3D1 to E3D4 was shifted onshore compare with that of the case without sand dredging E1. The shoreline retreat of cases E3D1 to E3D4 in 300 minutes after dredging is shown in Fig. 2.7. The results show that immediately after dredging, sand was transported offshore, which caused an abrupt retreat of the shoreline; however, the effect subsided after about 120 minutes in all the cases. As the beach profile approaches equilibrium, dictated by the incident waves, the net cross-shore sediment transport rate q decreases to zero at all points x along the profile. Thus, the shape of the transport rate distribution varies with time. Sawaragi and Deguchi[17] used an exponential decay to derive a time-dependent transport relationship; however, since the shape of the transport rate distribution also varies with time, a peak transport rate may not be the best indicator. The average absolute sediment transport rate was used to indicate the measure of transport activity along the profile[15]. The average absolute sediment transport rate was calculated as

$$Q_A = \frac{1}{x_1 - x_0} \int_{x_0}^{x_1} |q| dx \tag{2.13}$$

in which Q_A is average absolute sediment transport rate ($mm^3/mm/s$), x_1 is the seaward limit of the profile change (mm). In experiments E3D1–E3D4, after the sand dredging, the average absolute

sediment transport rate quickly decayed in the first 120 minutes and then stabilized in the subsequent last 180 minutes (Fig. 2.8).

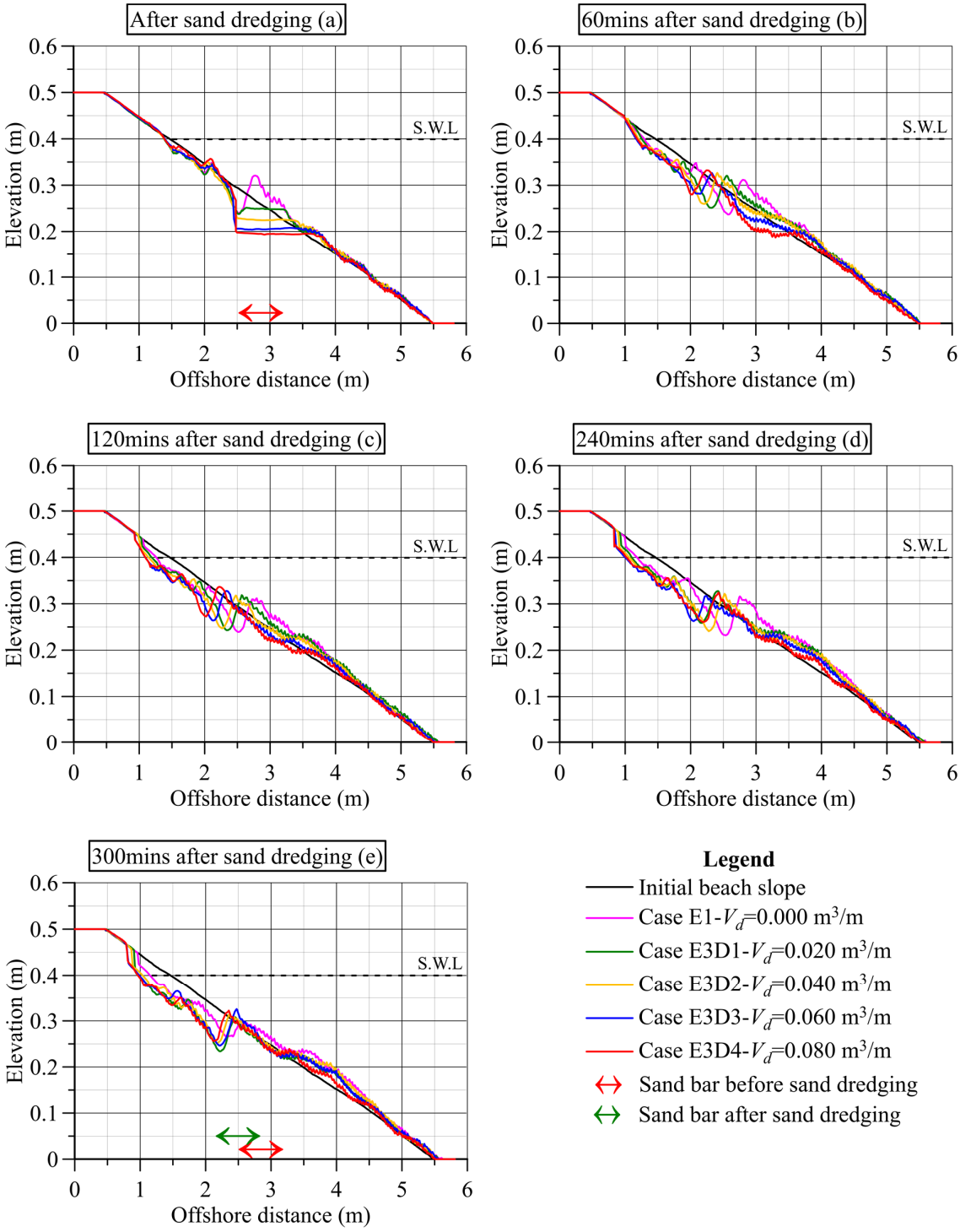

Fig. 2.6 Beach profiles of cases with different sand dredging volumes.

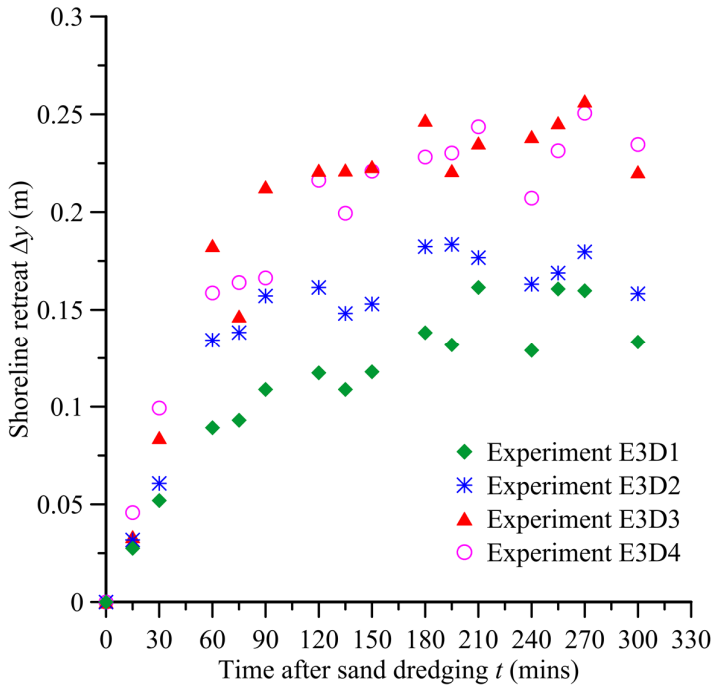

Fig. 2.7 Shoreline retreat after dredging different volumes of sand.

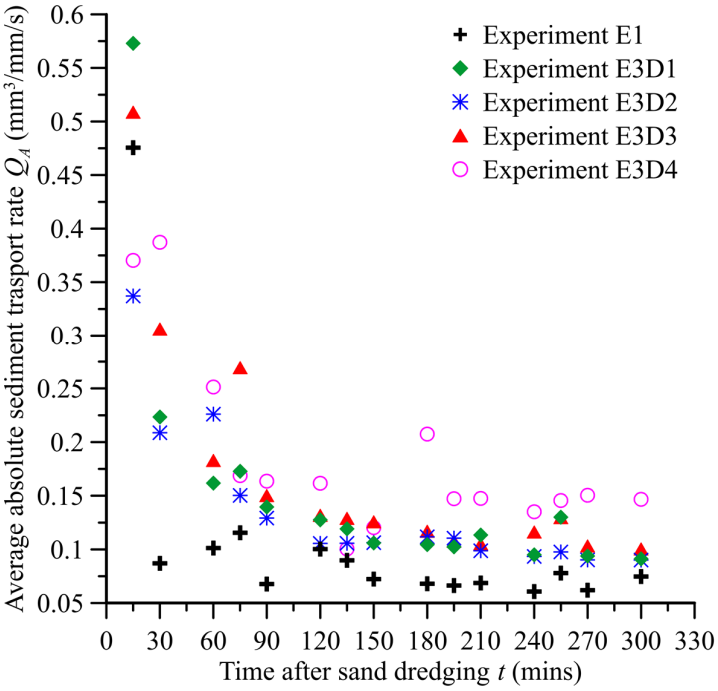

Fig. 2.8 Average absolute sediment transport rate of physical experiments.

The final shoreline retreats of the four cases after 300 minutes of wave generation in the experiments and numerical simulation show the same trend (Fig. 2.9). After 300 minutes, the final shoreline retreat increased with increasing sand dredging volume; however, the ratio between the final shoreline retreat and the dredged volume was not constant and shows a decreasing trend as the volume

increases. On the other hand, in the theoretical analysis, with small of sand dredged volume, the relationship between final shoreline retreat and sand dredged volume is assumed linearity and followed the Equation 2.7, i.e. the theoretical analysis underestimated the shoreline retreat with small dredged volume.

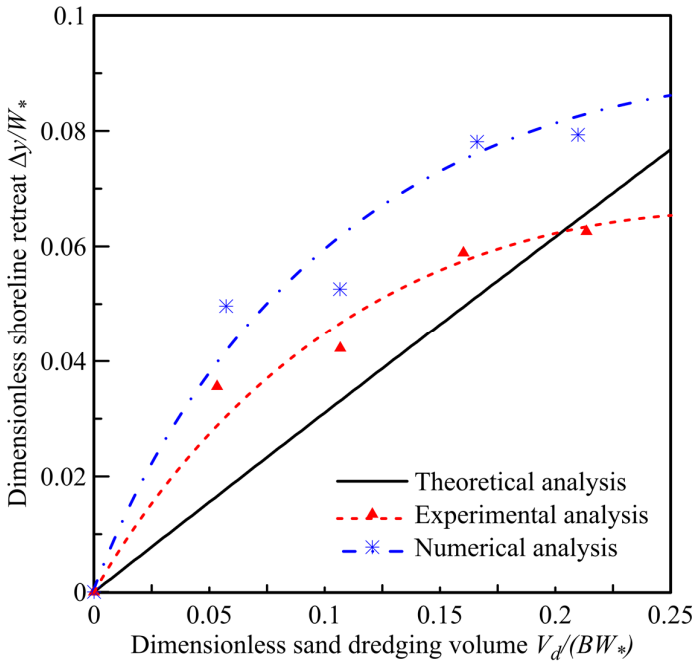

Fig. 2.9 Final shoreline retreat after near shore bar sand dredging (h^*/B=2.2).

Shoreline Retreat with Different Methods and Times of Sand Dredging

The volume of dredged sand in these experiments E2D and E5D was very close to that of the experiment E3D3. In the experiment E2D, the sand was periodically dredged at the sand bar every 60 minutes in erosive wave conditions, thus the speed of shoreline retreat was slower than that of one-time sand dredging case E3D3 (Fig. 2.10b, c). The shoreline retreat gradually increased during 300 minutes of wave generation (Fig. 2.11). In the experiment E5D, a berm was formed at the foreshore area in the accretive wave conditions (Fig. 2.10a). Although, the sand dredging volumes are similar, the speed of shoreline retreat of case E5D in the first 120 minutes after sand dredging is smaller than that of the case E3D3 (Fig. 2.10b, c). The shoreline retreats gradually increased in the first 180 minutes and then subsided in the subsequent 120 minutes. Despite the equal volumes of dredged sand, the process of shoreline retreats in each experiment varied significantly. The speed of shoreline retreats of the experiments E2D and E5D was slower than that of the experiment E3D3. However, the final shoreline retreat was very similar (Fig. 2.12). Therefore, in order to reduce the speed of shoreline retreat, sand dredging should be carried out in the calm wave season instead of storm wave season and used the method of periodic sand dredging.

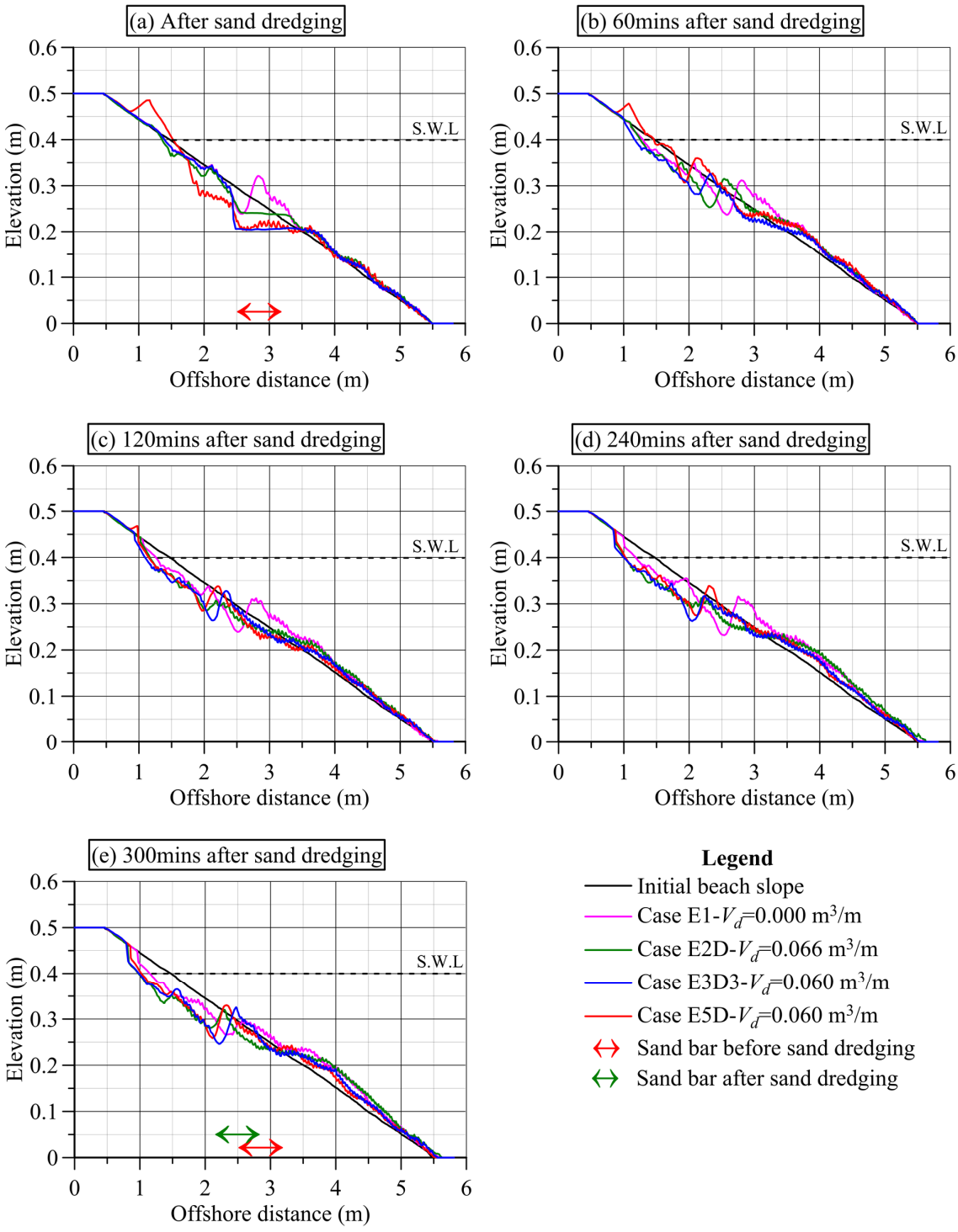

Fig. 2.10 Beach profiles of cases with different methods and times of sand dredging.

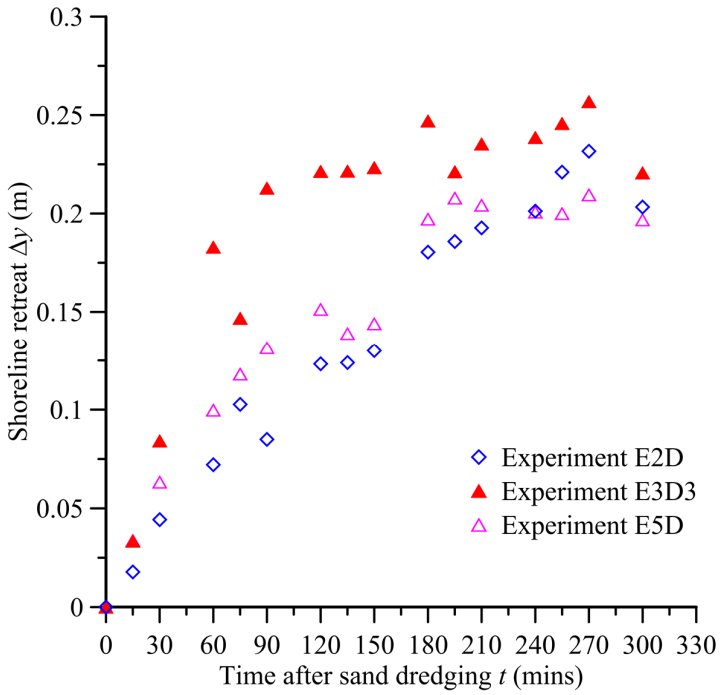

Fig. 2.11 Shoreline retreat with different methods and times of sand dredging.

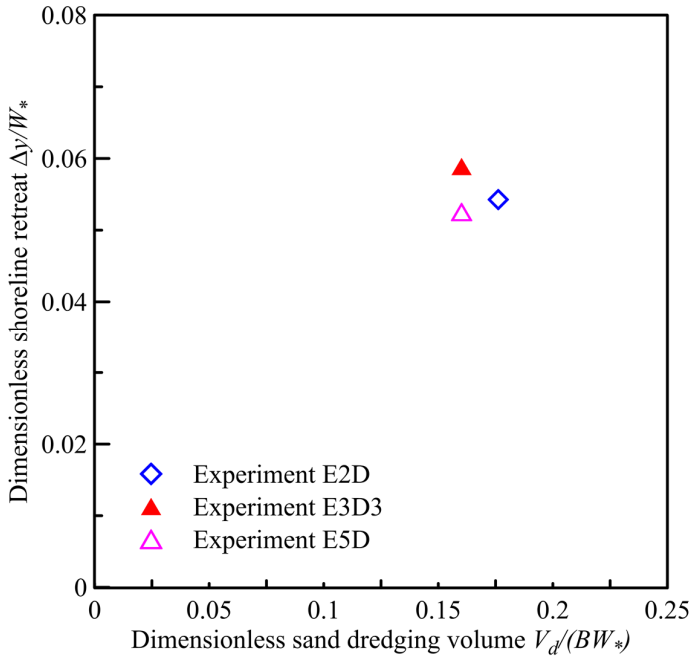

Fig. 2.12 Final shoreline retreat with different methods and times of sand dredging.

2.3 Position of Shoreline Change Caused by Near Shore Sand Dredging

To identify the location of accretion and erosion areas caused by nearshore sand dredging, three cases of experiments were conducted in 3D wave basin considering the wave refraction and diffraction processes at the nearshore zone. In addition, to evaluate the effect of the width of dredged hole to the

magnitude of shoreline retreat, the geometry of dredged hole was altered by changing the width with the same length of dredged hole.

The experiments were carried out in 3D wave basin that is 10 m long, 5 m wide, and 0.6 m deep (Fig. 2.13). Table 2.2 showed the summary of the experimental conditions. The median grain size of the sediment is 0.2 mm and the initial slope of the beach is 1:10 for all the cases. To create semi-equilibrium profiles with a bar, regular erosive waves were generated with incident wave height H = 14 cm and wave period T = 1 s[13]. Wave was generated for 240 minutes to obtain a barred profile from the initial beach slope, and then sand was dredged one-time. The geometry of dredged hole is *b* (m) in length, *a* (m) in width and *d* (m) in depth. After the sand dredging, the same wave condition was generated for 120 more minutes in all the cases.

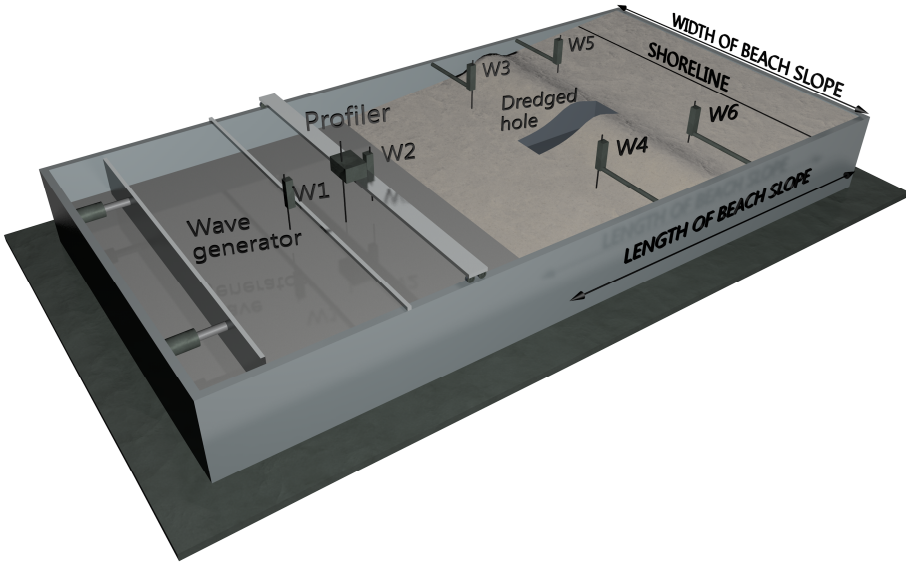

Fig. 2.13 Physical modelling for nearshore sand dredging in 3D wave basin (W: wave gauge No.).

Measurements of beach topography and wave height were repeated every 30 minutes in case E1. Because the dredged hole in the nearshore zone was filled up very quickly after sand dredging, the beach topography and wave height were measured at 10, 20, 30, 45, 60, 120 minutes after sand dredging in the dredged cases E2D1, E2D2. The wave gauge W2 was placed on a trolley car to measure the wave height distribution in the middle of the beach at 0.5-m interval (A-B line in Fig. 2.14). At each position, the wave height was measured for 10 s before moving to the next position.

Table 2.2 Experimental conditions in 3D wave basin.

Case No.	Dredging method	Dredged hole *a* x *b* x *d* (m)	Dredged volume (m^3)
E1	Without dredging	-	0.00
E2D1	One-time	0.25 x 1.20 x 0.15	0.02
E2D2	One-time	0.50 x 1.20 x 0.15	0.04
Note: geometry of dredged hole *a*: width (m), *b*: length (m), *d*: depth (m)			

Fig. 2.14 shows the shoreline of all cases after 240 minutes of wave generation from initial beach slope. In 3D wave basin, even in the same experimental conditions, it is very difficult to reproduce the same shoreline for all cases after 240 minutes of wave generation from initial beach slope. Therefore, the difference of shoreline changes between experiments with and without sand dredging is not discussed in this study. The shoreline after 240 minutes of wave generation is considered as the zero line in each case and the shoreline change is measured from this zero line. Fig. 2.15 and Fig. 2.16 showed the shoreline changes due to sand dredging in two experiments E2D1 and E2D2, respectively. The magnitudes of shoreline retreat of the 2D experiments E3D2 and E3D4 indicated in Table 2.1 are also shown in these figures to know the difference on shoreline change in 2D and 3D effects.

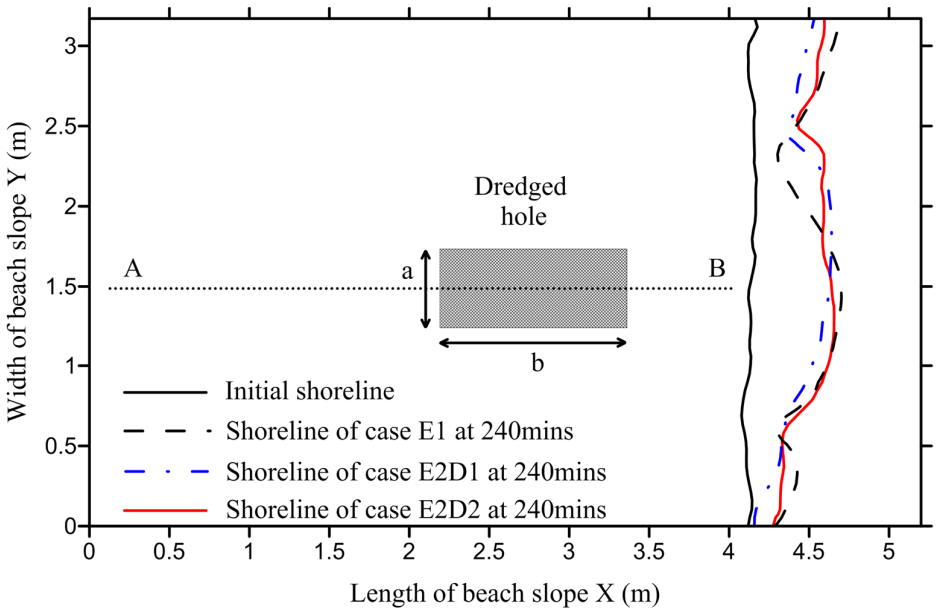

Fig. 2.14 Shoreline at 240mins of wave generation from initial beach.

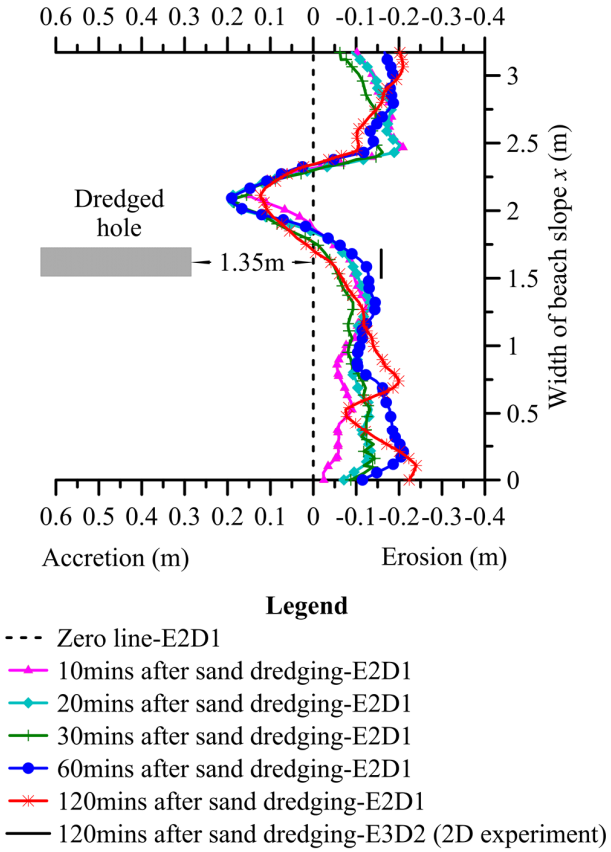

Fig. 2.15 Shoreline change of experiment E2D1 during 120 minutes after sand dredging.

When waves approach to the coast, the wave propagation direction may be changed by wave refraction and diffraction. If wave refraction and wave diffraction are considered independently, the wave refraction process causes the erosion at the lee of dredged hole flanked by two accretion areas while wave diffraction process behaves the opposite way[18]. In the experiments of sand dredging, wave breaking positions in the line A-B are further onshore, whereas in the case without sand dredging E1, it is further offshore (Fig. 2.17). The arrows in this figure show the direction of moving on/offshore of wave breaking points after sand dredging. Thus in dredging cases, the wave breaking positions in the dredged hole area move further onshore, while in both the sides of dredged hole it is stable or move offshore. At the side slope of dredged hole, wave refraction occurs. Therefore, wave propagation diverges away to both the sides (Fig. 2.18). The result is that the sediment at the lee of dredged hole transported to both the sides causes the erosion and flanked by two accretion areas (Fig. 2.15 & Fig. 2.16). It can be said that, in the nearshore sand dredging, with the short wave periods the wave refraction is a significant process to produce the shoreline pattern and the wave diffraction can be neglected.

By making a comparison of the magnitude of shoreline retreat of the cases E2D1 and E2D2, although increasing the width of dredged hole, the magnitude in either case looks similar (Fig. 2.15 & Fig. 2.16). This result is appropriate to the result of numerical modelling studied by Demir et al.[19].

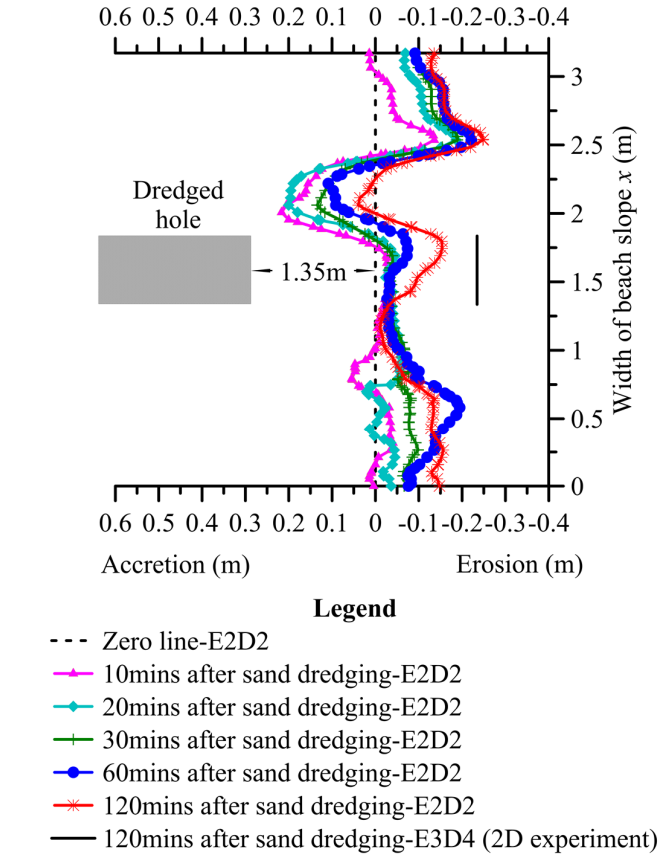

Fig. 2.16 Shoreline change of experiment E2D2 during 120 minutes after sand dredging.

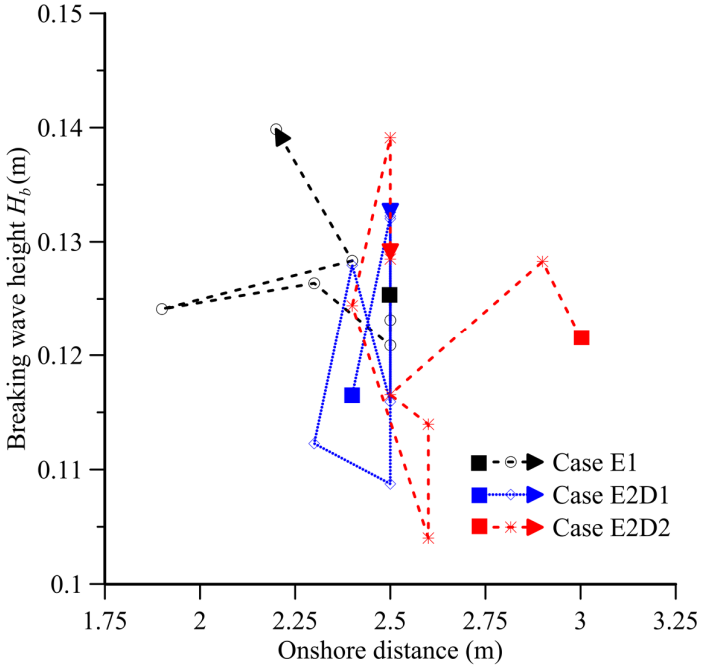

Fig. 2.17 Breaking wave height and location of wave breaking point in middle of beach slope (line A-B in Fig. 2.14).

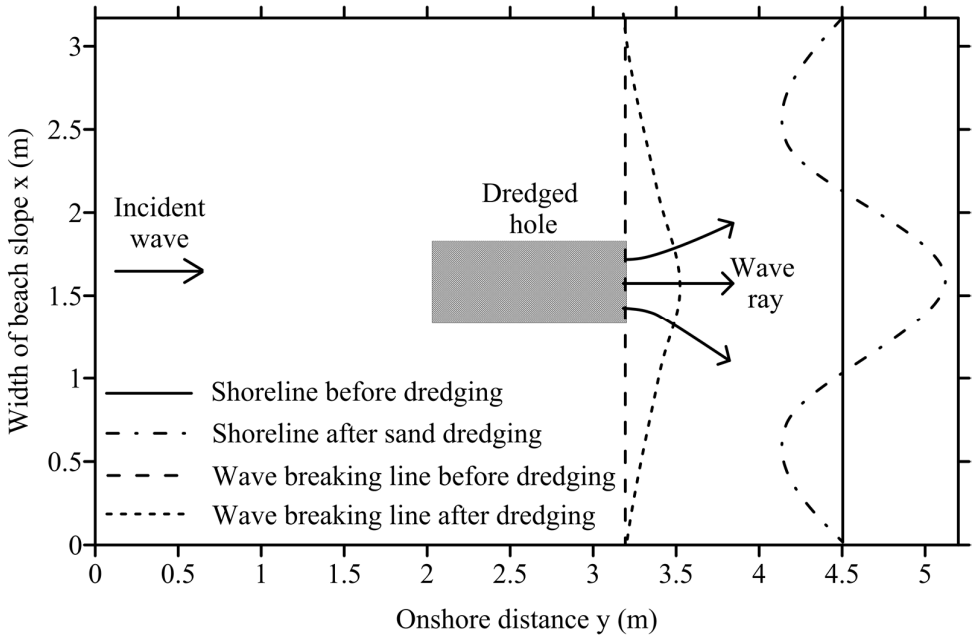

Fig. 2.18 Sketch of wave refraction induced by nearshore bar sand dredging results in shoreline change.

2.4 Infill Rate of Dredged Hole

In the experiments, the sand bar was located in the breaker zone, i.e. the most activation of seabed zone. Any change of bathymetry in this area can cause significant change of hydrodynamic conditions, thereby causing highly transport gradient, hence the profile. After the sand bar was dredged, under the same wave conditions, a new bar was formed by sediment that transported from foreshore area and located at new position.

The infill rate is calculated by dividing the filled volume of dredged hole by the dredged volume at a certain time after sand dredging. The results of experiment E3D4 in 2D wave flume showed that after sand dredging, the infill rate was very high in the first 15 minutes and gradually increases in last 105 minutes. However, dredged hole was not filled up (Fig. 2.19). On the other hand, in 3D wave basin experiment E2D2 the dredged hole was filled 80% in the first 60 minutes and completely filled up after 120 minutes. In the experiment E2D2, at 120 minutes after sand dredging the amount of sand from the lee of dredged hole is not sufficient to fill up the dredged hole (Fig. 2.20). Figure 2.21 shows that just after sand dredging a large amount of sand transported from both sides of dredged hole and then deposited in the dredged hole. In addition, by making a comparison of the magnitude of shoreline retreat at the lee of dredged hole between the 2D wave flume and 3D wave basin experiments, it is shown that the shoreline retreat in the 2D wave flume experiments is larger (Fig. 2.15 & Fig. 2.16). Thus the source of infilled sediment of the dredged hole is not only transported from the area behind the hole but also

from its both sides. It is clear to conclude that the dredged hole in nearshore zone is filled up very rapidly after nearshore sand dredging.

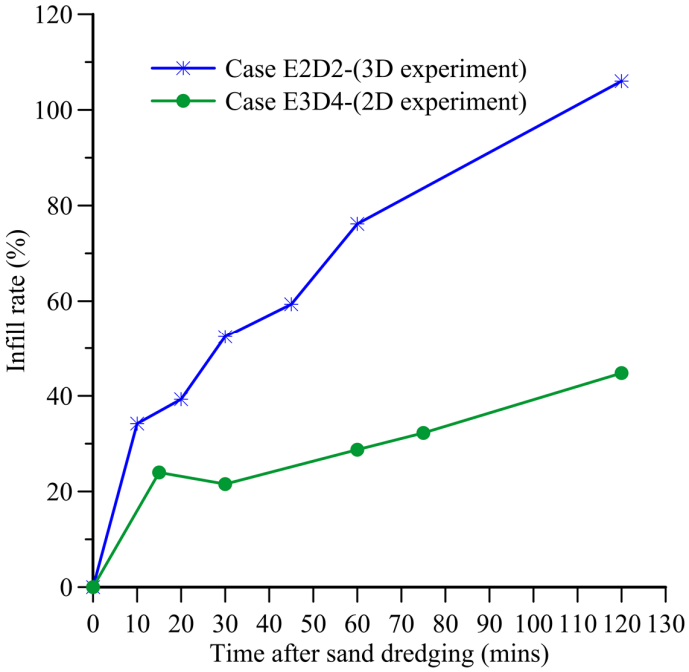

Fig. 2.19 Infill rate of dredged hole after sand dredging.

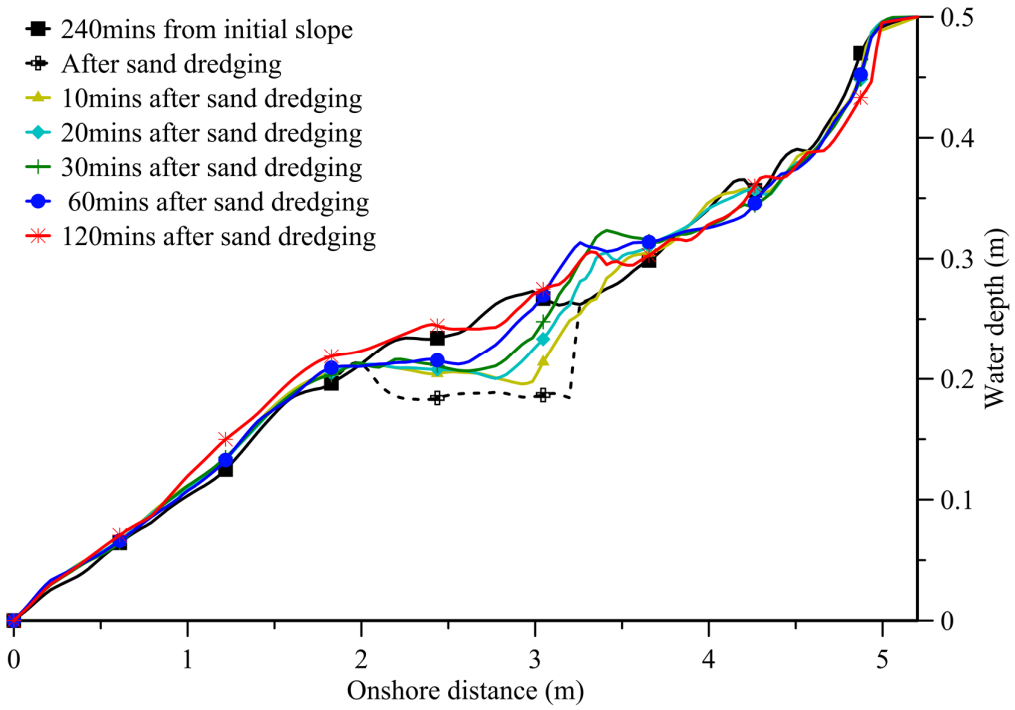

Fig. 2.20 Cross-shore beach profile in the middle of dredged hole x = 1.585 m (case E2D2).

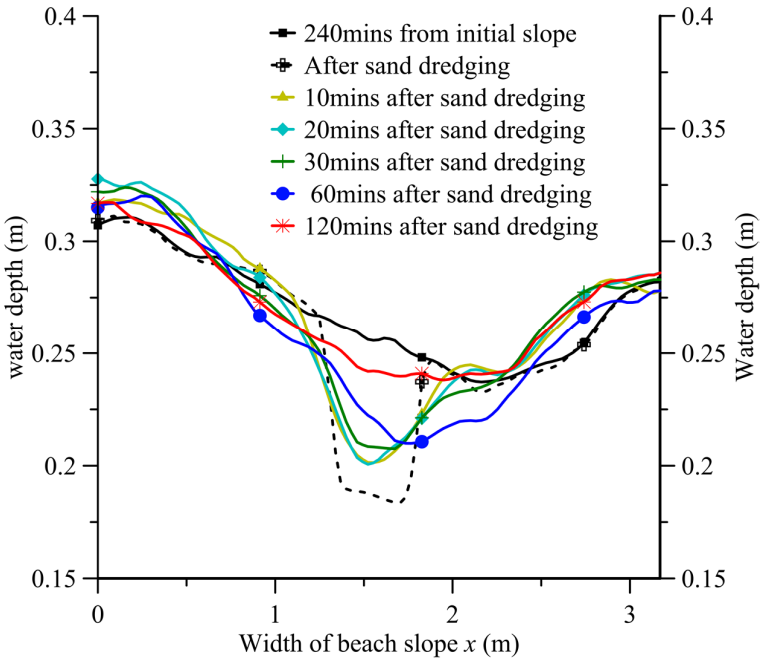

Fig. 2.21 Longshore beach profile in the middle of dredged hole y = 2.75 m (case E2D2).

2.5 Discussions

The relationship between the shoreline retreat and sand dredged volume of the three analysis methods: theoretical analysis, experimental analysis and numerical analysis were similar i.e. the shoreline retreat increased as increasing the sand dredged volume. In the beach nourishment, Dean[20] showed that it is reasonable to assume that in the case of the grain size of nourished sediment is equal to the native sediment, the advance profile after nourishment is similar to the original profile. Thus, the shoreline advance is proportional to the sediment nourished volume. In nearshore sand dredging, because a volume of sand was dredged, the sand from the foreshore was transported offshore formed a new equilibrium beach profile. The shape of the equilibrium beach profile after sand dredging was similar to the shape of the profile before sand dredging (Fig. 2.6e). However, the final equilibrium beach profile was shifted onshore caused shoreline retreat. Therefore, the final of shoreline retreat was also proportional to the sand dredged volume. The relationship between the shoreline retreat and sand dredged volume was simply quantified by Equation 2.7.

Sand bar is located at breaker zone, i.e. in the most activation of seabed zone. Any change of bathymetry in this area can cause significant change of hydrodynamic conditions within the nearshore zone, thereby causing highly transport gradient and profile change[12]. Whereas, the results of experiments in 2D wave flume and 3D wave basin showed that in erosive waves, the sediment was transported very quick offshore after sand dredging caused quick shoreline retreat, the sand dredging in accretive waves and periodic sand dredging method can delay the speed of the shoreline retreat. These results may play an important role for the next research of shore-face nourishment.

McDougal et al.[8] studied the variation of diffraction coefficient in the lee of dredged hole by changing the geometry of the dredged hole. The diffraction can be taken into account when $a/L \geq 1$, $b/L \geq 0.5$, $d/h = 3$. In this study, the dredged holes in the case of physical experiment was located in the nearshore zone, however, its depth and width are $d/h < 1$, $a/L < 0.5$. The results of experiment showed that the wave diffraction process was less significant than refraction process in the dredged hole area. Therefore, sand dredging in the nearshore zone caused erosion at the lee of dredged hole, flanked by two accretion areas.

2.6 Conclusions

The shoreline retreat caused by nearshore sand dredging is quantified by a simple relationship to the volume of sand dredging based on the equilibrium beach profile. According to the results of experiment and numerical analysis, the theoretical quantity of shoreline retreat is slightly under estimated. The shoreline retreat is almost proportional to the dredged volume.

One-time sand dredging at the nearshore zone under the erosive wave conditions caused quick retreat of the shoreline. Thus infill rate of nearshore dredged hole is very high. Just 60 minutes after sand dredging, 80% volume of dredged hole is filled. Although, the final magnitude of retreat of shoreline under periodic sand dredging and dredging in the accretive wave conditions is similar to one-time sand dredging, it can delay the process of shoreline retreat. This is a very important finding that is used for the shore-face nourishment discussed in the next chapter.

The sand dredging in the nearshore zone caused severe shoreline erosion at the lee of dredged hole and the vicinity areas. However, in order to make effective sediment management in coastal area, sand is sometimes dredged at the nearshore zone in the deposited areas and then nourished to the eroded areas. Under the global climate change and environmental problems, sediment management in terms of nearshore sand dredging is important for shore protection.

References

1) Price WA, Motyka JM, Jaffrey LJ. The effect of offshore dredging on coastlines. Coastal Engineering. 1978. 1347-1358.

2) Kojima H, Ijima T, Nakamuta T. Impact of offshore dredging on beaches along the Genkai Sea, Japan. Coastal Engineering. 1986. 1281-1295.

3) Marine Habitat Committee. Report of the working group on the effects of extraction of marine sediments on the marine ecosystem. Rep. No. ICES CM 2000/E:07, Gdansk, Poland. 2000.

4) Horikawa K, Sasaki T, Sakuramoto H. Mathematical and laboratory models of shoreline changes due to dredged holes. J. Fac. Eng. Univ., Tokyo. 1977. 34: 49-57.

5) Motyka JM, Willis DH. The effect of refraction over dredged holes. Proc. of 14th Int. Conf. on Coastal Engineering, ASCE. New York. 1974. 615-625.

6) Bender CJ. Wave field modifications and shoreline response due to offshore borrow areas. MS thesis, Univ. of Florida, Gainesville, Fla. 2001.

7) Work PA, Fehrenbacher F, Voulgaris G. Nearshore impacts of dredging for beach nourishment. J. Waterway, Port, Coastal, Ocean, Eng. ASCE. 2004. 130: 303-311.

8) McDougal WG, William AN, Furukawa K. Multiple-pit breakwaters. J. Waterway, Port, Coastal, Ocean, Eng. ASCE. 1996. 122(1): 27-33.

9) Gonzalez M, Medina R, Espejo A, Tintore J, Martin D, Orfila A. Morphodynamic evolution of dredged sandpits. Journal of Coastal Research. 2010. 26(3): 485-502.

10) Dolah RF, Van BJ, Digre, Gayes PT, Donovan-Ealy P, Dowd MW. An evaluation of physical recovery rates in sand borrow sites used for beach nourishment projects in South Carolina. prepared for The South Carolina Task Force on Offshore Resources and the Mineral Management Service, Office of International Activities and Marine Minerals, S.C. 1998.

11) Bruun P. Coast erosion and the development of beach profiles. Beach Erosion Board. 1954.

12) Chu DT, Himori G, Saito Y, Bui TV, Aoki S. Study of beach erosion and evolution of beach profile due to nearshore bar sand dredging. Proc. of 8th International Conference on Asian and Pacific coast. Department of Ocean Engineering, IIT Madras, India. 2015.

13) Sunamura T, Horikawa K. Two dimensional beach transformation due to waves. Coastal Engineering. 1974. 920-938.

14) Chu DT, Himori G, Bui TV, Aoki S. An experimental study of the effect of offshore bar sand dredging on beach erosion. Journal of Japan Society of Civil Engineers, Ser. B2 (Coastal Engineering). 2014. 70 (2): I_531-I_535.

15) Larson M, Kraus NC. Sbeach: Numerical model for simulating storm-induced beach change. Report 1: Empirical foundation and model development. Coastal Engineering Research Center, Waterways Experiment Station, Corps of Engineers. 1989. 129-137.

16) Pugh CA. Sediment transport scaling for physical models. Appendix C. sedimentation engineering: processes, measurements, modeling, and practice. ASCE (New York). 2008. 110.

17) Sawaragi T, Deguchi I. On-offshore sediment transport rate in the surf zone. Proceedings of the 17th Coastal Engineering Conference, American Society of Civil Engineers. 1981. 1194-1214.

18) Bender CJ, Dean RG. Wave field modification by bathymetric anomalies and resulting shoreline changes: a review with recent results. Coastal Engineering. 2003. 125-153.

19) Demir H, Otay EN, Work PA, Borekci OS. Impacts of dredging on shoreline change. J. Waterway, Port, Coastal, Ocean Eng. 2004. 170-178.

20) Dean RG. Beach nourishment: theory and practice (advanced series on ocean engineering). World Scientific Pub Co Inc. 2003. 18: 37-77.

Chapter 3 Shore-face Nourishment

3.1 Introduction

The coastal zone often subjected to natural hazard phenomena such as storm, tsunami, flooding, landslide/cliff collapse, beach erosion. There is a little room for doubt that the climate change causes sea level rise and the frequency of tremendous storm surges. During the storm surge significant volume of sediment in the foreshore is flushed offshore and the sand bar has been formed, i.e. storm attack causes beach erosion and after the storm surge the shoreline moves landward. In the post-storm period, the shoreline will be recovered because the sediment is transported onshore in calm or accretive wave conditions (Fig. 3.1). However in some area, the shoreline recovers very slowly for some of reasons such as sea level rise, intensity of storm increase, multiple erosion events that could exist within the recovery period, reduction of supplied sediment to the littoral coast in some areas[1) 2) 3)]. Corbella and Stretch[2)] studied the post-storm shoreline recovery in east coast of Southern Africa and showed that some locations had been recovered very quickly within the first 2 years, but in other locations it took 4-5 years to recover. Morton et al.[4)] studied the post-storm beach response and classified it into four categories as: (1) erosion and continuous loss of beach volume, (2) partial recovery and subsequent erosion, (3) complete recovery and (4) continuous gains in beach volume that greatly exceeds the volume eroded by the storm.

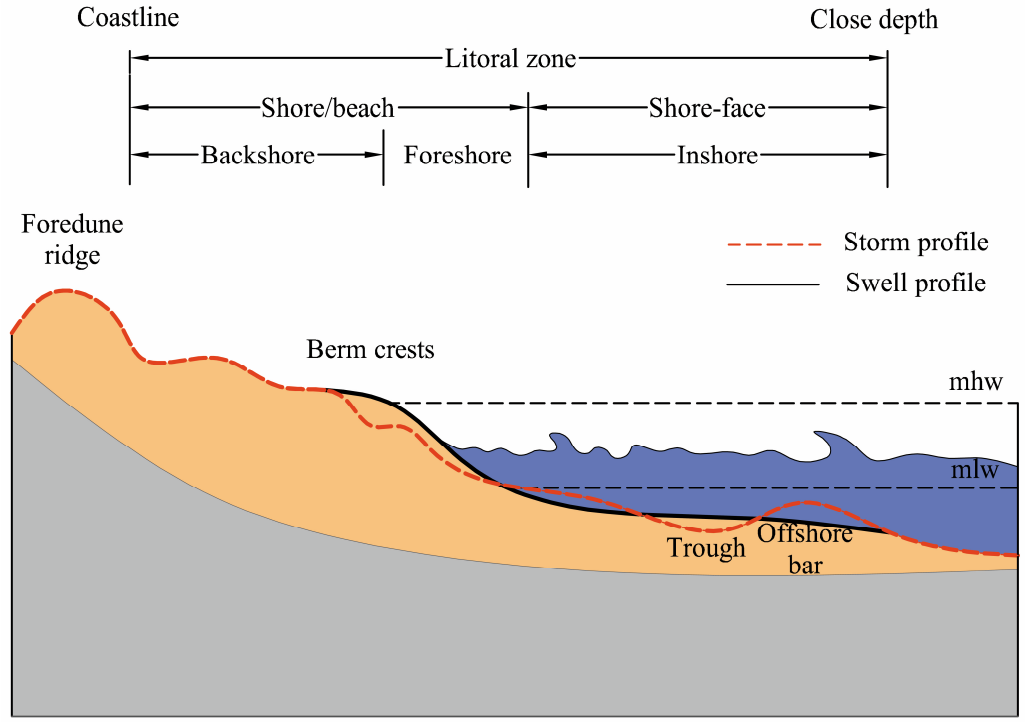

Fig. 3.1 Accretive and erosive profile in littoral zone (mhw: mean high water level; mlw: mean low water level).

Duin et al.[5] studied the shoreline protection in Egmond, Netherland by the shore-face nourishment. The sediment was taken from other littoral cells and nourished at the offshore side of the outer bar. The shore-face nourishment functions as a reef that partially blocks the wave-driven longshore current, and shoaling waves that generates onshore transport. A large volume of sediment is needed for this project. In addition, the location of shore-face nourishment area is far from the shoreline. The time period at which the sediment feeds the beach zone is in the order of 5-10 years. Therefore, the shore-face nourishment had a minimal direct effect on the beach.

In this study, the artificial acceleration of onshore sediment transport rate was taken into account by dredging sand at the offshore sand bar and nourished at the shore-face, i.e. shore-face nourishment method to make quick recover of beach after storm. One of the advantage of this method is the nourished sediment is dredged in the littoral cell and filled on the same littoral cell. A large volume of nourished can be saved for shore protection.

To investigate the effectiveness and feasibility of the shore-face nourishment, the physical experiments were conducted in 2D wave flume under regular and irregular waves. Two parameters, shoreline recovery ratio and berm volume, are calculated for evaluation. The results showed that the shoreline was quickly recovered in the case of shore-face nourishment, whereas those of without nourishment was recovered very slowly. In addition, some factors that affect the acceleration of onshore sediment transport rate after shore-face nourishment such as accretive wave conditions, position of nourished area, nourished volumes, water levels, nourished methods are also discussed.

3.2 Shore-face Nourishment in Regular Waves

3.2.1 Effectiveness of Shore-face Nourishment on Beach Recovery

To validate the effectiveness of shore-face nourishment, twenty-two cases of physical experiments were conducted in 2D wave flume as described in detail in Chapter Two (Fig. 3.2). The conditions of the experiments are shown in Table 3.1. The median grain size of the sediment is 0.2 mm and the initial slope of the beach is 1:10 for all the cases. The regular waves were generated by a piston type wave generator. By generating the same erosive wave condition with incident wave height H = 0.14 m and wave period T = 1 s[6] for 60 minutes from the initial beach slope in every case, eroded profile was formed with the bar at the breaker zone. Some amount of sand was dredged one-time at the sand bar and then filled on the different positions of shore-face of beach profile. After moving the sand, the erosive wave was shifted to the accretive wave condition H = 0.08 m and T = 1.5 s[6] and generated for 120 more minutes in all the cases except for cases E03S and E04S. In these cases, the sand was dredged two-time with the same amount of volume at each time. In the first dredge time, sand was filled on the shore-face, and then the accretive wave was generated for 30 minutes. Thereafter, the same volume of sand was dredged and filled one more time and then accretive waves were generated for the last 90 minutes. In some cases, the conditions of accretive wave, position of shore-face area, dredged

and nourished volume, method of nourishment and water levels were also changed after shore-face nourishment. During the 120 minutes of accretive wave generation, accreted profile was formed with the berm at the shore area.

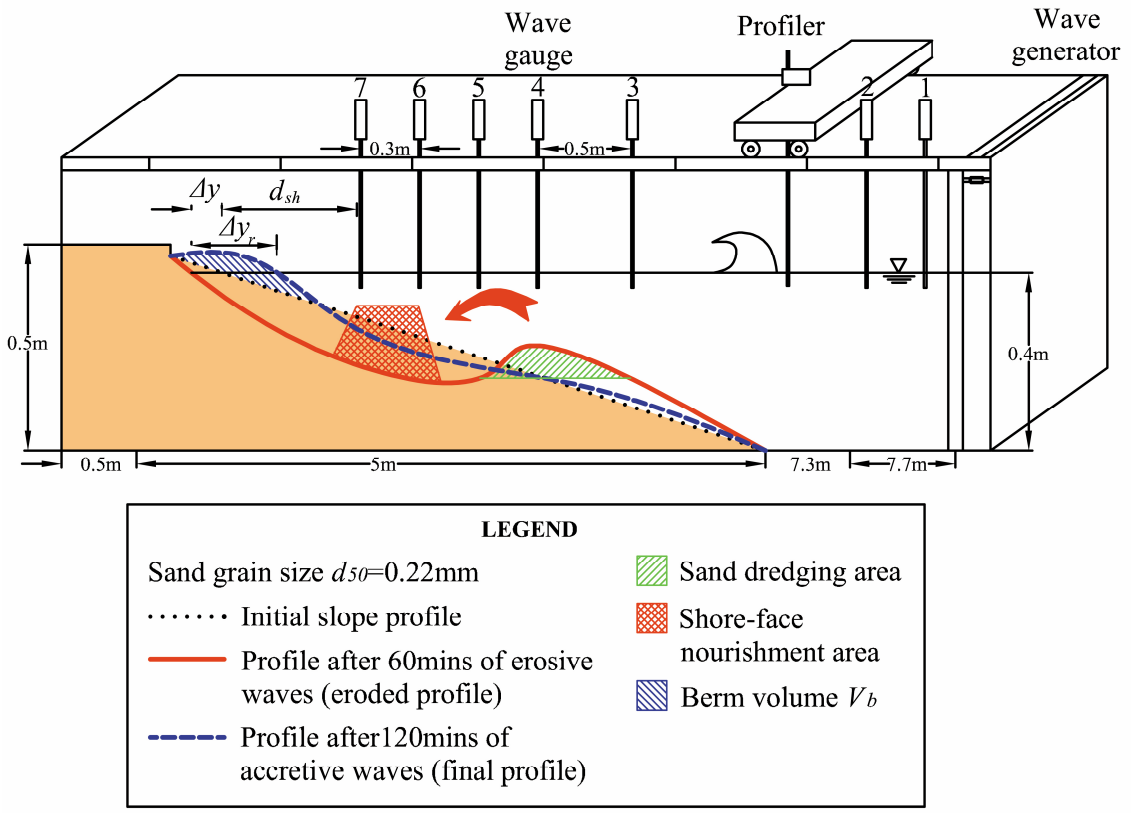

Fig. 3.2 Physical modelling of shore-face nourishment in 2D wave flume.

The beach profile was measured at 2-cm intervals by an optical bottom profiler placed on a trolley car. Beach profile measurement was carried out at the initial beach slope, 60 minutes after erosive wave generation, after sand dredging and shore-face nourishment, 30, 60, 120 minutes after accretive wave generation consecutively. The wave height was measured along the 2D wave flume by the seven wave gauges during the wave generation.

In order to evaluate the effectiveness of the shore-face nourishment on beach recovery, two parameters i.e. shoreline recovery rate and berm volume were taken into account. The shoreline recovery rate is defined as ratio of distance Δy_r between the final recovered shoreline and the eroded shoreline to distance Δy between the eroded shoreline and the initial shoreline. The berm volume V_b is defined as the difference between net onshore volume at the shore of the accreted profiles and initial profile. Sediment transport rate is calculated from the mass conservation equation showed in Equation 3.1. The change of sediment transport rate based on the alteration of depth between two profiles. The profile after shore-face nourishment is defined as the base profile for calculation of the sediment

transport rate at a given time. The sediment transport rate was calculated at 30, 60, 120 minutes after the shore-face nourishment.

$$q(y) = \int \frac{\Delta h}{\Delta t} dy \tag{3.1}$$

in which *q(y)* is the sediment transport rate at position *y* (m^3/m/h); *y* is the cross-shore coordinate (m) (positive directed seaward), Δh is change of water depth between two beach profile (m), Δt is time period after shore-face nourishment (hour).

Three pairs of experiments E01S and E07S, E13S and E28S, E15S and E16S were conducted in order to assess the applicability of the shore-face nourishment to the acceleration of the post-storm recovery rate of beach. Each pair cases of the experiments were conducted with/without (W/WO) shore-face nourishment, respectively. The same erosive/accretive wave conditions were generated for each pair cases of experiment. However, three pair cases are different in accretive wave condition. In the left hand side of Fig. 3.3, the profiles of the cases without shore-face nourishment were shown and the profiles of the cases with shore-face nourishment were shown in the right hand side. In comparison of each pair of experiments, after 120 minutes of accretive wave generation, in the cases without shore-face nourishment, although a small volume of sediment of bar transports onshore, significant amount of volume still remained at the bar, particularly in the case E01S. On the other hand, in the cases with shore-face nourishment, most of nourished sediment was transported onshore.

Table 3.1. Cases of physical modelling of shore-face nourishment in regular waves.

Case No.	Erosive wave (regular wave)		Post-storm accretive wave (regular wave)		Nourished area (m)	Dredged area (m)	Sand dredging volume (m^3/m)	Shore-face nourishment	eroded/ accreted water level (m)
	Wave height H_e (m)	Wave period T_e (s)	Wave height H_a (m)	Wave period T_a (s)					
E01S	0.14	1.0	0.040	1.5	-	-	0.0	None	0.4/0.4
E02S			0.080	1.5	1.6-2.0	2.2-2.75	0.014	Nourishment	0.4/0.38
E03S			0.080	1.5	1.6-2.0	2.4-3.1	0.015+0.015	Nourishment	0.4/0.4
E05S			0.080	1.5	1.6-2.0	2.2-2.75	0.014	Nourishment	0.4/0.37
E07S			0.040	1.5	1.6-2.0	2.2-2.85	0.02	Nourishment	0.4/0.4
E08S			0.040	2.0	1.6-2.0	2.2-2.85	0.02	Nourishment	0.4/0.4
E09S			0.060	1.5	1.6-2.0	2.2-2.85	0.02	Nourishment	0.4/0.4
E10S			0.080	1.5	1.6-2.0	2.7-3.05	0.008	Nourishment	0.4/0.4
E11S			0.080	1.5	1.6-2.0	2.2-2.75	0.014	Nourishment	0.4/0.4
E12S			0.080	1.5	1.6-2.0	2.4-3.1	0.03	Nourishment	0.4/0.4
E13S			0.080	1.5	-	-	0.00	None	0.4/0.4
E15S			0.100	1.5	-	-	0.00	None	0.4/0.4
E16S			0.100	1.5	1.6-2.0	2.2-2.85	0.02	Nourishment	0.4/0.4
E17S			0.085	1.0	1.6-2.0	2.2-2.85	0.02	Nourishment	0.4/0.4
E18S			0.060	1.0	1.6-2.0	2.2-2.85	0.02	Nourishment	0.4/0.4
E19S			0.095	2.0	1.6-2.0	2.2-2.85	0.02	Nourishment	0.4/0.4
E25S			0.080	1.5	1.3-1.7	2.2-2.85	0.02	Nourishment	0.4/0.4
E26S			0.080	1.5	1.4-1.8	2.2-2.85	0.02	Nourishment	0.4/0.4
E27S			0.080	1.5	1.5-1.9	2.2-2.85	0.02	Nourishment	0.4/0.4
E28S			0.080	1.5	1.6-2.0	2.2-2.85	0.02	Nourishment	0.4/0.4
E29S			0.080	1.5	1.7-2.1	2.2-2.85	0.02	Nourishment	0.4/0.4

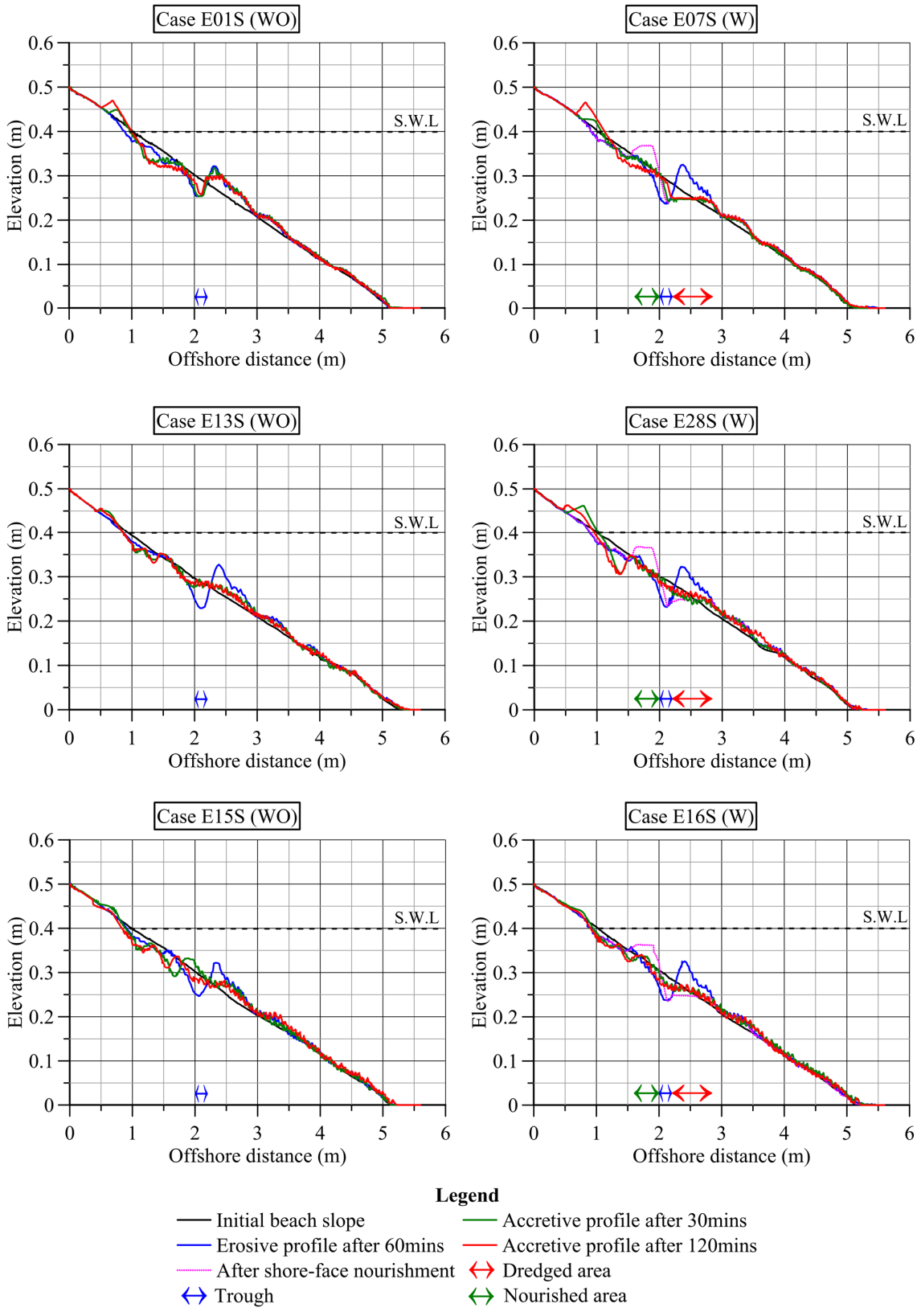

Fig. 3.3 Beach profiles of cases with/without (W/WO) shore-face nourishment.

The post-storm shoreline recovery and berm volume of three pair cases of experiments were shown in Fig. 3.4 and Fig. 3.5, respectively. The differences of accretive wave conditions of these pairs gave the different results of the shoreline recovery and the berm volume. These differences will be discussed in section 3.2.2.2 of this chapter. In this section, the differences of shoreline recovery and berm volume of each pair with and without shore-face nourishment were discussed. Some of discussion points were elaborated as follows.

First, it is clear that post-storm shoreline recovery and berm volume of the cases with shore-face nourishment is higher than those of the cases without shore-face nourishment under the same accretive wave condition. In the cases without shore-face nourishment E15S & E13S, the sediment of the bar was transported onshore and deposited at trough of the profile in the first 30 minutes of accretive wave generation (Fig. 3.6a, b). In the case E01S, a small volume of sediment at the bar was transported to the trough (Fig. 3.6c). In these cases, the volume of sediment that was deposited on the backshore during 30 minutes after accretive wave generation was transported from the foreshore. The sediment that was trapped at the trough cannot be transported much onshore thus, the sediment transport rate significantly decreases in the last 90 minutes (Fig. 3.7 and Fig. 3.8). On the other hand, in the cases with shore-face nourishment, a volume of sediment was dredged at the bar and nourished on the shore-face, over the trough. Most of the volume of nourished sediment was transported onshore and deposited on the backshore during 120 minutes of accretive wave generation. Therefore, the increment of shoreline recovery and berm volume may result. It is reasonable to say that the shore-face nourishment can be considered as effective method for accelerating the rate of shoreline recovery after storm.

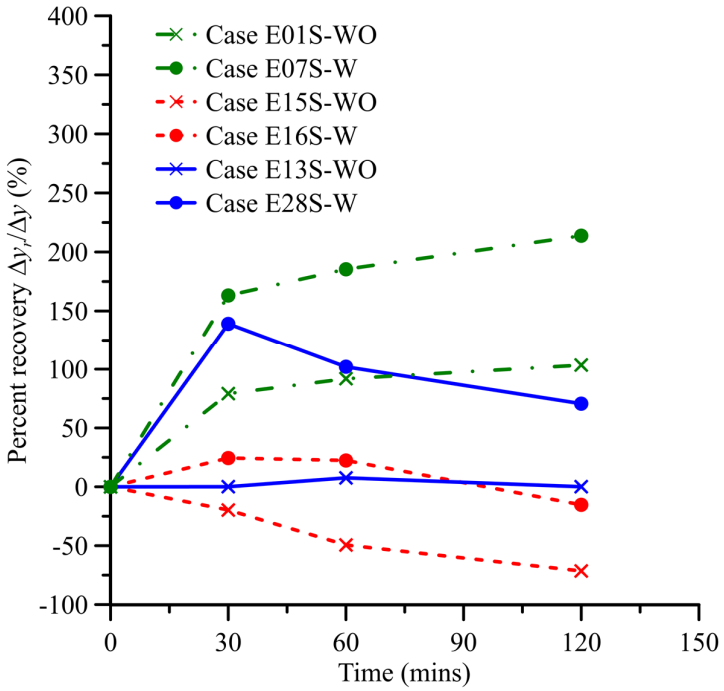

Fig. 3.4 Post-storm shoreline recovery of cases with/without (W/WO) shore-face nourishment.

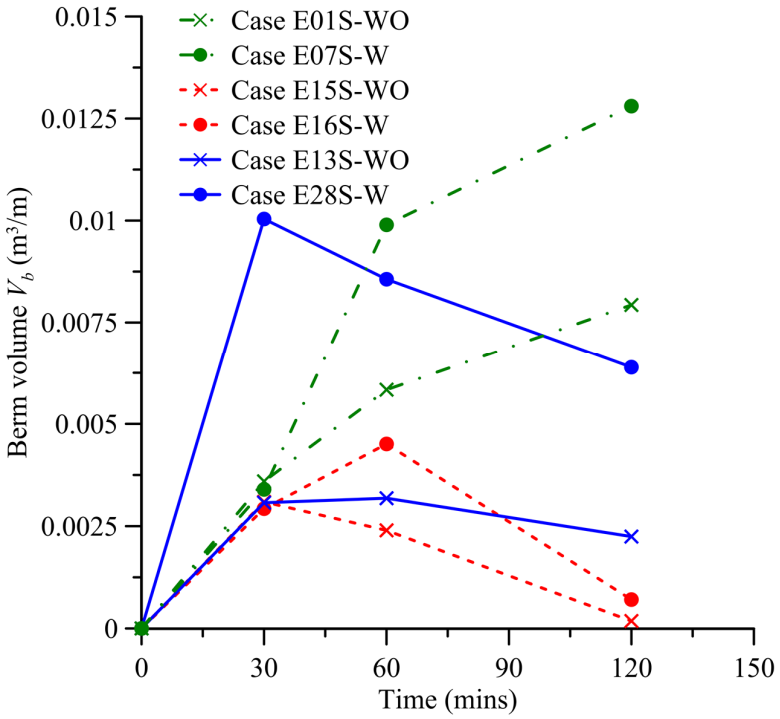

Fig. 3.5 Post-storm berm volume of cases with/without (W/WO) shore-face nourishment.

Second, in the cases without shore-face nourishment, the post-storm shoreline recovery rate and berm volume rapidly increases in the first 30 minutes of accretive wave generation and then stabilize or slightly decreases, except for case E01S (Fig. 3.4 and Fig. 3.5). The sediment transport rate of these cases was comparatively high just a short period after storm and then quick decreased (Fig. 3.6, Fig. 3.7 and Fig. 3.8). Morton et al.[4)] studied the recovery of post-storm shoreline in southeastern Texas, the United State of America and showed that 40% eroded shoreline was recovered in the first year post storm and the rate of recovery quickly decreases in the next years. This is similarity with the results of most of the cases of physical experiments with/without shore-face nourishment.

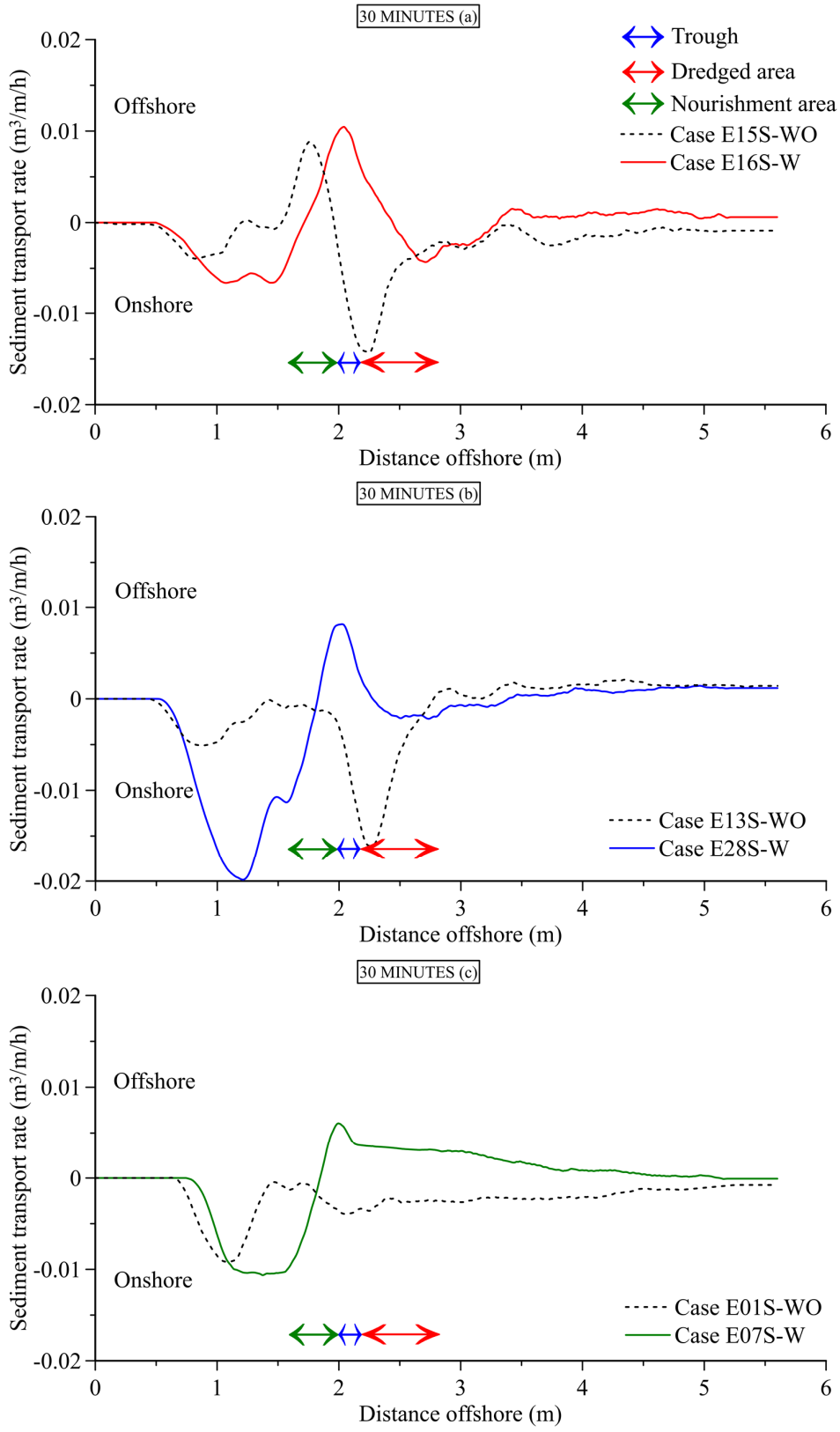

Fig. 3.6 Cross-shore sediment transport rate of the cases with/without (W/WO) shore-face nourishment in 30mins.

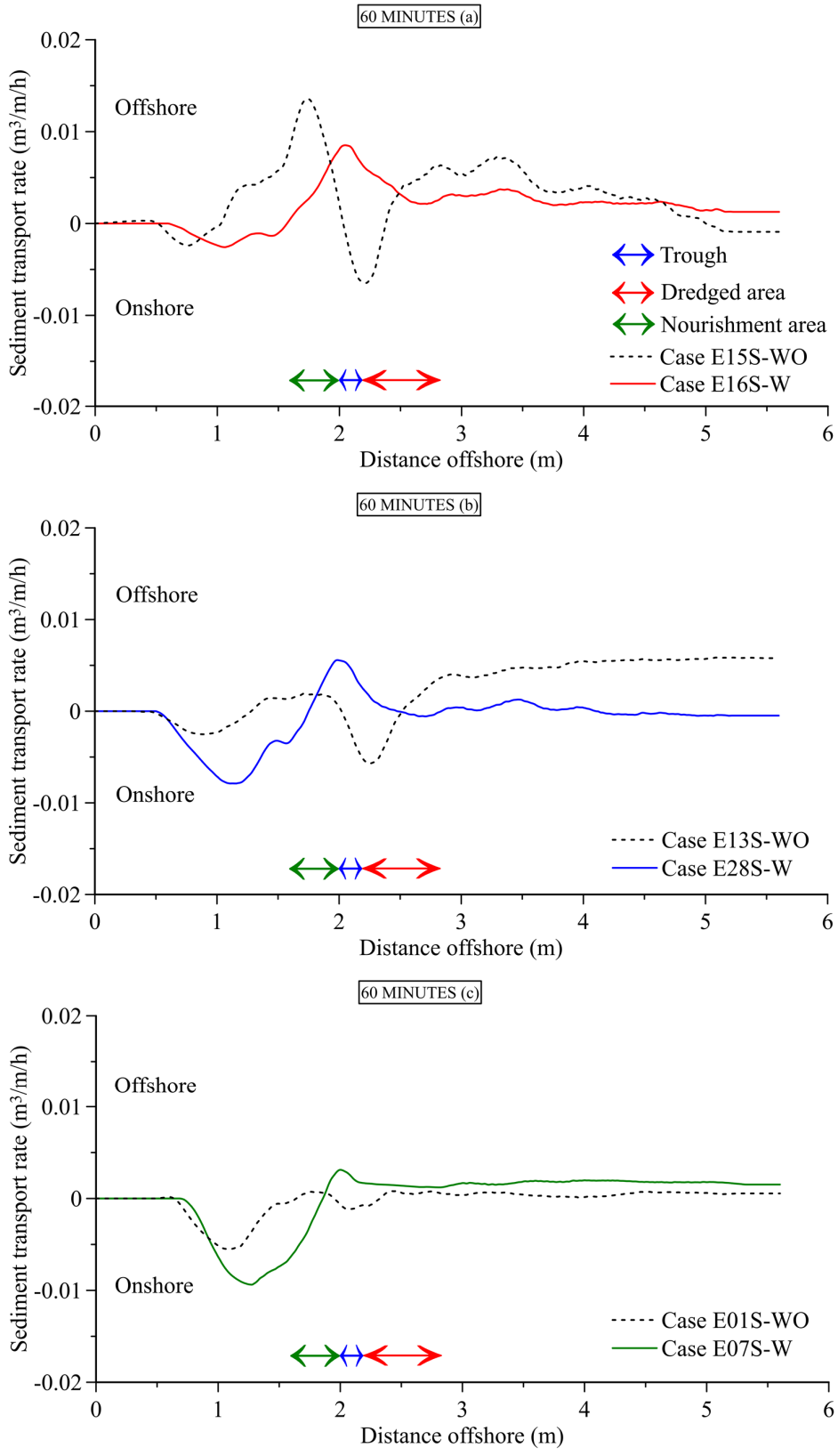

Fig. 3.7 Cross-shore sediment transport rate of the cases with/without (W/WO) shore-face nourishment in 60mins.

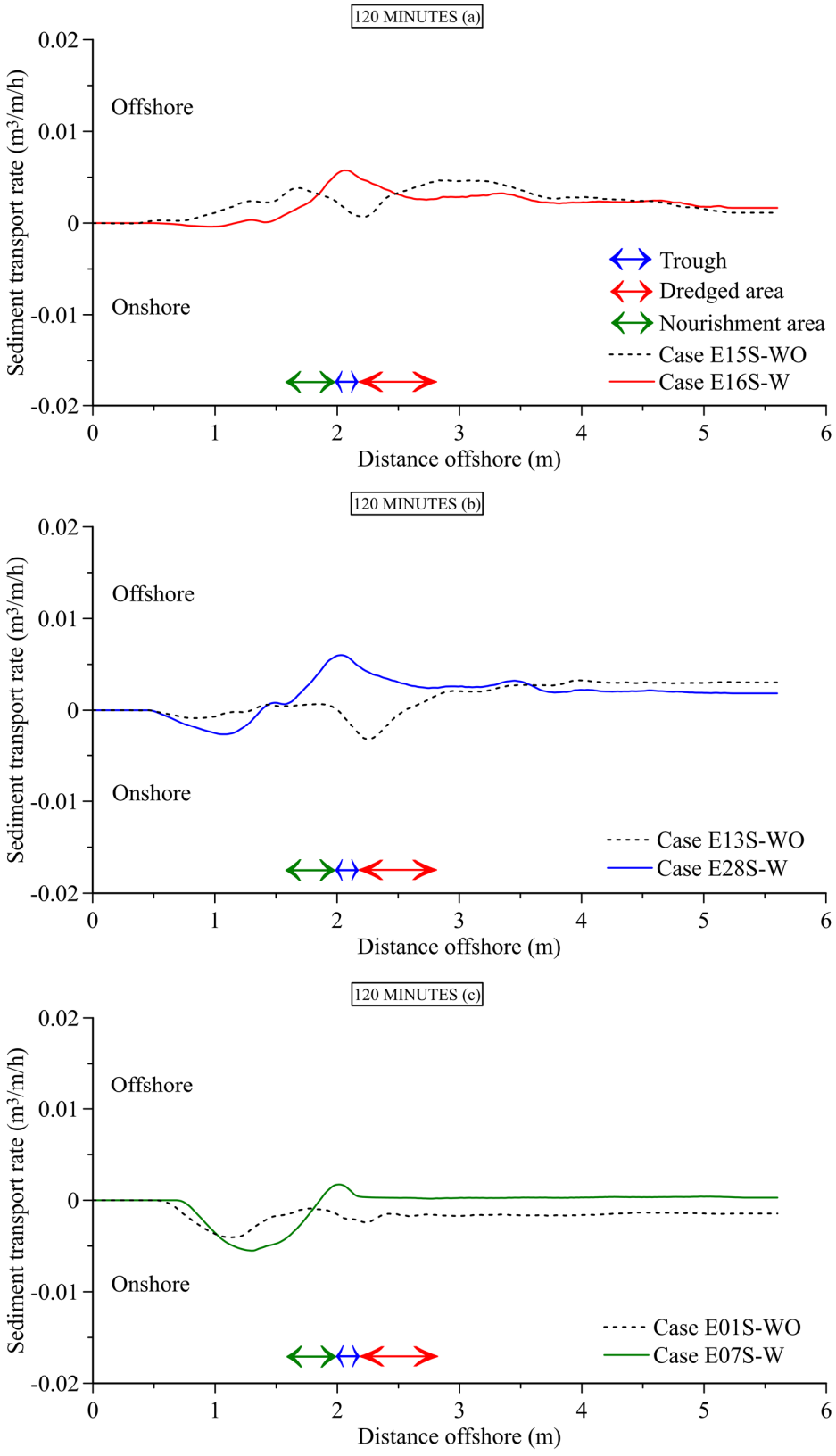

Fig. 3.8 Cross-shore sediment transport rate of the cases with/without (W/WO) shore-face nourishment in 120mins.

3.2.2 Beach Recovery Rate under Different Shore-face Nourishment Conditions

In this section, several important conditions that can affect the acceleration of shoreline recovery rate were taken into account such as shore-face nourishment position, post-storm accretive wave condition, nourishment volume of sediment, post-storm water level and nourishment method. The effects of these conditions were investigated by the physical experiments. The similar storm wave conditions i.e. wave height H = 14 cm; wave period T = 1 s were used for generating the erosive profile. Thereafter, these conditions were changed before generating the accretive waves. The results and discussions were shown in the following.

3.2.2.1 Shore-face Nourishment Position

To evaluate the effects of shore-face nourishment positions on the rate of post-storm beach recovery five cases of experiment E25S, E26S, E27S, E28S and E29S were conducted. The experimental conditions were shown in Table 3.1. First, the constant volume of sediment was dredged at the sand bar and nourished at several locations on the shore-face of the beach with different distance d_{sh} from the initial shoreline. The distances d_{sh} for five cases of experiment E25S, E26S, E27S, E28S and E29S were 1.3, 1.4, 1.5, 1.6 and 1.7 m, respectively. The most effective position was the case that gives the results of the highest shoreline recovery rate and the largest berm volume. The beach profiles and wave height distribution just after nourishment and final accreted beach profiles of the five cases were shown in Fig. 3.9. Just after the shore-face nourishment, the wave breaking points of all cases located on the nourished area (Fig. 3.9a). After 120 minutes of accretive wave generation, beach profiles of all cases were nearly similar and wave breaking points in all the cases located at the similar position (Fig. 3.9b).

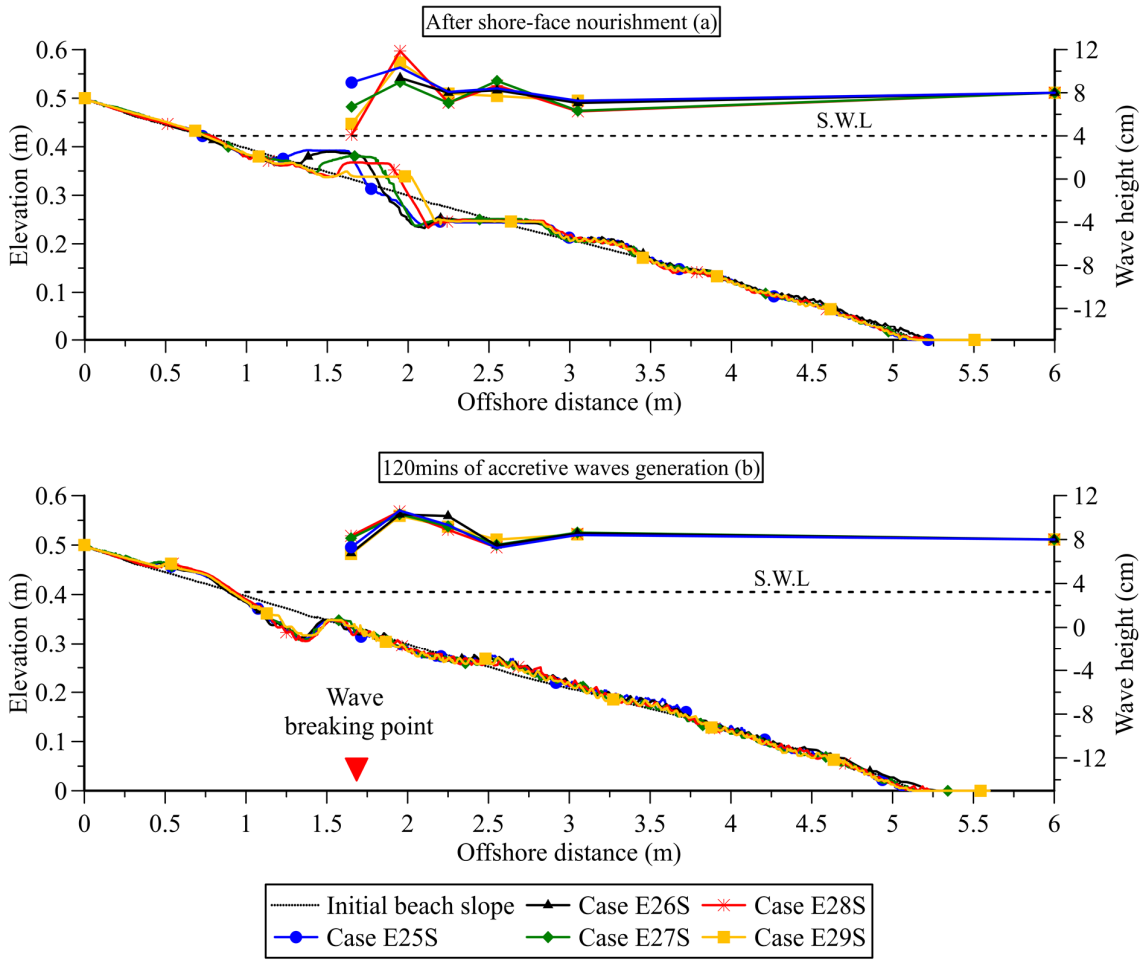

Fig. 3.9 Cross-shore profiles and wave height distribution of shore-face nourishment cases in different nourished positions d_{sh}.

The difference of shore-face nourishment positions gives the different results of on/offshore sediment transport rate along the profile (Fig. 3.10). Surprisingly, Fig. 3.10a shows that the cases E25S and E29S in which the nourished positions were the closest and furthest from the shoreline, respectively, the sediment transport rates along the profile, however, were smaller than those in the other cases. Onshore sediment transport rates of cases E26S, E27S and E28S were comparatively high, particularly at the backshore area. Therefore, the berm volume and the shoreline recovery rate of these cases were higher than those of the cases E25S and E29S after 120 minutes of accretive wave generation (Fig. 3.11 and Fig. 3.12).

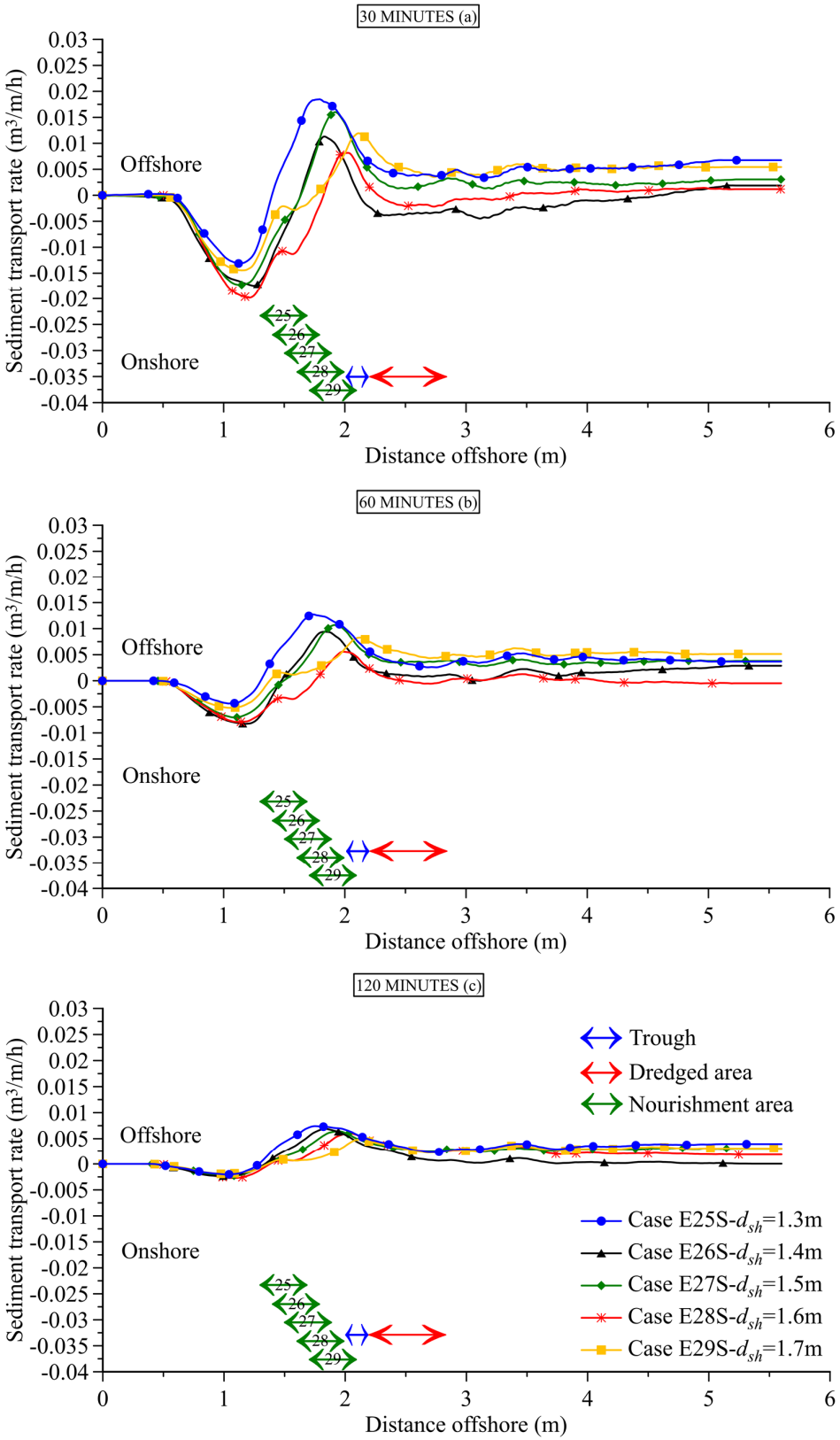

Fig. 3.10 Cross-shore sediment transport rate of shore-face nourishment cases in different positions of shore-face nourishment d_{sh}.

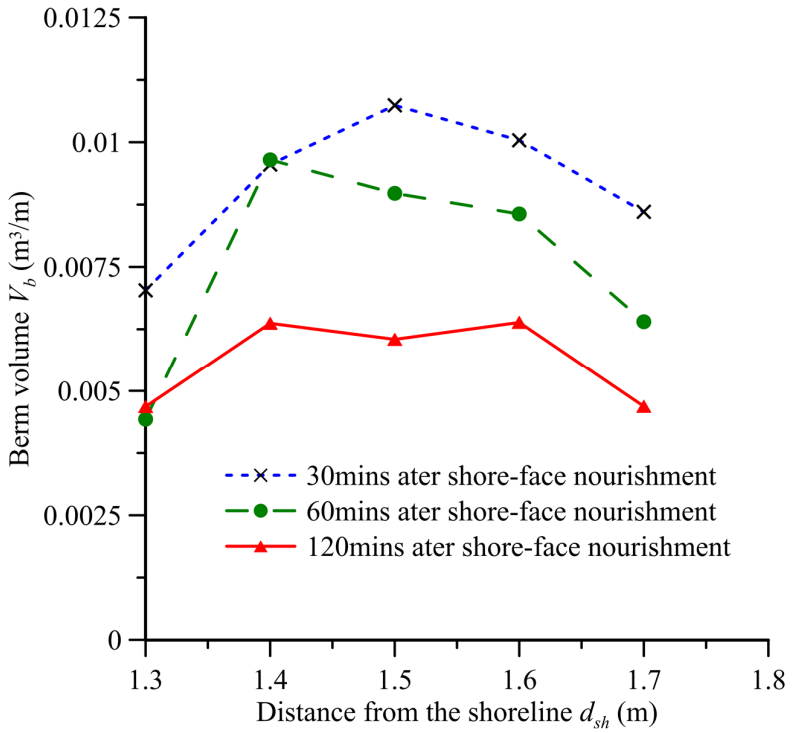

Fig. 3.11 Post-storm berm volume of shore-face nourishment cases in different shore-face nourishment positions d_{sh}.

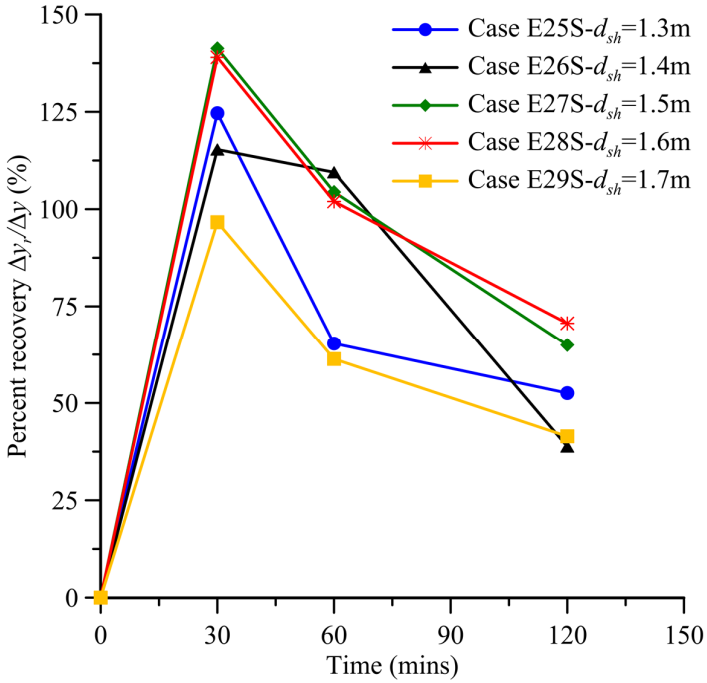

Fig. 3.12 Post-storm shoreline recovery of shore-face nourishment cases in different shore-face nourishment positions d_{sh}.

Figure 3.13 showed the change of topography after shore-face nourishment around the nourished area during the first 30 minutes of accretive wave generation, where the profiles were detected from the photographs. The nourished sediment of the cases E25S and E26S transported onshore rapidly after accretive wave generation caused quick advance of the shoreline. As a result, a scouring hole behind the breaking point was formed earlier than the other cases. Once the scouring hole was formed, whereas the suspended load behind the wave breaking point tends to move offshore, the bed load and sheet flow move onshore (Fig. 3.14). Small bar was formed as most of the sediment volume of this bar was transported from the foreshore because of the significant suspended load. Thus, once the scouring hole has been formed, the sediment was transported offshore. In the first 5 minutes of accretive wave generation, the topography at the nourished area of the case E29S was changed very slowly. The top of nourished area was deep below the water surface; thus the wave was not broken on the nourished area but on its behind. The scouring hole was also formed rapidly within next 5 minutes. At the beginning of accretive wave generation, the sediment at the foreshore area of the cases E27S and E28S transports further offshore and deposited in front of the nourished area. This volume of sediment and nourished sediment slower the formation of scouring hole. The slower formation of scouring hole, the sediment sheet flow and bed load were dominant. Thus the more sediment was transported onshore (Fig. 3.10a). The high rate of shoreline recovery and the large berm volume of these cases may result.

The wave breaking position and water depth of nourished area were important factors in the determination of the most effective positions for shore-face nourishment. In the cases E25S and E26S, the nourished areas were located at the wave breaking position (Fig. 3.9). In the case E29S, as the depth of nourished area was too deep, the accretive wave did not activate much on the nourished sediment once the scouring hole has not been formed. Therefore, the proper positions of nourished area are located offshore side of wave breaking point as it is shallow enough for activation by the accretive wave on the nourished sediment.

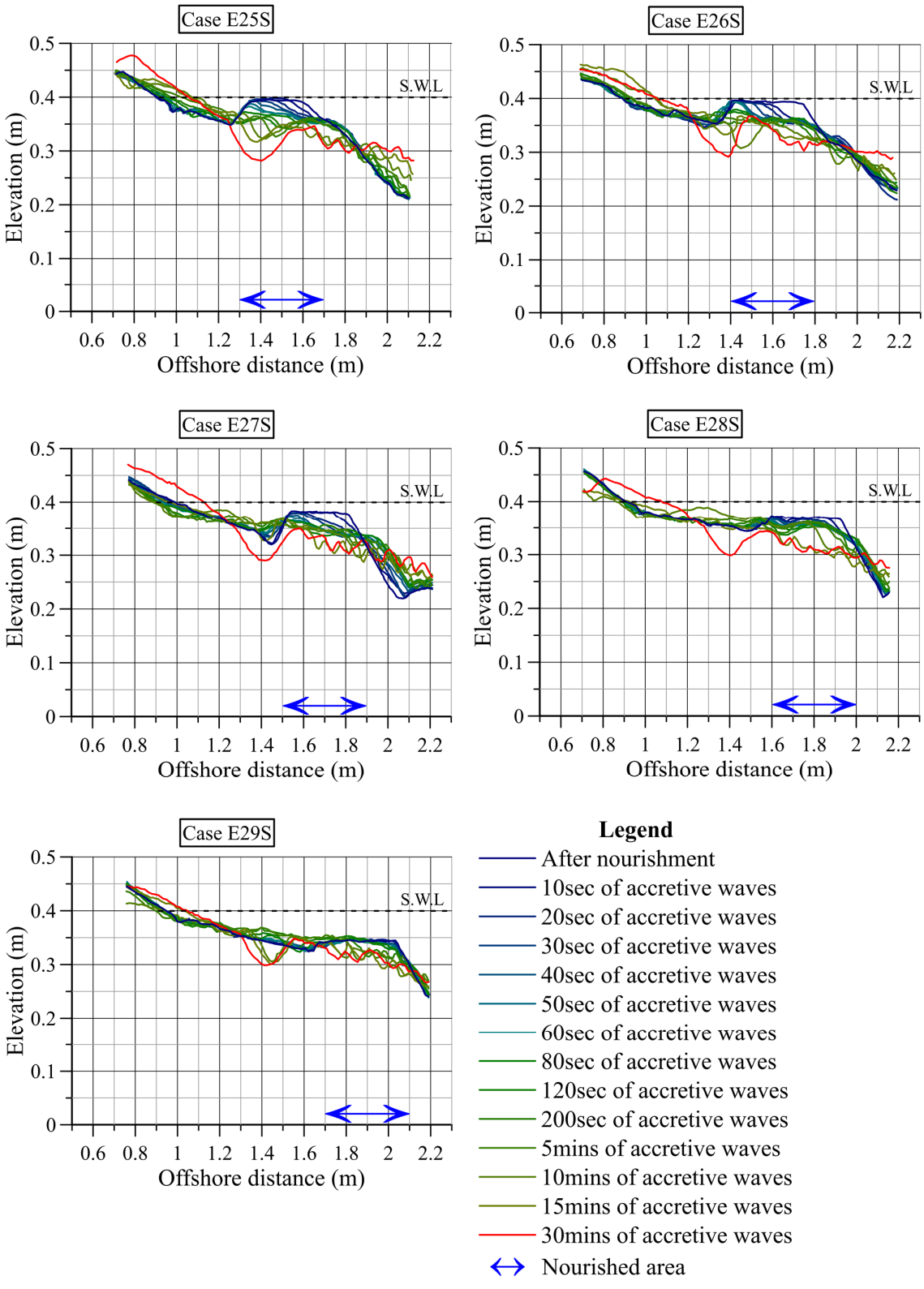

Fig. 3.13 Change of topography at the nourishment area in the first 30 minutes after shore-face nourishment in different shore-face nourishment positions d_{sh}.

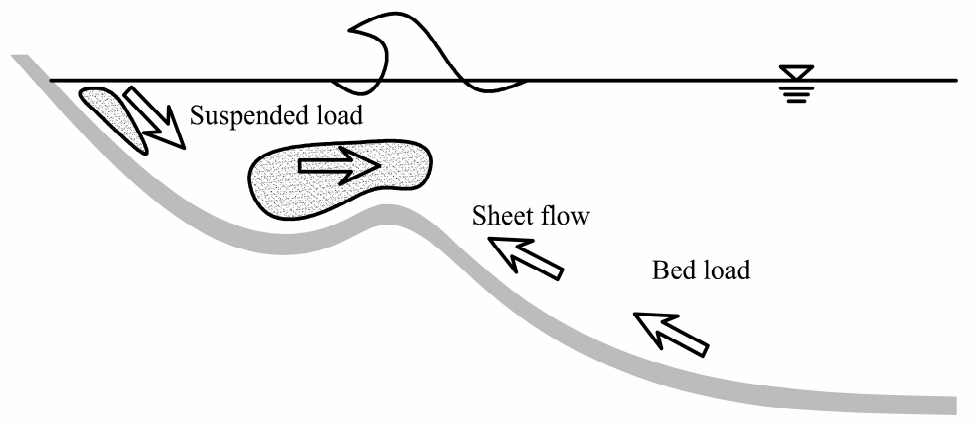

Fig. 3.14 Net sediment transport in cross-shore section[7)].

The post-storm berm volumes at 120 minutes of accretive wave generation of cases E26S, E27S and E28S are more or less similar (Fig. 3.11). The post-storm shoreline recovery rate of case E27S and E28S was almost the same and higher than those of case E26S during the accretive wave generation (Fig. 3.12). Thus the most effective positions of shore-face nourishment area in the experimental conditions were the distance d_{sh}=1.5-1.6 m. The distance d_{sh}=1.6 m of case E28S was selected for the other experimental cases.

3.2.2.2 Post-storm Accretive Wave Condition

In accretive wave condition, the nourished sediment was transported onshore. Thus the most important factor that directly affects the effectiveness of shore-face nourishment on the post-storm beach recovery was accretive wave condition acting after storm. The effects of accretive wave condition on the shoreline recovery were evaluated by conducting five cases of experiments E08S, E07S, E09S, E28S and E16S. The conditions of experiment were shown in Table 3.1. The steepness of accretive wave H_a/L_a was increased from 0.0064-0.0285. Fig. 3.15 and Fig. 3.16 showed that during the first 30 minutes of accretive wave generation in the cases of high steepness of the accretive wave, E28S and E09S, a part of volume of nourished sediment was transported to the foreshore area and the other part was transported back offshore and deposited at dredged area. On the other hand, in the cases of low steepness accretive wave, E08S, E07S and E09S, most volume of nourished sediment was transported to the foreshore area. Whereas, in the first 30 minutes of accretive wave generation of the case E28S a significant volume of nourished sediment transported to this foreshore area, however, during the last 90 minutes, a part of the volume transported offshore. In the cases of low steepness accretive wave, the sediment was continuously transported onshore.

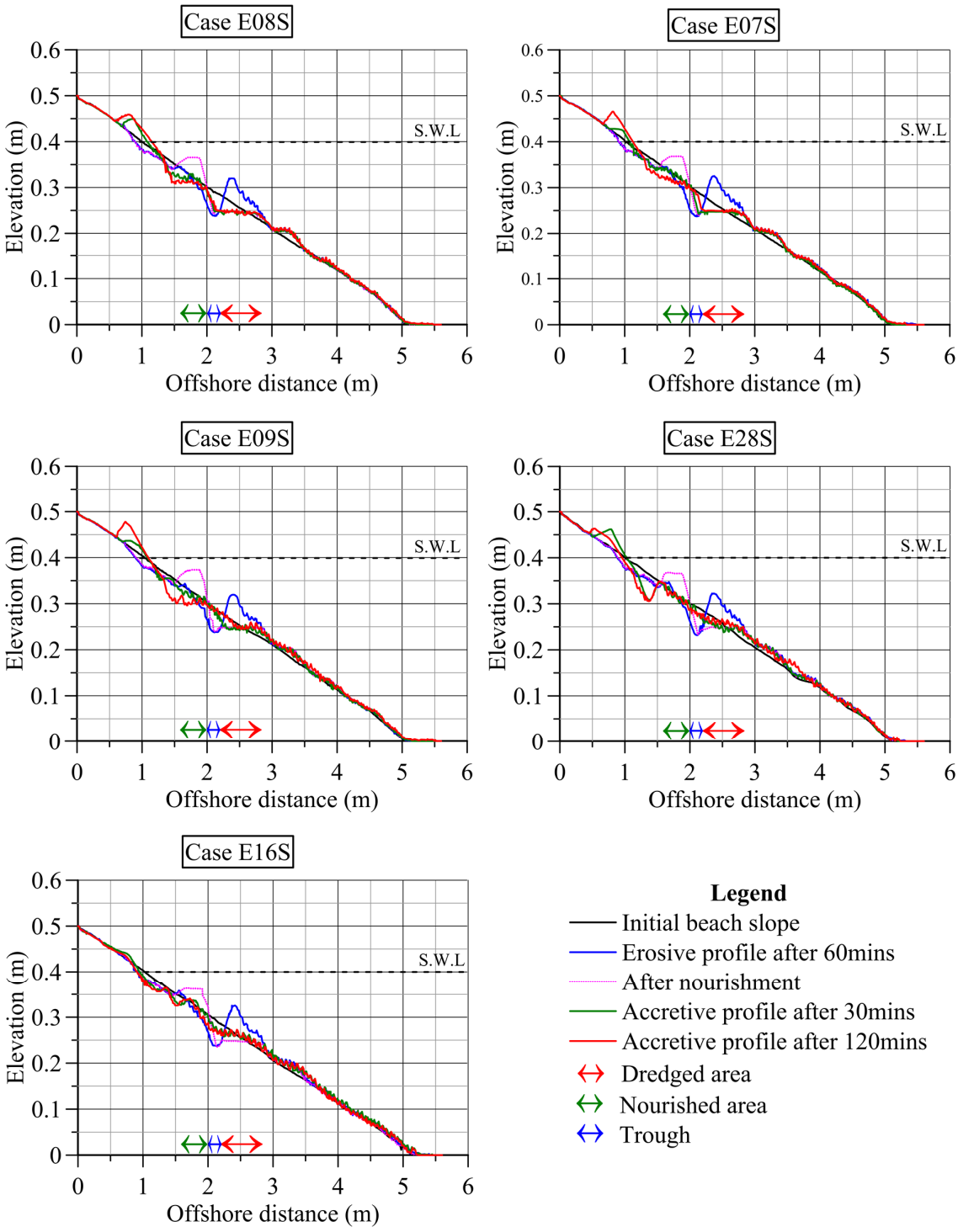

Fig. 3.15 Beach profiles of shore-face nourishment cases in different accretive wave conditions.

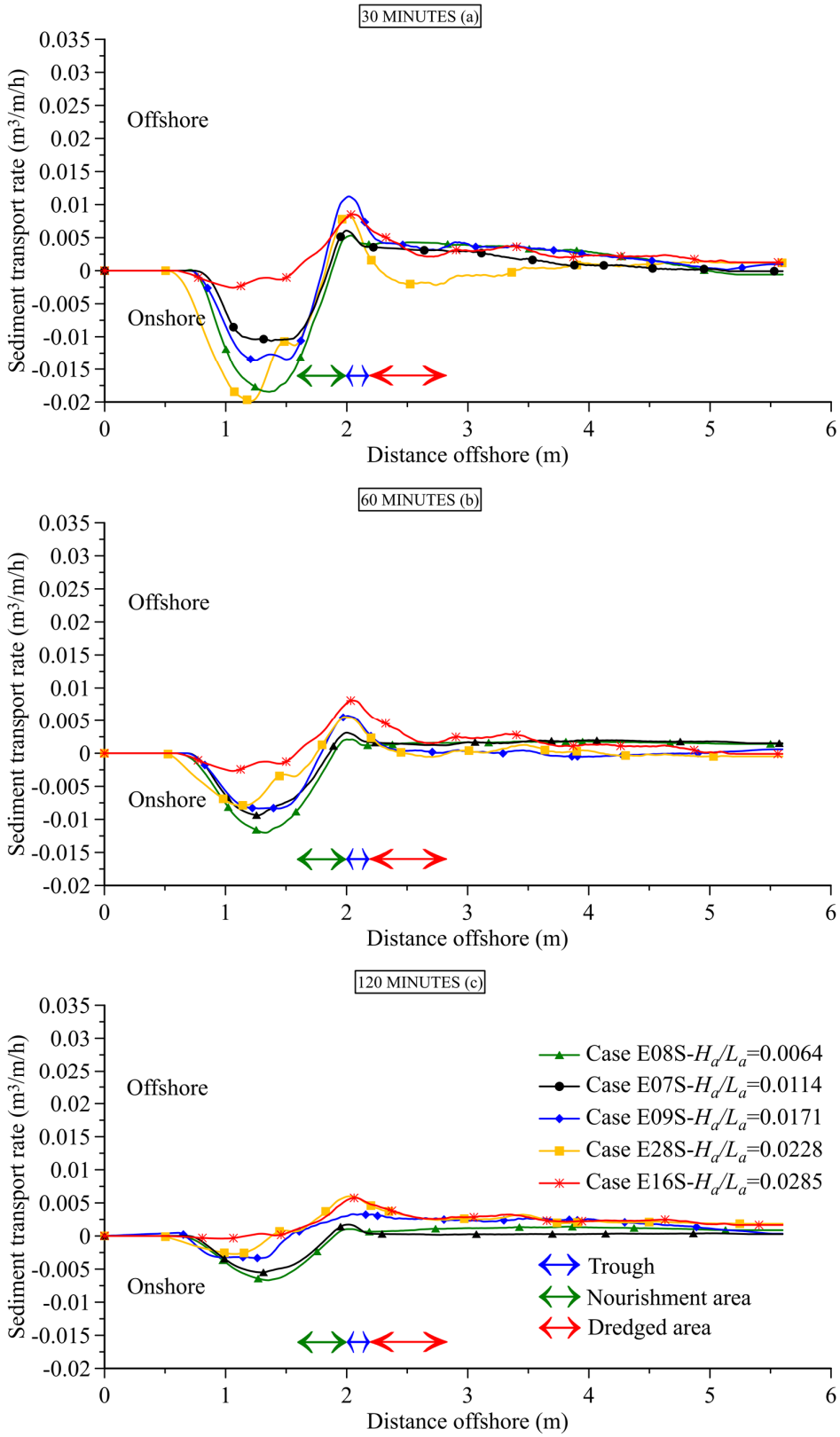

Fig. 3.16 Cross-shore sediment transport rate of shore-face nourishment cases in different accretive wave conditions.

The results of post-storm shoreline recovery show that the higher steepness of accretive wave caused low shoreline recovery rate (Fig. 3.17). In the cases with low accretive wave steepness, the shoreline quickly recovered within the first 30 minutes of accretive wave generation and then nearly stabilized during the last 90 minutes. After the first 30 minutes of high rate recovery in the case E28S, the shoreline recovery rate slightly decreased. In comparison with the previous cases, with the highest steepness of accretive wave, the shoreline of the case E16S slightly recovered in the first 60 minutes and then quickly retreated. In addition, after 120 minutes of accretive wave generation, the shoreline of this case was rather retreated than that of before shore-face nourishment.

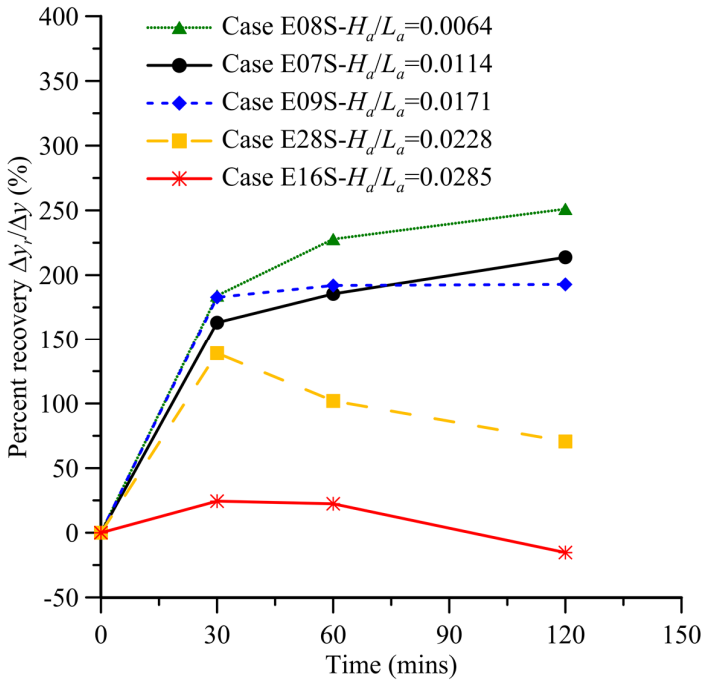

Fig. 3.17 Shoreline recovery of shore-face nourishment cases in different accretive wave conditions.

In another aspect of consideration, the berm volume that gains after shore-face nourishment also evaluates an impact. Logically, the shoreline recovery is surely related to the berm volume. Therefore, after 120 minutes of accretive wave generation of all cases, the berm volume decreased as the steepness of accretive wave increased (Fig. 3.18). In the case E28S, the berm volume increased very quick at the first 30 minutes of accretive wave generation. However, it decreased rapidly in the next 90 minutes. The accretive wave condition of the case E28S can be considered as a critical accretive wave condition for shore-face nourishment. It can be said that the lower steepness of accretive wave yields the higher beach recovery rate.

As accretive wave condition directly relates to the applicability of shore-face nourishment method, it could be identified as the most important factor among others. In this section, the classification of applicable and inapplicable accretive wave conditions in the shore-face nourishment

was also discussed. The final percentage of shoreline recovery rate of experimental results were classified into three categories i.e. the shoreline recovery percentage less than 0%, from 0-100%, and more than 100%. The relationship between the percentage of shoreline recovery and the accretive wave steepness as well as the grainsize of sediment i.e. settling velocity (w) of sediment were plotted on Fig. 3.19.

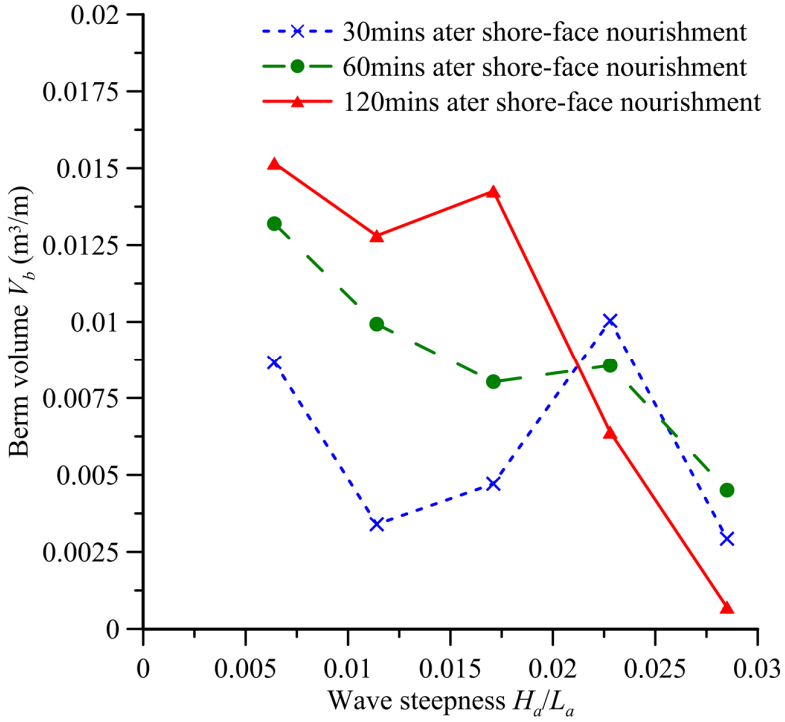

Fig. 3.18 Post-storm berm volume of shore-face nourishment cases in different accretive wave conditions.

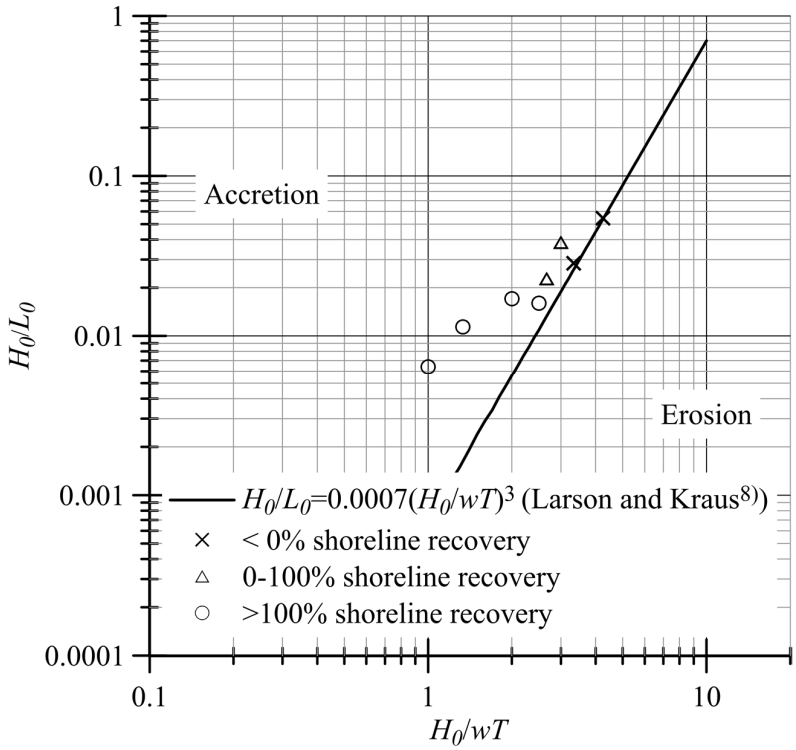

Fig. 3.19 Criterion of regular accretive wave condition for shore-face nourishment.

3.2.2.3 Shore-face Nourished Volume of Sediment

One of the important factors that affects the effectiveness of the artificial acceleration of post-storm beach recovery rate was the nourished volume of sediment. As discussed in the section 3.2.1, the significant volume of sand at bar could not be transported onshore after 120 minutes of accretive wave generation in the cases without shore-face nourishment. The beach recovery rate can be artificially accelerated by shore-face nourishment, the sediment at the bar was dredged and nourished on the shore-face area. Thus, it is important to find out how much of the nourished volume is sufficient for the complete beach recovery. The selection of the sufficient nourished volume was investigated by conducting five cases of physical experiments in 2D wave flume: E13S, E10S, E11S, E28S and E12S. The conditions of experiment were shown in Table 3.1. The results showed that the more volume of nourished sediment, the more increment of sediment transport from the nourished area to the foreshore area (Fig. 3.20 and Fig. 3.21).

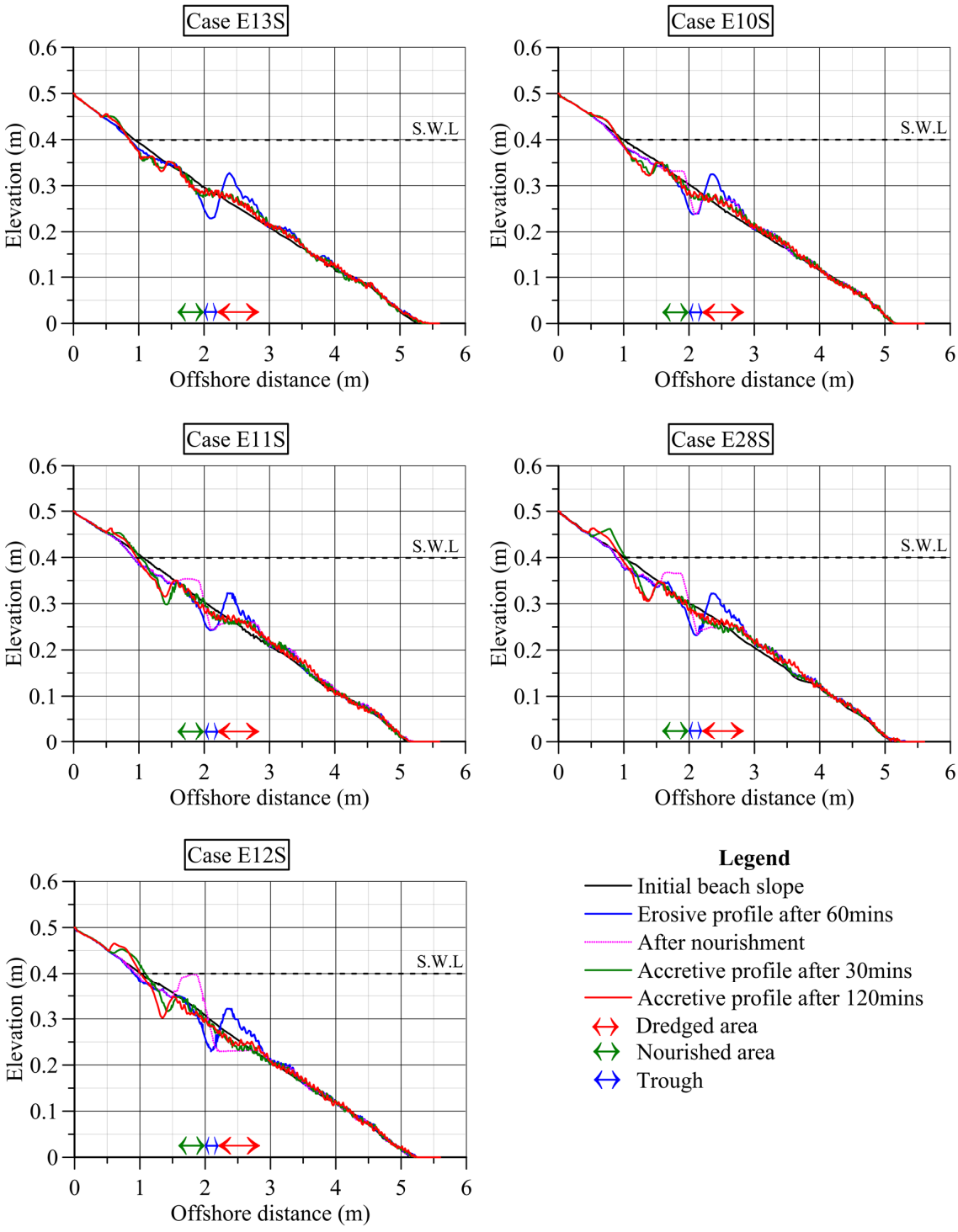

Fig. 3.20 Beach profiles of shore-face nourishment cases in different nourished volumes.

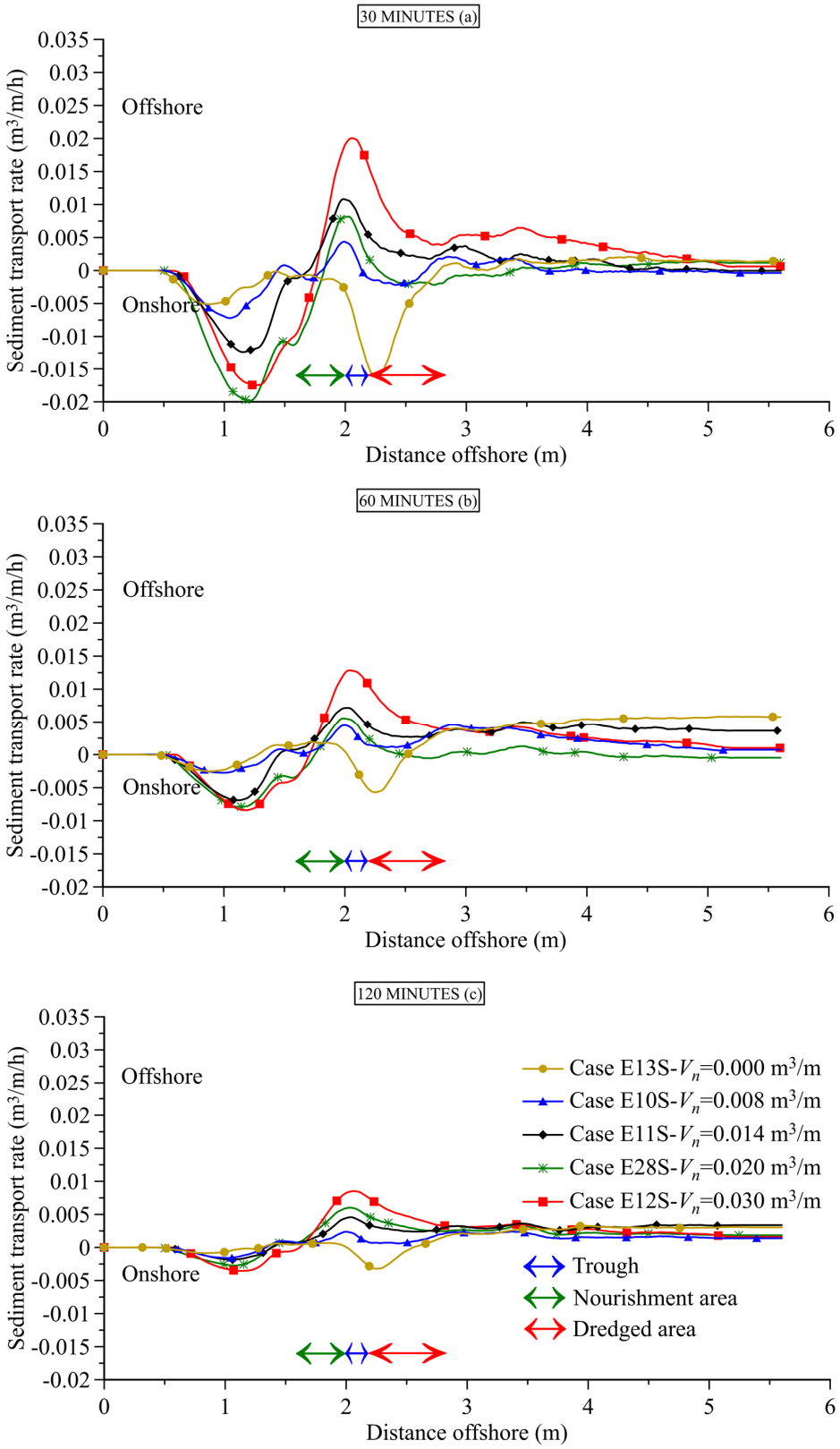

Fig. 3.21 Cross-shore sediment transport rate of shore-face nourishment cases in different nourished volumes.

With insufficient volume of nourished sediment, the percentage of post-storm beach recovery of the case E10S was insignificant (Fig. 3.22). The final shoreline recovery of this case was less than about 30%, whereas in the case E12S, with the sufficient nourished volume, the shoreline recovery percentage was more than 100%. The increment of nourished sand volume increased the percentage shoreline recovery and the relationship between them seems to be linear (Fig. 3.23). However, the relationship between the berm volume and the nourished sand volume was not linear. As the nourished sand volume increased over 0.014 m^3/m, the berm volume dramatically increases (Fig. 3.24). Therefore, in the experimental conditions the sufficient nourished sand volume should be over 0.014 m^3/m. The proper selection of dredged and nourished volume was the key for successful application of the shore-face nourishment method. The proper selection of dredged and nourished volume can be done by analyzing the theory of equilibrium beach profile and field data of beach profile after storm.

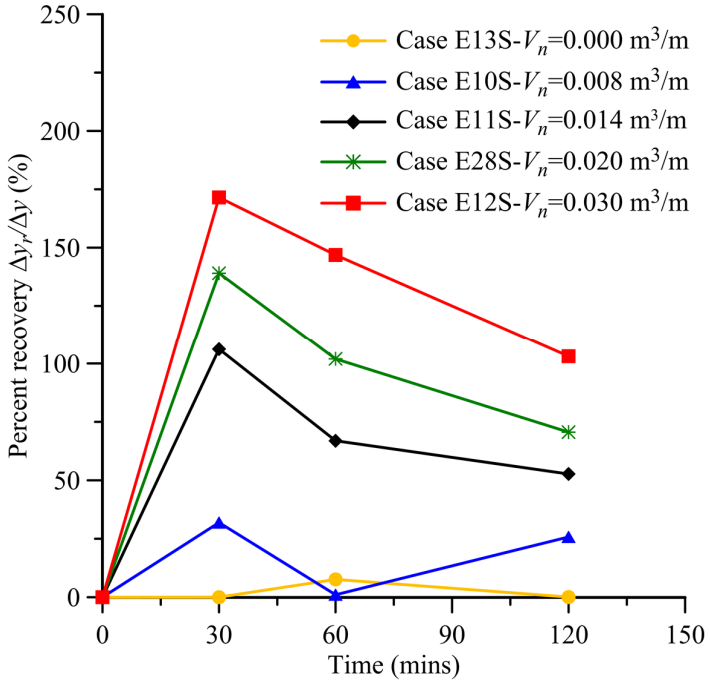

Fig. 3.22 Post-storm shoreline recovery of shore-face nourishment cases in different nourishment volumes.

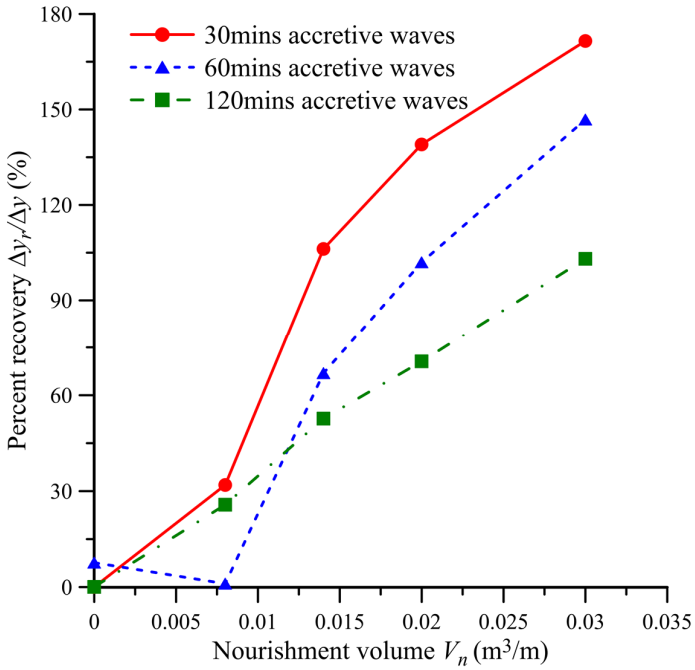

Fig. 3.23 Post-storm shoreline recovery of shore-face nourishment cases in different nourished sand volume.

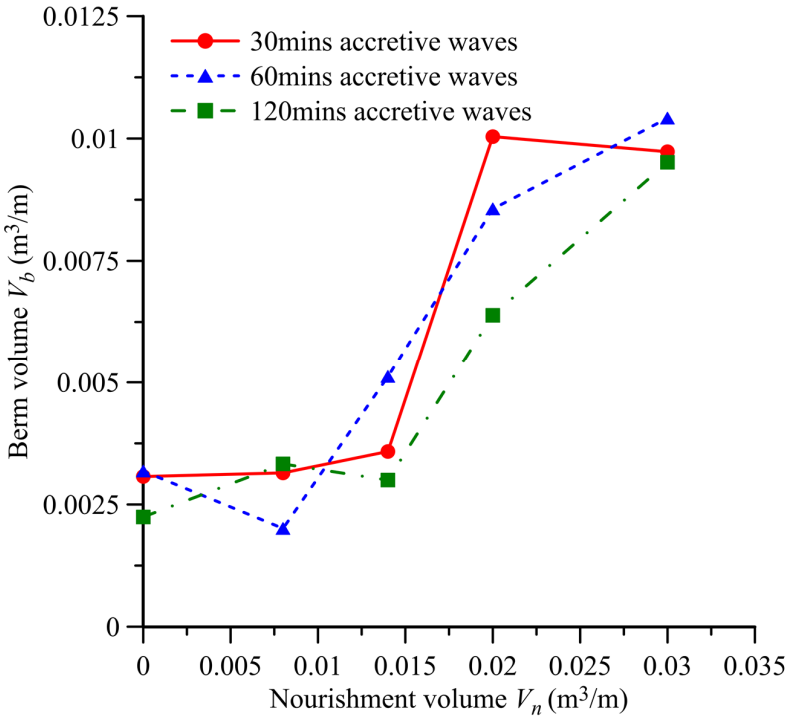

Fig. 3.24 Post-storm berm volume of shore-face nourishment cases in different nourished sand volume.

3.2.2.4 Water Level after Storm

In this section, the impact of water level was discussed on the effectiveness of shore-face nourishment. Three experimental cases E05S, E02S and E11S were conducted with different water levels in the time of accretive wave generation. All cases were subjected to the same storm and accretive waves condition. During 60 minutes of erosive wave generation, the water level was kept at 0.4 m in all cases. After shore-face nourishment, the water levels of each case were changed and the accretive waves are generated for 120 minutes (Table 3.1).

In the cases E02S and E11S, the nourished sediment was transported further onshore in the foreshore area (Fig. 3.25). At the first 30 minutes of accretive wave generation, the onshore sediment transport rate of the high water level cases E02S and E11S was higher than that of the low water level case E05 (Fig. 3.26). However, in the next 30 minutes, whereas, the onshore sediment transport rate of the case E02S significantly decreased and in the case E11S sediment tends to transport offshore, the onshore sediment transport of case E05 gradually increased. The scouring holes of the higher water level cases i.e. the cases E02S and E11S were formed rapidly after nourishment (Fig. 3.25). As discussed in section 3.2.2.1, once the scouring hole was formed, the onshore sediment transport rate will be decreased and the offshore sediment transport was predominant.

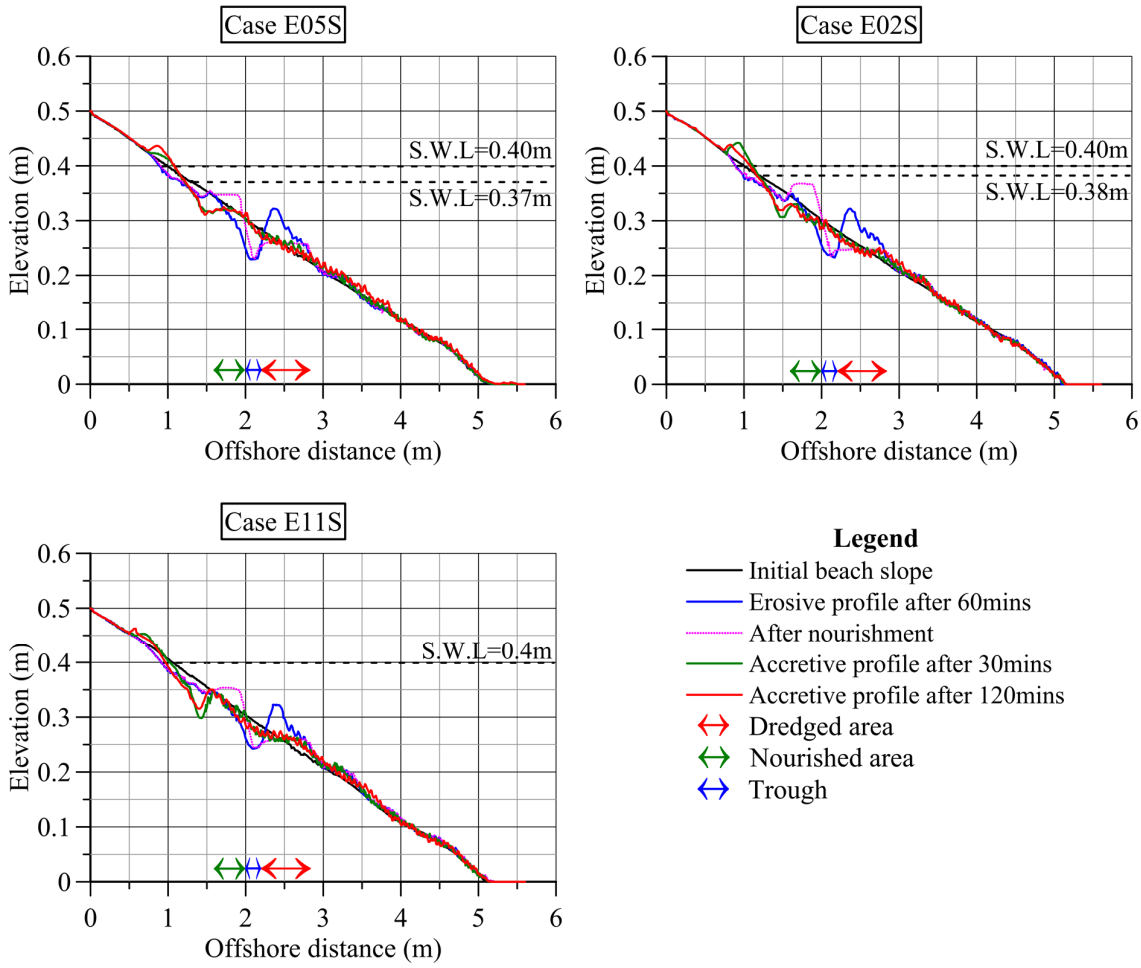

Fig. 3.25 Beach profiles of shore-face nourishment cases in different water levels after shore-face nourishment.

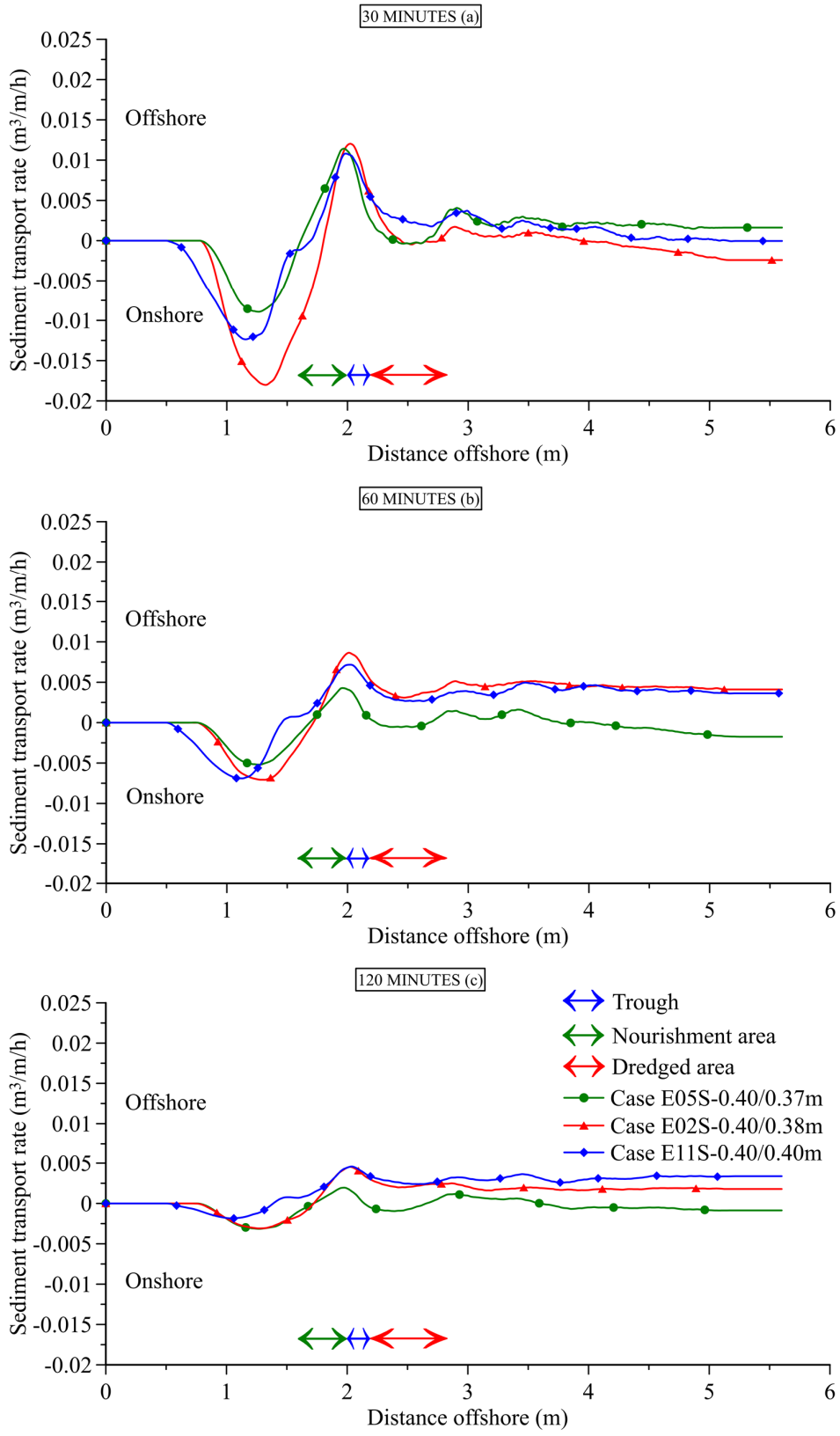

Fig. 3.26 Cross-shore sediment transport rate of shore-face nourishment cases in different water levels after storm.

The post-storm shoreline recovery rates in the cases E05S and E02S with lower water level were similar and higher than that of the high water level case E11S (Fig. 3.27). Despite the fact that the berm volumes of the cases E02S and E11S were larger than those of the lowest water level case E05S in the first 60 minutes of accretive wave generation. Whereas, in the last 30 minutes of accretive wave conditions, the berm volume of the case E05S increased, those of the other cases decreases (Fig. 3.28). The lower water level cases showed the higher rate of beach recovery and larger berm volume. Furthermore, after storm the water level decreased rapidly. Therefore, there is a little room for doubt that the beach recovery rate can be increased by the shore-face nourishment.

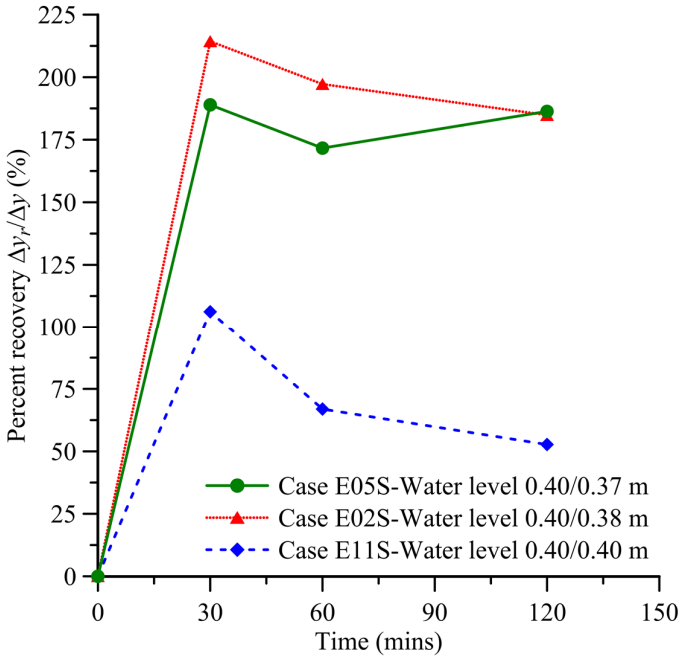

Fig. 3.27 Post-storm shoreline recovery of shore-face nourishment cases in different water levels after storm.

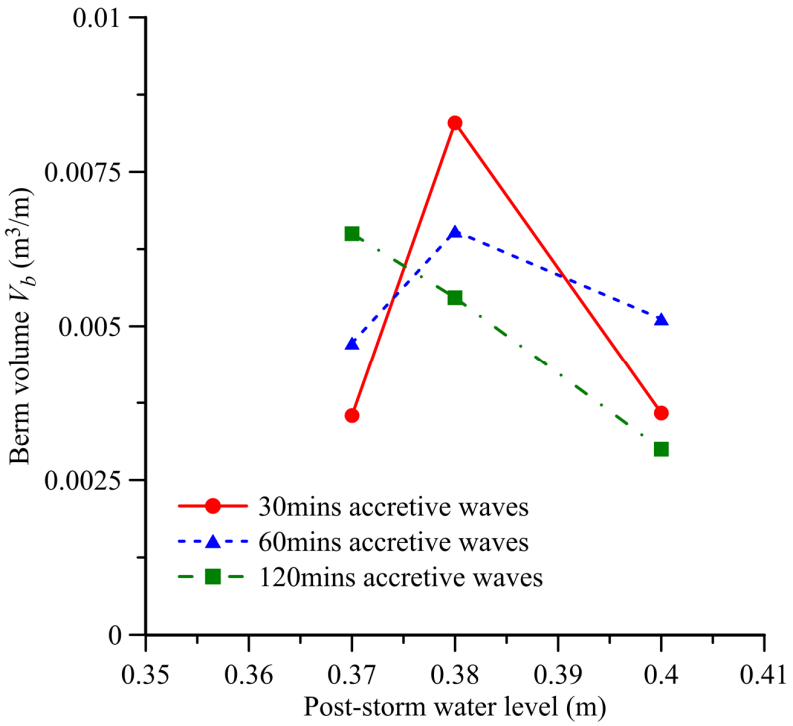

Fig. 3.28 Post-storm berm volume of shore-face nourishment cases in different water levels.

3.2.2.5 Method of Shore-face Nourishment

In this section, schedule of sand dredging and shore-face nourishment was discussed. There are two methods that a volume of sand was dredged one-time or two-times, thereafter nourished it on the shore-face. One-time shore-face nourishment was similar to the conditions of the cases that were described in previous sections, i.e. after 60 minutes of erosive wave generation, a volume of sand was dredged one-time at the sand bar and nourished on the shore-face then the accretive wave was generated for 120 minutes. In the two-time shore-face nourishment, a half of determined volume of sand was dredged at the sand bar and nourished on the shore-face after 60 minutes of erosive wave generation. Thereafter, accretive waves were generated for 30 minutes, and another half volume of sand was dredged again at the sand bar and nourished on the shore-face. Finally, the same accretive wave was generated in the last 90 minutes.

A pair of experimental cases E12S and E03S were conducted in the 2D wave flume with the same erosive wave and accretive wave conditions (Table 3.1). The total nourished volumes were 0.03 m^3/m. The results of post-storm shoreline recovery rate and berm volume of each test condition were compared. The post-storm profiles at 120 minutes in all the cases appear similar (Fig. 3.29). Fig. 3.30 showed that in the case with one-time nourishment, the onshore sediment transport rate was higher than that of the case of two-time nourishment during the first 30 minutes of accretive wave generation. Whereas, in the next 30 minutes of accretive wave generation, the onshore sediment transport rate of one-time nourishment was decreased and the sediment at the foreshore tends to move offshore, the

onshore sediment transport rate of the two-times nourished method was continuously increased. During the last 60 minutes of accretive wave generation, the sediment transport rates of all cases were stable.

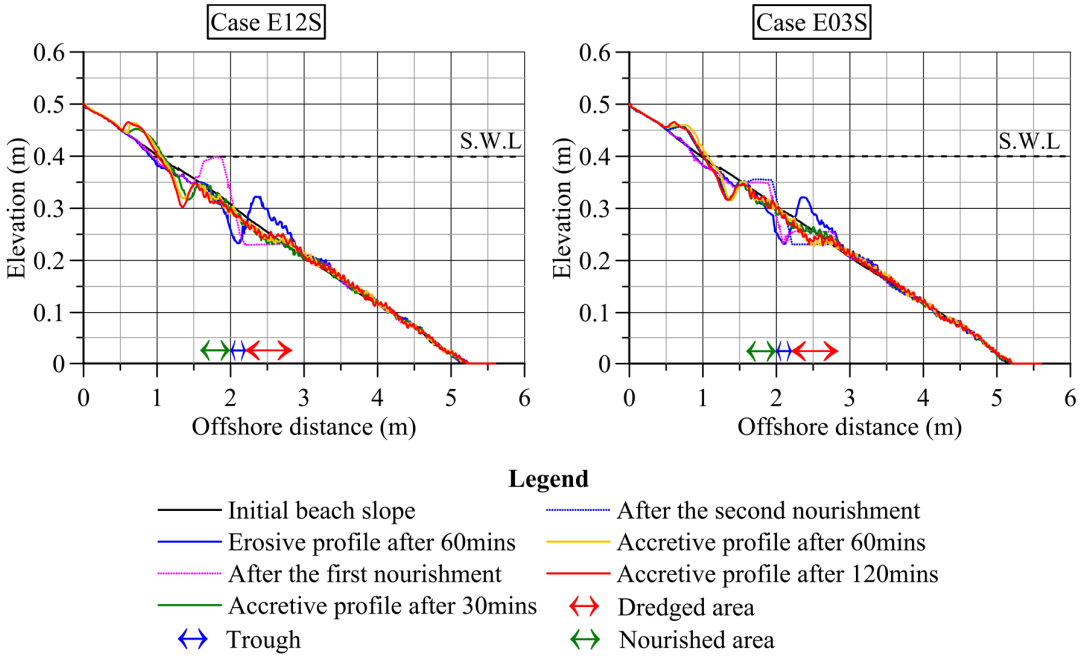

Fig. 3.29 Beach profiles of shore-face nourishment cases in different nourishment methods.

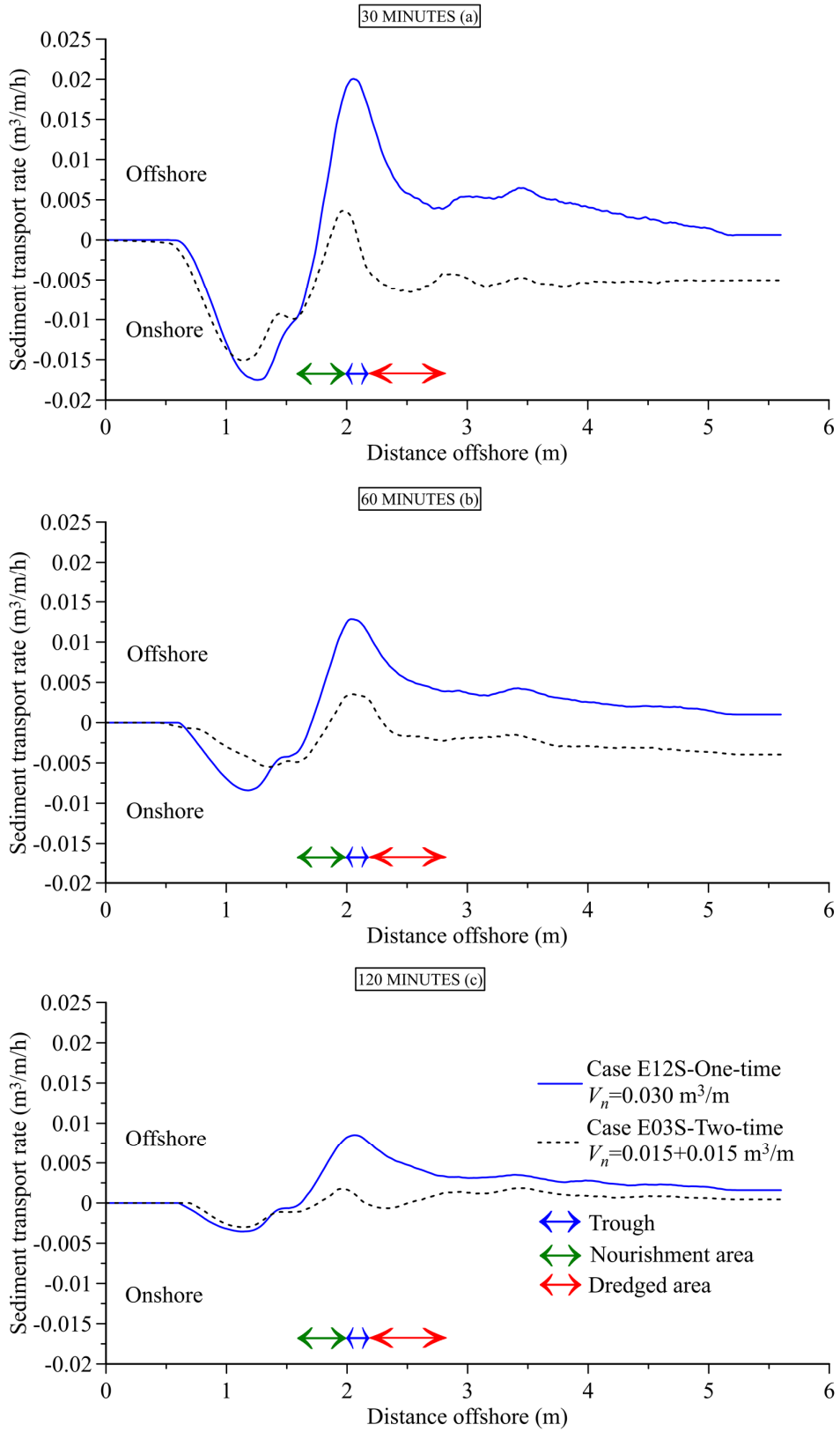

Fig. 3.30 Cross-shore sediment transport rate of shore-face nourishment cases in different nourishment methods (V_n=0.03 m^3/m).

The post-storm shoreline of one-time nourishment method was quickly recovered due to the big volume of nourished sediment during the first 30 minutes of accretive wave generation, however in the last 60 minutes, it gradually decreased (Fig. 3.31). In the two-time nourishment method, the shoreline was still recovered after the second nourishment by 30 more minutes and then gradually retreated in the last 60 minutes. The maximum of shoreline recovery of both cases appears similar. The post-storm berm volume of the experimental results showed the same trend as the shoreline recovery (Fig. 3.32). Therefore, it is clear that the two-time shore-face nourishment was not showed the significantly effective on the increment of the acceleration of beach recovery rate.

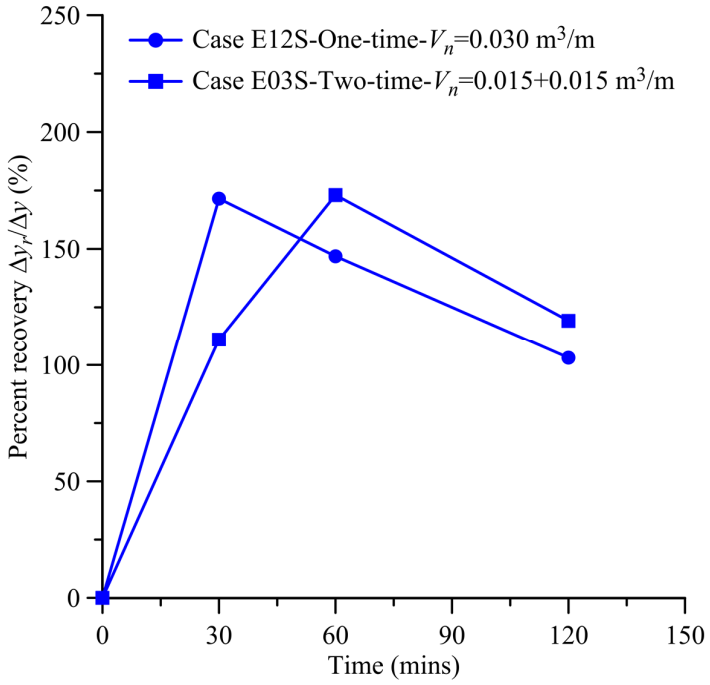

Fig. 3.31 Post-storm shoreline recovery of shore-face nourishment cases in different nourishment methods.

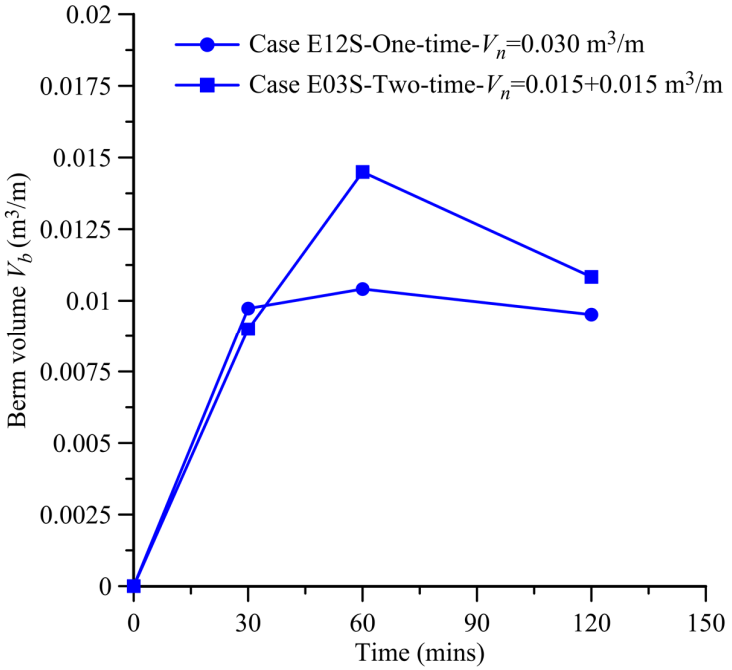

Fig. 3.32 Post-storm berm volume of shore-face nourishment cases in different nourishment methods.

3.3 Shore-face Nourishment in Irregular Waves

In the actual field, water waves were generated by different forces like natural wind, tide, seismic etc. in conjunction with gravity effect. Thus, the waves are irregular in wave heights and periods. However, in the sections 3.2, the regular waves were used for all the cases of experiments. The results showed that the shore-face nourishment can be applied for artificial acceleration of post-storm beach recovery in regular wave conditions. In this section, the applicability of shore-face nourishment in irregular wave conditions was focused by conducting some experiments in 2D wave flume. Similar evaluated parameters i.e. shoreline recovery rate and berm volume were used for assessment. In addition, the different results between shore-face nourishment in regular and irregular waves were also discussed.

3.3.1 Effect of Shore-Face Nourishment on Beach Recovery in Irregular Waves

Four additional experiments were conducted in 2D wave flume to validate the applicability of shore-face nourishment on the artificial acceleration of the shoreline recovery rate in irregular wave conditions. Experimental conditions were presented in Table 3.2 . Conditions of irregular accretive wave of cases E21S, E22S and E23S were adjusted equivalently in wave energy with the regular wave cases E07S, E09S and E28S, respectively. Irregular waves having a Bretschneider-Mitsuyasu spectrum[9) 10)]. The spectra were approximated by the following formula

$$S(f) = 0.257 H_s^2 T_s^{-4} f^{-5} \exp\left(-\frac{1.05}{(T_s f)^4}\right) \tag{3.2}$$

in which H_s is significant wave height (m), T_s is significant wave period (s), f is frequency (Hz).

The regular erosive waves were generated for 60 minutes with wave height H = 0.14 m and wave period T = 1 s[6)] to obtain an barred type beach profile from the initial slope. A volume of sand was dredged at the sand bar and then nourished on the same place of shore-face in all the cases. Thereafter, wave was shifted to irregular accretive wave condition and generated for 120 minutes. The beach profiles were measured by bottom profiler at the beginning, and after 60 minutes of the erosive waves, after shore-face nourishment and after 30, 60, 120 minutes of accretive wave generation consecutively.

Table 3.2 Cases of physical modelling of shore-face nourishment in irregular waves.

Case No.	Erosive wave (regular wave)		Post-storm accretive wave (irregular wave)		Nourished area (m)	Dredged area (m)	Sand dredging/ nourished volume (m^3/m)	Shore-face nourishment	Storm/ swell water level (m)
	Wave height H_e (m)	Wave period T_e (s)	Significant wave height H_s (m)	Significant wave period T_s (s)					
E21S	0.140	1.0	0.060	1.5	1.6-2.0	2.2-2.85	0.02	Nourishment	0.4/0.4
E22S			0.085	1.5	1.6-2.0	2.2-2.85	0.02	Nourishment	0.4/0.4
E23S			0.113	1.5	1.6-2.0	2.2-2.85	0.02	Nourishment	0.4/0.4
E24S			0.085	1.5	-	-	-	None	0.4/0.4

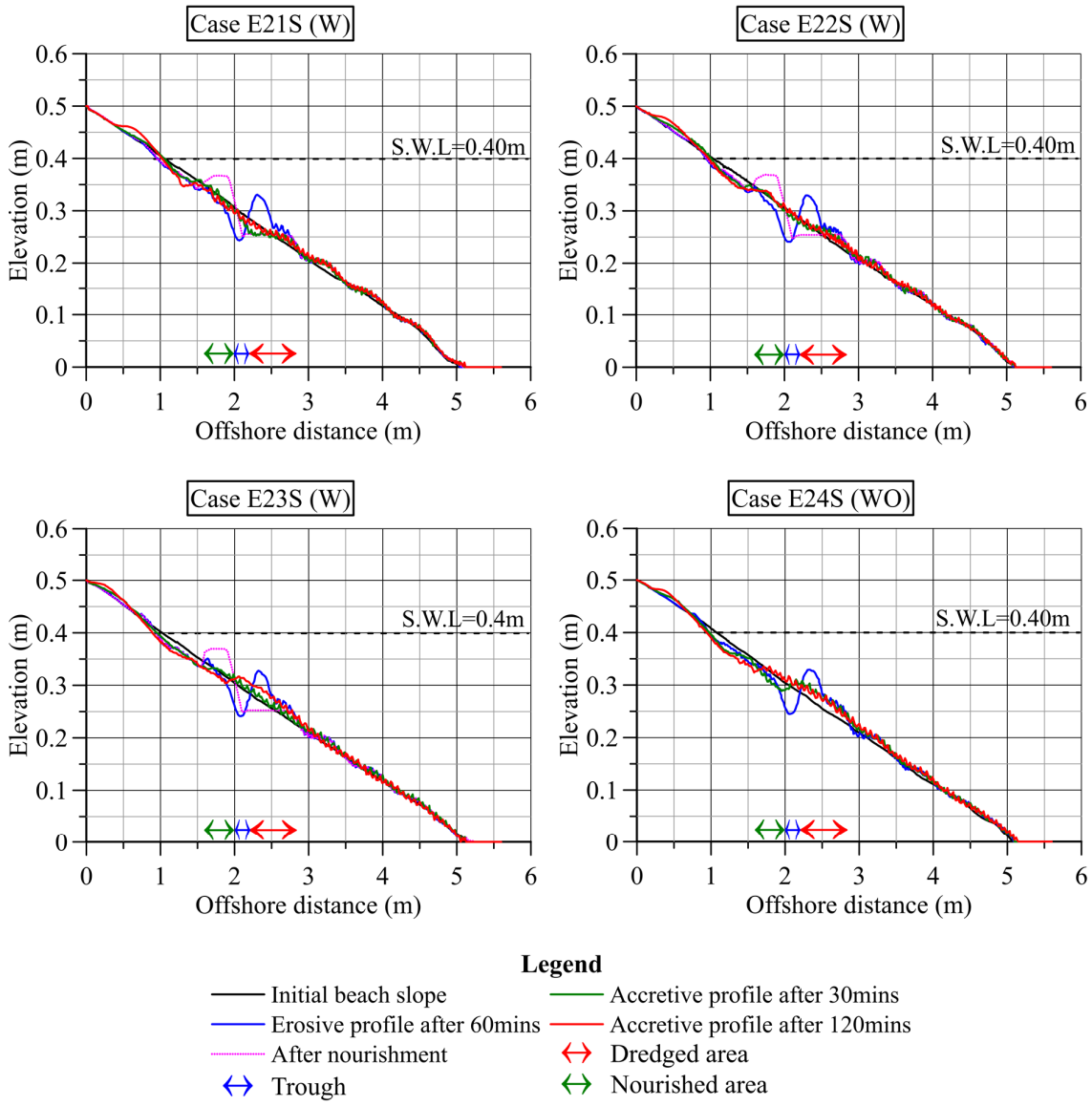

Fig. 3.33 Beach profiles of shore-face nourishment cases in different irregular wave after with/without (W/WO) shore-face nourishment.

Fig. 3.33 and Fig. 3.34 showed the beach profiles and sediment transport rate after shore-face nourishment, respectively. Similar to the results of the cases without shore-face nourishment in regular waves, a volume of sediment at the offshore bar was transported onshore in the case E24S without shore-face nourishment, however, most of them deposited at trough of the beach profile after storm (Fig. 3.34). Most of sediment that was transported to the foreshore was from the area near the shoreline. Therefore, the shoreline recovery in this case was very low during the first 30 minutes of accretive wave generation (Fig. 3.35). In addition, during last 90 minutes of accretive wave generation, the shoreline was further retreated. Whereas, in equivalent wave energy with the case E24S, the shoreline of the case

E22S was quickly recovered in the first 30 minutes and slightly retreated in the last 90 minutes of accretive wave generation.

As the wave steepness of irregular accretive wave increased, sediment transported further onshore at foreshore area (Fig. 3.33). The case with the highest steepness wave E23S, during the first 30 minutes of accretive wave generation, the sediment rapidly transported onshore, however, during the last 90 minutes it is transported offshore (Fig. 3.34). During the last 90 minutes of accretive wave generation, shoreline was retreated even more than before shore-face nourishment (Fig. 3.35). Regarding the cases with low steepness waves E21S and E22S, during the first 30 minutes of accretive wave generation, shoreline was quickly recovered then in the last 90 minutes it was slightly decreased. As it was observed the shoreline recovery decreases when the wave steepness increases.

The berm was formed during the accretive wave generation in all cases. With the time of the accretive wave generation, the berm volume was more and more increased, particularly during the first 30 minutes (Fig. 3.36). In the case E24S, the berm volume increased without shore-face nourishment, the amount of sediment, however, was smaller than the cases E22S with shore-face nourishment under the same irregular accretive wave conditions. After 120 minutes of the accretive wave generation, it was observed that the accretive wave steepness and the berm volume were inversely proportional. In addition, it could be mentioned from the observation that the berm volume continuously increased i.e. the sediment was ceaselessly transported onshore.

These results of the shoreline recovery and the berm volume in irregular wave conditions showed the similar trend to the results of experiments in the regular wave conditions. It could be shown that the beach was recovered quickly by the shore-face nourishment in irregular accretive wave conditions.

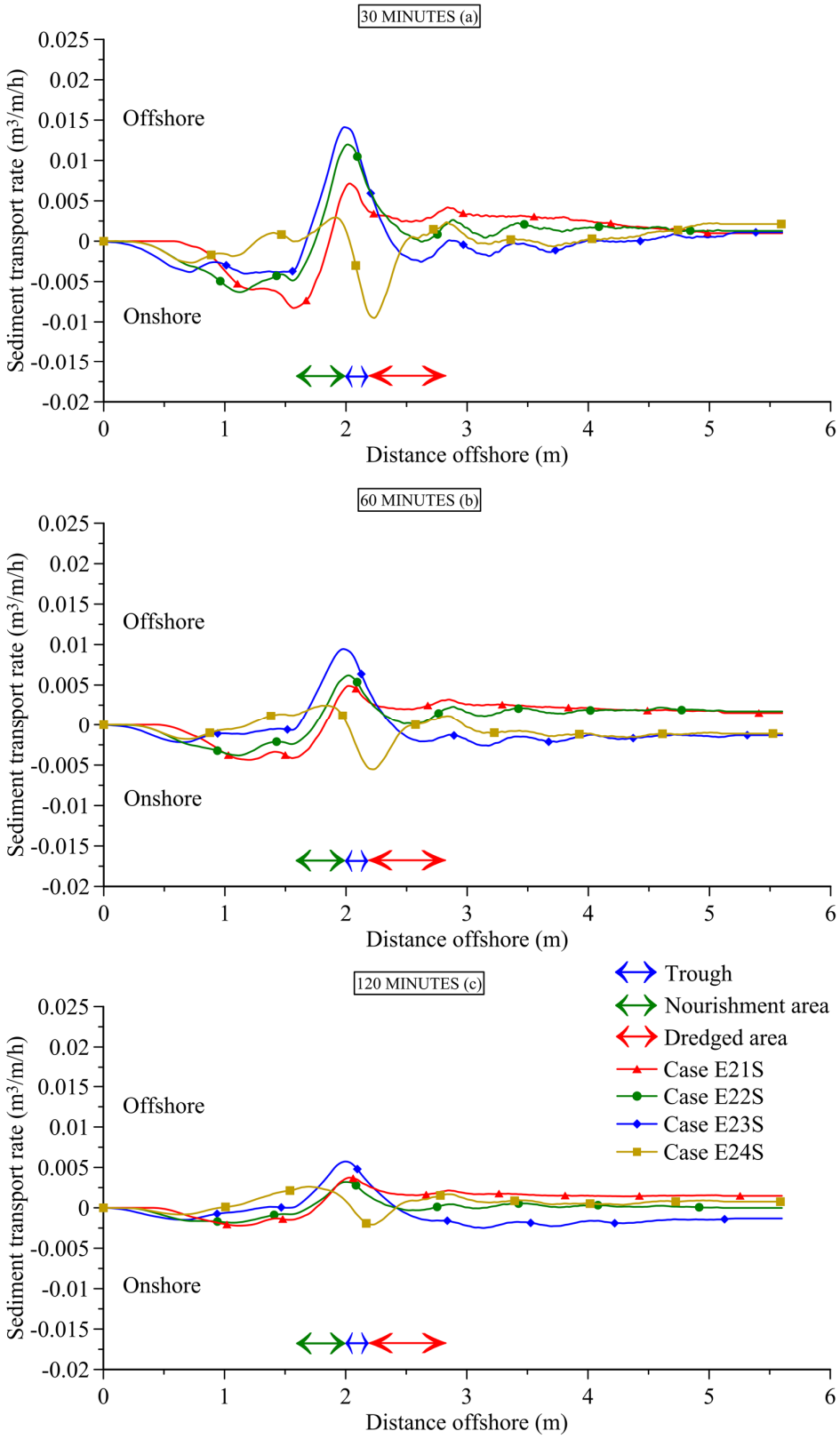

Fig. 3.34 Cross-shore sediment transport rate of shore-face nourishment cases in different irregular wave conditions.

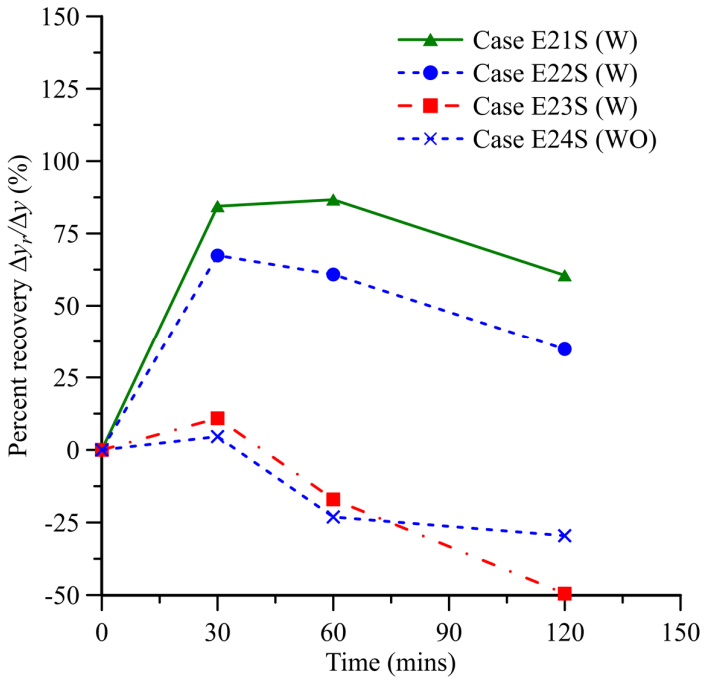

Fig. 3.35 Post-storm shoreline recovery of shore-face nourishment cases in different irregular wave conditions.

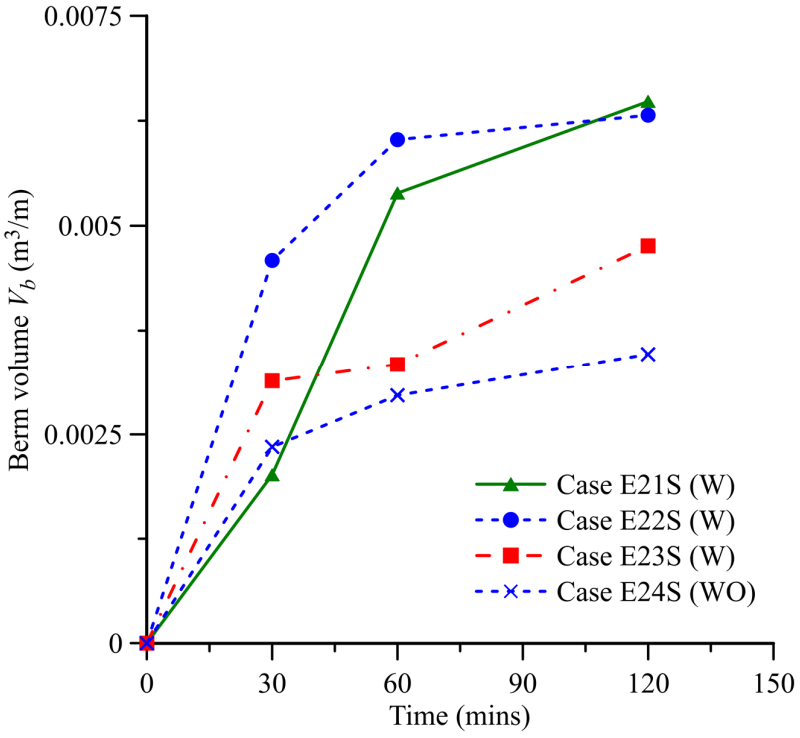

Fig. 3.36 Post-storm berm volume of with/without (W/WO) shore-face nourishment cases in different irregular wave conditions.

3.3.2 The Differences of Shore-face Nourishment in Regular and Irregular Waves

The differences of shore-face nourishment under regular and irregular waves were discussed by the results of three pairs of cases of experiments E07S and E21S, E09S and E22S, E28S and E23S. Wave conditions i.e. significant wave height of irregular waves and wave height of regular waves were set up equivalently in wave energy for the each pair of experimental cases (Table 3.3).

Table 3.3 Cases of physical modelling of shore-face nourishment in regular and irregular accretive waves.

Case No.	Erosive wave		Post-storm accretive wave		Wave energy of post-storm accretive wave ($N\text{-}m/m^2$)	Regular/irregular wave condition *(R/I)*
	Wave height (m)	Wave period (s)	Wave height (m)	Wave period (s)		
E07S	0.140	1.0	0.040	1.5	2.00	*R*
E21S			0.057	1.5	2.03	*I*
E09S			0.060	1.5	4.50	*R*
E22S			0.085	1.5	4.56	*I*
E28S			0.080	1.5	8.00	*R*
E23S			0.113	1.5	8.06	*I*

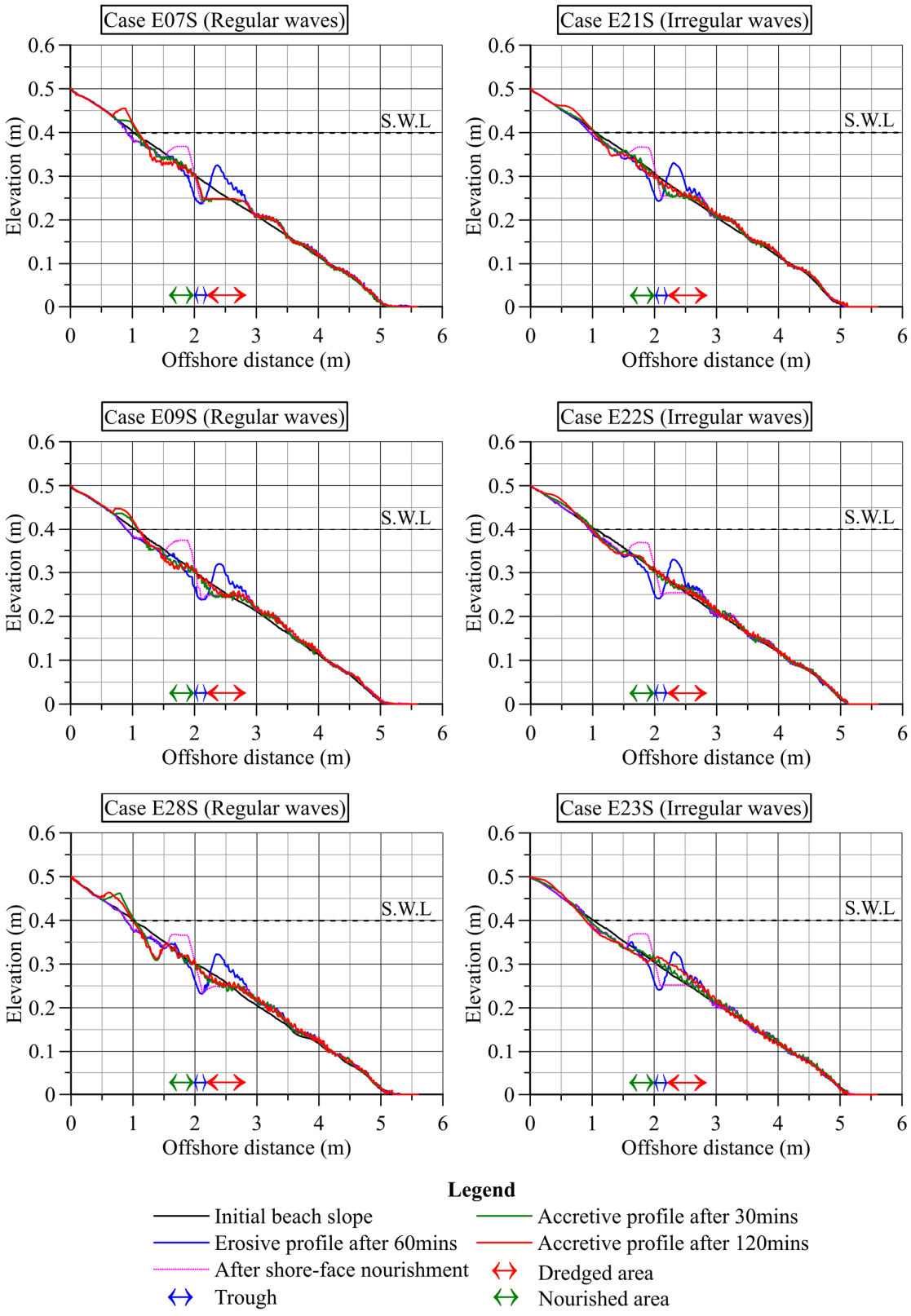

Fig. 3.37 Beach profiles of shore-face nourishment cases in different regular/irregular waves after shore-face nourishment.

The beach profiles in regular and irregular waves were shown in left and right hand side of Fig. 3.37, respectively. In the irregular waves, the sediment was transported further onshore and the beach profiles were smooth. In the wave train of irregular waves, there were low waves with long periods as well as high waves with short periods (Fig. 3.38). The low waves with long periods flushed the nourished sediment further onshore, thus the berms in the irregular wave cases were formed and located further onshore than those in the regular wave cases. For instance, whereas, the berm after 120 minutes of accretive wave generation in the case E07S was located around 0.7-1.2 m, in the case E21S, it was located around 0.4-1.0 m. On the other hand, the high waves with short period of irregular wave train dragged the nourished sediment offshore. In the regular waves, there were only single accretive waves, thus the nourished sediment was always flushed onshore. Therefore, with the equivalent wave energy, the shoreline recovery rate as well as berm volume in regular waves were always higher than those in irregular waves (Fig. 3.39 and Fig. 3.40).

It can be said that in the irregular waves, the post-storm shoreline recovery rate and berm volume were smaller than those in the regular waves cases, however, in comparative analysis between the cases with and without shore-face nourishment, the post-storm shoreline recovery rate and berm volume were comparative high in the case with shore-face nourishment. Therefore, the combination of nearshore sand dredging and shore-face nourishment can effectively accelerate the post-storm beach recovery rate.

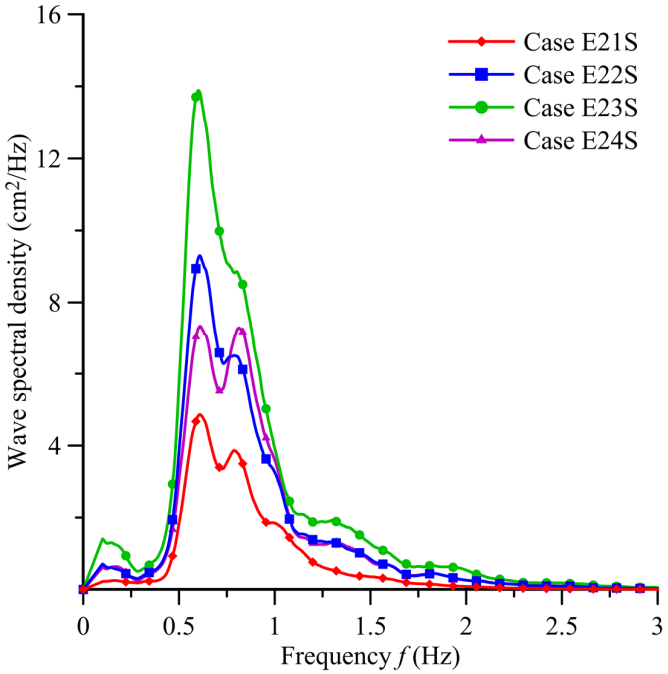

Fig. 3.38 Wave spectrum of irregular waves at wave gauge No. 3.

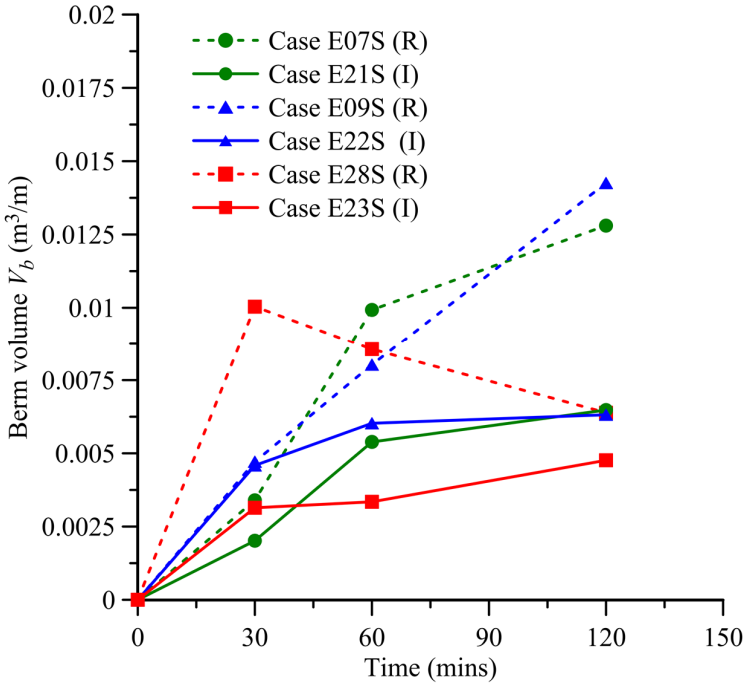

Fig. 3.39 Post-storm berm volume of shore-face nourishment cases in different regular/irregular waves conditions.

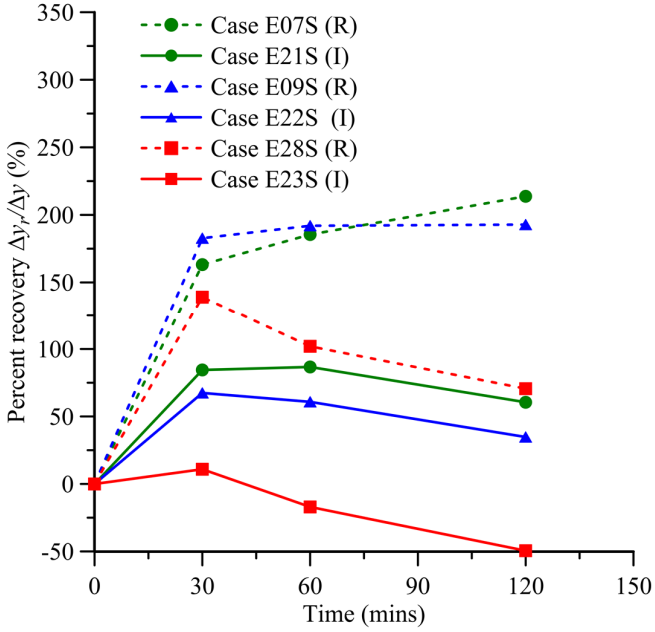

Fig. 3.40 Post-storm shoreline recovery of shore-face nourishment cases in different regular/irregular wave conditions.

3.4 Discussions

The results of shore-face nourishment in regular and irregular waves showed the effectiveness of shore-face nourishment method on accelerate post-storm beach recovery, hence the shore protection. The beach recovery was proportional to the nourished volume of sediment. In the case E10S, the small nourished volume was not enough for the completed recovery. On the other hand, in the case of large nourished volume E28S and E12, at 30 minutes after nourishment, a large volume of nourished sediment was transported onshore, thereafter a part of that volume was transported offshore (Fig. 3.20). In these cases, the volume of nourished sand was more than enough for shore-face nourishment. Therefore, a sufficient volume should be calculated for the shore-face nourishment. The sufficient volume can be assumed base on the equilibrium beach profile of the area in calm wave season and the volume of eroded sediment caused by storm.

The accretive wave conditions played as the most important role for the applicability of shore-face nourishment. The less wave steepness of the accretive waves, the higher applicability of the method (Fig. 3.17). The condition of accretive regular waves shows effectiveness of shore-face nourishment was follow the criterion of Larson and Kraus[8] (Fig. 3.19). In the application criterion of regular accretive waves for the shore-face nourishment, the grain size of sediment was also taken into account.

Because of the global warming, the frequency of tremendous storms has been increased[11], thus in some coasts, the shoreline is continuously retreated during the recovery period. In some worst cases, the shoreline may never recover. Therefore, the quick recovery was the important key of the shore-face nourishment. As discussed in Chapter Two, the sand dredging in accretive waves and periodic sand dredging method can delay the speed of the shoreline retreat. In this chapter, the results of the periodic sand dredging and shore-face nourishing of the case E03S showed insignificant effectiveness. The experiment results of the shore-face nourishment showed that in the low water level i.e. after storm, the effectiveness of shore-face nourishment increased. Therefore, in order to reduce the negative effects of the sand dredging and improve the effectiveness of shore-face nourishment method, the shore-face nourishment should be carried out in calm wave season. Furthermore, the dredged sand should be immediately nourished on the shore-face of the beach after sand dredging.

Duin et. al[5] studied the effectiveness of shore-face nourishment on shore protection. In their study, the function of shore-face nourishment was as a reef in which dissipating energy of storm waves. Because the sediment was nourished at a place between the inner bar and outer bar in which far from the shoreline, thus the nourished sediment insignificantly transported to the foreshore area. In addition, in this project, a huge additional volume of nourished sediment was needed. The results of this study showed that the shore-face nourishment can protect the shore without using additional volume of nourished sediment by dredging sand at the sand bar and nourishing it on the shore-face.

3.5 Conclusions

During the storm the sediment is dragged offshore which causes the beach erosion. After the storm, the eroded sediment is transported back onshore and the shoreline will be gradually recovered. Because of the global climate change, with the increase in frequency of tremendous storm and successive storm, and sea water level rise, the shoreline recovers very slowly, even it cannot be recovered. By dredging some amount of sediment that was eroded away from the shoreline by storm and nourishing it on the shore-face areas, the post-storm beach may be recovered quickly. This idea was validated by number of physical experiments. This method was name the shore-face nourishment and its effectiveness and applicability on accelerating the post-storm beach recovery was confirmed.

By dredging sand from the offshore bar and filled it on the shore-face, without adding volume of sand i.e. the combination of nearshore sand dredging and shore-face nourishment may change the concept of the "nourishment" term. "Nourishment" used here means recovering the shoreline by the sediment of the littoral cell itself. In addition, the shore-face nourishment can save a huge amount of additional nourished sediment and does not use any structure. The shore-face nourishment can be considered as nature-friendly shore protection method under the global climate change.

Post-storm wave condition i.e. accretive wave condition is the most important factor that directly influences the applicability of the shore-face nourishment method. In some accretive wave conditions, effectiveness of the shore-face nourishment method is insignificant. The other factors are dominant parameters in the post-storm beach recovery, for instances, volume of nourished sand, sea water level and position of nourishment area. In the field, the shore-face nourishment may be influenced by sea level, tide, longshore current etc. Therefore, field conditions should be well investigated before implementations of shore-face nourishment.

To enhance effectiveness of the shore-face nourishment, sediment should be dredged with sufficient volume, and nourished immediately on the shore-face of the beach. In addition, regarding the equilibrium beach profile, sediment grain size and the volume of eroded sediment caused by storm in the study area, the sufficient volume can be calculated.

References

1) Hepner T, Gibeaut J. Tracking post-storm beach recovery using data collected by Texas high school students. Shore & Beach. 2004. 72: 5-9.

2) Corbella S, Stretch D. Shoreline recovery from storms on the east coast of Southern Africa. Natural Harzards and Earth System Sciences. 2012. 12: 11-22.

3) Houser C, Wernette P, Rentschlar E, Jones H, Hammond B, Trimble S. Post-storm beach and dune recovery: Implications for barrier island resilience. Geomorphology. 2015. 234: 54-63.

4) Morton RA, Gibeaut JH, Paine JG. Stages and durations of post-storm beach recovery, Southeastern Texascoast, U.S.A. Journal of Coastal Research. 1994. 10: 884-908.

5) Duin MJP van, Wiersma NR, Walstra DJR, Van Rijn LC, Stive MJF. Nourishing the shoreface: observations and hindcasting of the Egmond case, The Netherlands. Coastal Engineering. 2004. 51: 813-837.

6) Sunamura T, Horikawa K. Two dimensional beach transformation due to waves. Coastal Engineering. 1974. 920-938.

7) Aoki S. Sediment transport and beach deformation. Lecture note, 2015. 1-65.

8) Larson M, Kraus NC. Sbeach: Numerical model for simulating storm-induced beach change. Report 1: Empirical foundation and model development. Coastal Engineering Research Center, Waterways Experiment Station, Corps of Engineers. 1989. 129-137.

9) Bretschneider C. Significant waves and wave spectrum. Ocean Industry. 1968. 40-46.

10) Mitsuyasu H. On the growth of spectrum of wind-generated waves (2)-Spectral shape of wind waves at finite fetch. In JSCE (Ed.), Proc., 17th Japanese Conf. Coastal Engineering. 1970. 1-7 (in Japanese).

11) WGII_AR5. Climate Change 2014: impacts, adaptation, and vulnerability. Cambridge, United Kingdom and New York, NY, USA: Cambridge University Press. 2014.

Chapter 4 Perched Beach Nourishment

4.1 Introduction

Beach nourishment is an effective method for coastal protection that has been applied commonly all over the world. The source of replenishing materials is becoming more and more exhausted and costly; therefore, the reduction of the amount of replenishing materials is a solution of reducing the cost of beach nourishment projects. Perched beach nourishment is an appropriate solution for this issue. In Japan and the United States of America, the method of perched beaches is considered as a new phase in coastal defense systems. With the perched beaches, the coastal defense system is strengthened and the beach is widened. This gives opportunities for restoration and preservation[1].

There were of studies on the responses of perched beach profile by conducting physical experiments in irregular waves[2) 3) 4) 5)] and regular waves[6)]. The results of these studies are very practical in the design of perched beach nourishment. However, in these studies, the experiments were separately conducted in regular and irregular waves. Therefore, these experiments showed different results of responses of perched beach. In addition, Chatham[6)] studied the responses of perched beach profile by conducting physical experiments in regular storm waves. The regular storm waves were generated for 3 to 12 hours continuously until the perched beach profile had reached an equilibrium condition. Sorensen and Beil[2)] conducted experiments to investigate the responses of perched beach profile under 42 hours of irregular storm waves generation. The results of scour depth and the volume loss of the perched beach of these two studies are comparatively high. In real time scale, storm attacked the beach for several hours. Thus, the time scale of experiment in these two researches was not realistic time scale. This research addresses the gaps between experiment and real time scale of storm waves attack on perched beach.

The purpose of this study is to identify the effectiveness of perched beach nourishment on shore protection in storm waves by conducting physical experiments in the 2D wave flume. The scour depth and volume loss were taken into account for evaluation. The different responses obtained in regular and irregular wave experiments were discussed in term of equivalent wave height and wave energy. First, in the equivalent wave height and wave period, the results showed that the profiles caused by regular storm waves yield much more deformation and volume loss than those by irregular waves. In addition, even in the cases where the perched beaches in regular waves showed eroded profiles, irregular waves yielded accreted profiles.

As the energy of the regular waves was set equally to that of the irregular waves, the responses of perched beach profiles in regular and irregular waves were similar except for the scour depth. Larson and Kraus[7)] studied the responses of beach profile in regular waves and classified the beach profiles based on the wave conditions and sediment grain size. In this study, the classification of a perched beach

profile in irregular waves was also proposed. This was based on the results of this study's experiments and empirical results of Larson and Kraus[7].

Table 4.1 Cases of physical modelling of perched beach nourishment.

Cases No.	Water level (m)	d/h_e	Wave height (m)	Wave period (s)	Regular/ Irregular (*R/I*)	Wave condition
E01P	0.067	0.528	0.040	0.822	*R*	1-Normal waves
E02P	0.067	0.528	0.040	0.822	*I*	
E03P	0.100	0.626	0.040	0.822	*R*	
E04P	0.100	0.626	0.040	0.822	*I*	
E05P	0.067	0.528	0.080	1.095	*R*	2-Normal waves
E06P	0.067	0.528	0.080	1.095	*I*	
E07P	0.100	0.626	0.080	1.095	*R*	
E08P	0.100	0.626	0.080	1.095	*I*	
E10P	0.067	0.528	0.133	1.588	*I*	3-Erosive waves
E11P	0.100	0.626	0.133	1.588	*R*	
E12P	0.100	0.626	0.133	1.588	*I*	
E14P	0.067	0.528	0.153	1.570	*I*	5-Erosive waves
E15P	0.100	0.626	0.153	1.570	*R*	
E16P	0.100	0.626	0.153	1.570	*I*	
E17P	0.067	0.528	0.136	1.607	*R*	4-Erosive waves
E18P	0.067	0.528	0.136	1.607	*I*	
E19P	0.124	0.673	0.136	1.607	*R*	
E20P	0.124	0.673	0.136	1.607	*I*	
E21P	0.190	0.760	0.136	1.607	*R*	
E22P	0.190	0.760	0.136	1.607	*I*	
E24P	0.067	0.626	0.094	1.588	*R*	6-Erosive waves
E25P	0.067	0.626	0.108	1.570	*R*	7-Erosive waves
Note: *d*: depth above the submerged breakwater crown (m), h_e: water depth at the seaward of the toe structure (m)						

4.2 Equivalent Wave Height of Regular and Irregular Waves

Twenty-two cases of experiments were conducted in a 2D wave flume of 30 m long, 0.7 m wide and 0.7 m deep (Fig. 4.1). Irregular waves having a Bretschneider-Mitsuyasu spectrum[8) 9)] that was described in Chapter Three were used for all of irregular wave cases. The wave height and wave period of experiments varied from normal to storm wave conditions (Table 4.1). The water level changed as low water level (*LWL*), mean water level (*MWL*), high water level (*HWL*) and highest water level (*HHWL*) with the depth above the submerged breakwater crown d = 0.067, 0.100, 0.124, 0.190 m, respectively. From the initial beach slope, waves were generated by a piston-type wave generator for 60 minutes in both regular and irregular waves. The wave heights were measured at 0.5-m intervals along the profile all the time of wave generation. On the five lines along the wave flume, beach profiles were measured by an optical bottom profiler at the beginning and after 60 minutes of wave generation.

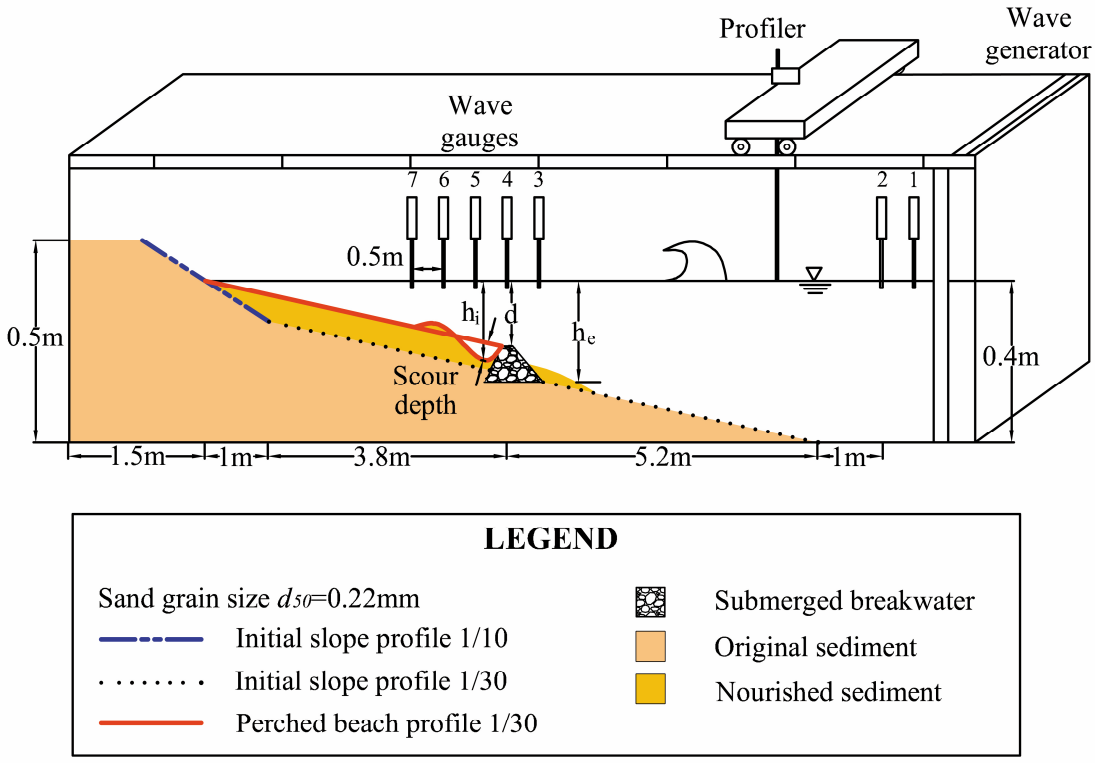

Fig. 4.1 Physical modelling of perched beach nourishment in 2D wave flume.

The scour depth was measured by taking maximum deformation between the initial profile of perched beach and its profile after 60 minutes of wave generation. The volume loss was measured by taking volume of sediment that was lost offshore over a submerged breakwater. The volume loss was shown as negative net volume in the later discussions. Because of measurement error, the volume losses of some cases were positive. However, the volume losses of these cases were insignificant comparatively to the cases with the large volume loss.

The total wave energy of irregular waves was expressed as

$$E_I = \rho g \int_0^{+\infty} S(f) d(f) \tag{4.1}$$

in which ρ is density of water (kg/m^3), g is gravity acceleration (m/s^2), f is wave frequency (Hz), $S(f)$ is frequency spectrum (m^2/Hz).

Frequency spectrum was suggested by Bretschneider-Mitsuyasu spectrum[8) 9)] as

$$S(f) = 0.257 H_s^2 T_s^{-4} f^{-5} \exp\left(-\frac{1.05}{(T_s f)^4} \right) \tag{4.2}$$

in which H_s is significant wave height (m), T_s is significant wave period (s).

Chose a substitution function

$$x = T_s f \tag{4.3}$$

Thus, the differentiation of x was obtained as

$$dx = T_s df \tag{4.4}$$

When Equation 4.2 and 4.4 were combined the following equation of energy of irregular waves is obtained

$$E_I = \rho g \int_0^{+\infty} 0.257 H_s^2 x^{-5} e^{-1.05 x^{-4}} dx \tag{4.5}$$

The wave energy of regular waves was expressed as Equation 4.6.

$$E_R = \frac{1}{8} \rho g H^2 \tag{4.6}$$

In the case of equivalent in energies of regular and irregular waves, the relationship between H and H_s was given as

$$H_s = \frac{H}{\sqrt{2}} \tag{4.7}$$

In the case of equivalent in wave height, the relationship between the wave energy of regular and irregular waves can be expressed as

$$E_R = 2 E_I \tag{4.8}$$

In this section, the equivalent in wave height of regular and irregular waves was taken into account. In each wave condition in the first five wave conditions i.e. from the cases E01P to E22P, the

regular and irregular waves were set equivalently in wave height and wave period (Table 4.1). The wave energy of the regular and irregular waves with the equivalent wave height was shown in Fig. 4.2. In spite of similarity in wave height and wave period, the wave energy of the irregular waves is a half of that of regular waves. The wave spectrum was measured by wave gauges along beach profile in 60 minutes of wave generation. The wave spectrum was calculated by Fast Fourier Transform and smoothed by using Bartlett window with filter number was 160[10]. The offshore wave spectrums that was measured at wave gauge No. 1 of five conditions indicated in Table 4.1 of the irregular waves were shown in Fig. 4.3. In the wave component of wave conditions 3, 4, 5 there were some low frequency waves 0.1-0.3 Hz existed with small energy density. The wave energy of irregular and regular waves at each wave gauge was calculated by Equation 4.1 and 4.6, respectively.

4.2.1 Effect of Wave Conditions on Response of Perched Beach Profile

To assess the effects of normal and erosive waves on the different responses of perched beach profile in the regular and irregular waves, four pair cases of experiment E03P and E04P, E07P and E08P, E11P and E12P, E15P and E16P were conducted at mean water level (MWL). And some other experiments E01P and E02P, E05P and E06P, E10P, E14P were conducted in low water level (LWL) (Table 4.1). In each pair case of the experiments, similar wave height and wave period were generated with regular and irregular waves, respectively.

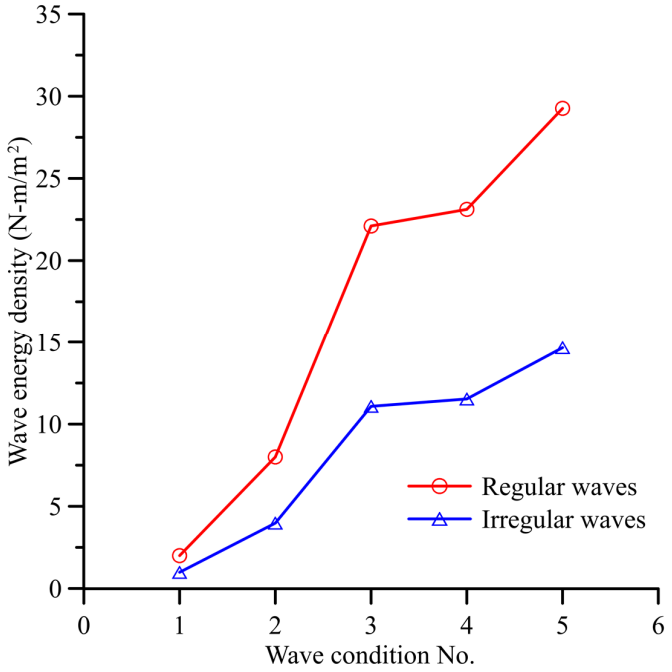

Fig. 4.2 Wave energy density of regular and irregular waves.

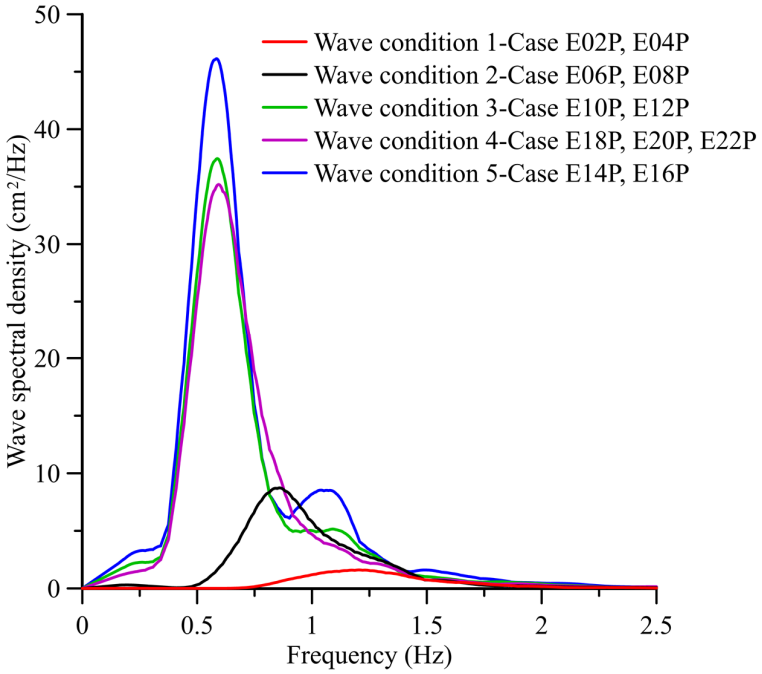

Fig. 4.3 Spectrums of irregular waves at the offshore-wave gauge No.1.

The perched beach profiles after 60 minutes of wave generation were shown from Fig. 4.4 to Fig. 4.7. In the normal wave conditions, the deformation of perched beach profiles was insignificant at the vicinity of the submerged breakwater. As the wave height increases to erosive wave conditions, the deformations of perched beach profile in regular and irregular waves were different. In regular waves, the deformation was very large at the vicinity of submerged breakwater, particularly in the case E15P (Fig. 4.5 and Fig. 4.7). In this case, the sediment was lost very much offshore over the submerged breakwater in the nearshore area, however, the perched beach profiles were nearly stable in foreshore zone. On the other hand, in irregular waves, the deformation was insignificant at the vicinity of the submerged breakwater. Also, at the foreshore, the sediment transported onshore formed the berm (Fig. 4.4 and Fig. 4.6).

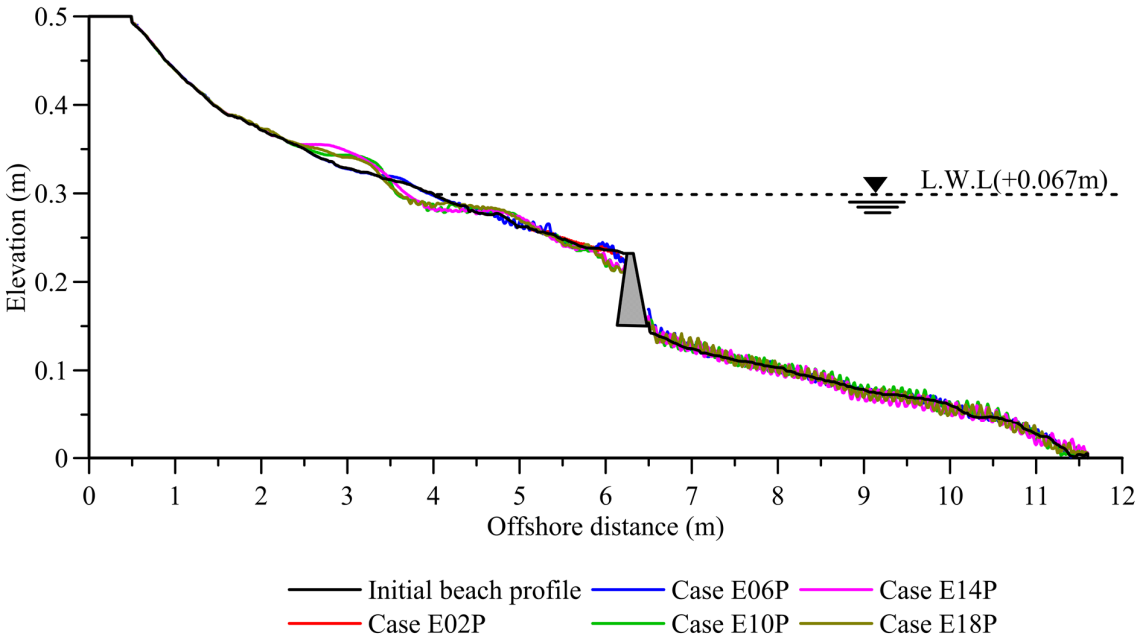

Fig. 4.4 Beach profile in irregular waves at low water level (LWL) after 60mins of wave generation.

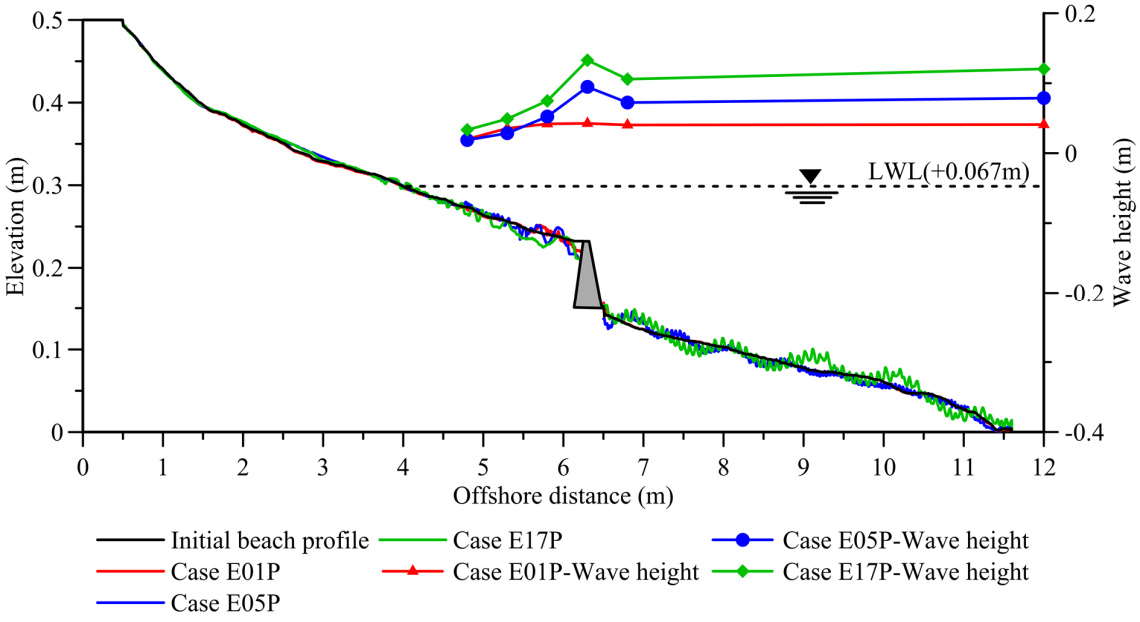

Fig. 4.5 Beach profile in regular waves at low water level (LWL) after 60mins of wave generation and wave height distribution just after perched nourishment.

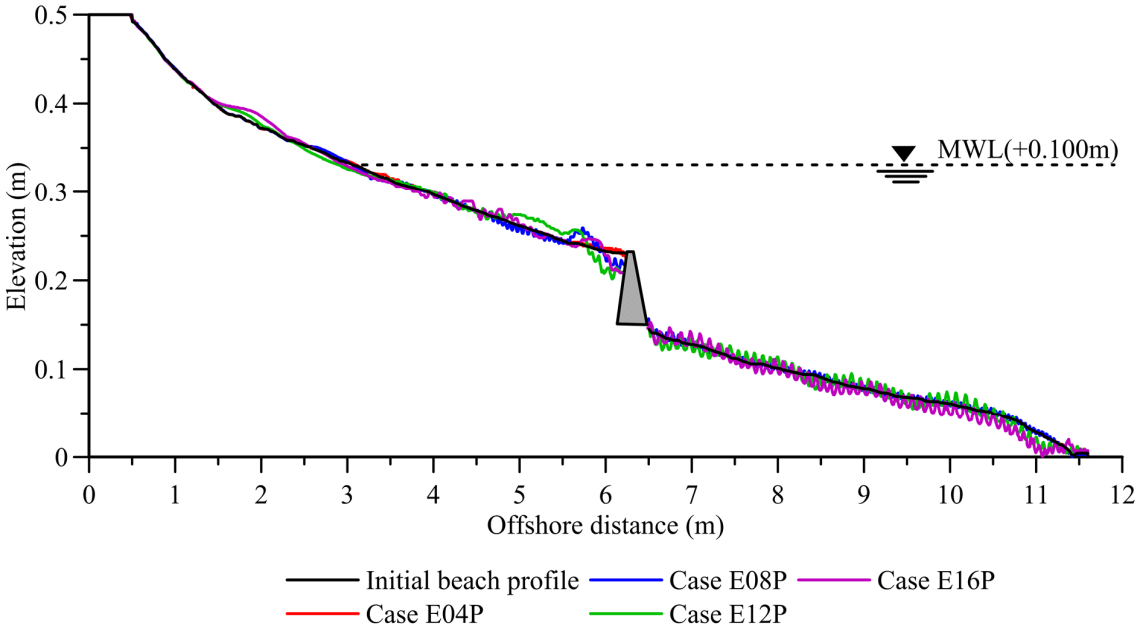

Fig. 4.6 Beach profile in irregular waves at mean water level (MWL) after 60mins of wave generation.

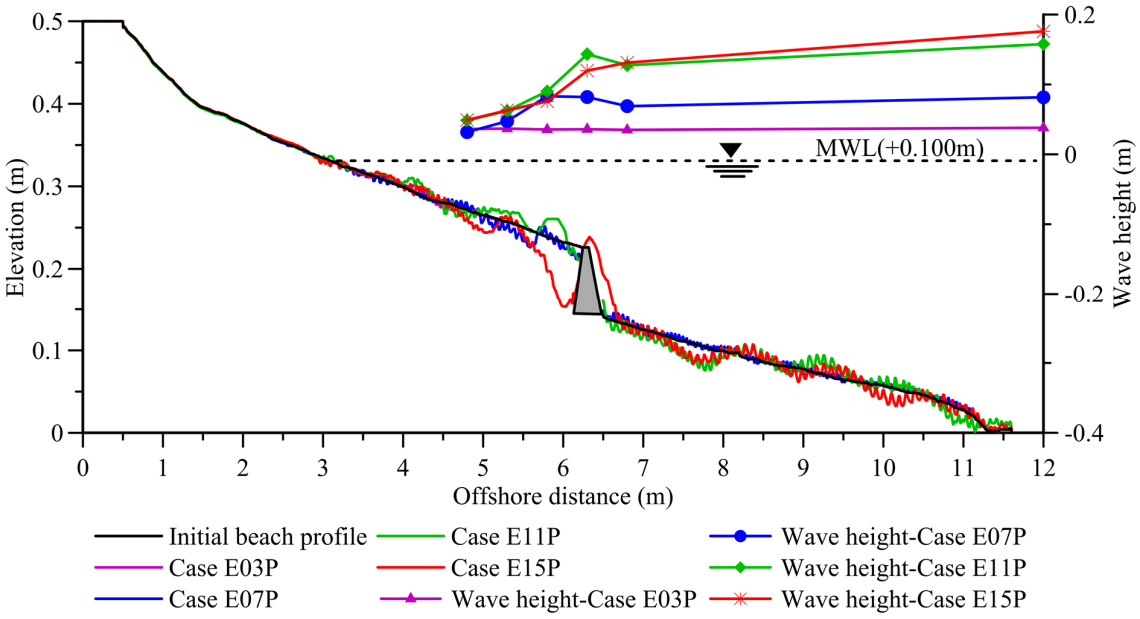

Fig. 4.7 Beach profile in regular waves at mean water level (MWL) after 60mins of wave generation and wave height distribution just after perched nourishment.

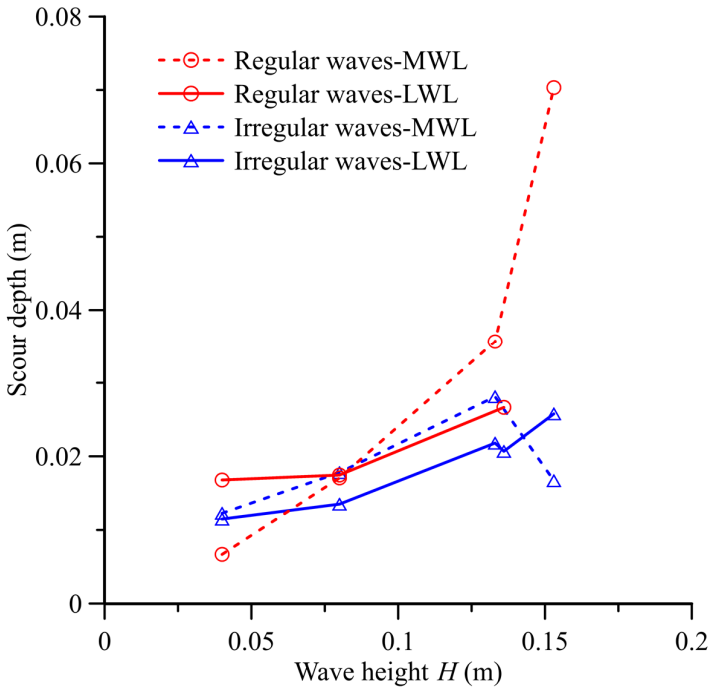

Fig. 4.8 Scour depth in different wave height at low/mean water level (LWL/MWL) after 60mins of wave generation.

The maximum scour depth of perched beach profiles in different wave heights was shown in Fig. 4.8. As the wave height increased the scour depth also increased for all the cases. Whereas, the scour depth increased dramatically by the erosive regular waves with wave height of 0.153 m, in the irregular wave cases, the scour depth was gradually changed. The wave energy dissipation was high in the region of breaking waves, this maintains grains in suspension, and more sediment was transported than in regions of non-breaking waves[7]. In the irregular wave train, there were low waves as well as high waves. The wave breaking positions were distributed along the perched beach. Thus, the energy was dissipated in a long distance on the perched beach (Fig. 4.9c, d). In the regular waves, however, the wave broke at the same position on the perched beach. Fig. 4.9b, c, d show that on the submerged breakwater, the energy of regular waves was higher than that of irregular waves. However, it decreases quickly in a short distance from the wave breaking point. After dissipation it became lower than the energy of the irregular waves. The most of the energy of regular waves dissipated in the area near the submerged breakwater. In the regular waves the sediment in wave breaking regions receives more wave energy and was easily transported. Therefore, the scour depth in regular waves became larger than that of the irregular waves.

In another aspect, the volume loss of the perched beach profile in the irregular waves was insignificant, whereas in the regular waves, it significantly increased as the wave height increased (Fig. 4.10). The maximum cross-shore transport rate appears to be located in the vicinity of plunging point where maximum energy dissipation occurs[7]. In the physical experiments, the wave plunging point was

not easy to measured. The wave plunging point occurs after the wave breaking point; thus, the wave breaking point was taken into account for discussion instead of wave plunging point. In regular erosive waves, the wave breaking positions of the cases E11P, E15P and E17P were close to the submerged breakwater, the wave breaking positions of other cases in normal regular waves, however, were further onshore (Fig. 4.5 and Fig. 4.7). Moreover, the higher wave height, the more energy was dissipated on the areas after wave breaking. In regular erosive waves, the sediment in the vicinity of the submerged breakwater received much more wave energy. Thus, the sediment was easily transported offshore causing the large volume loss over submerged breakwater.

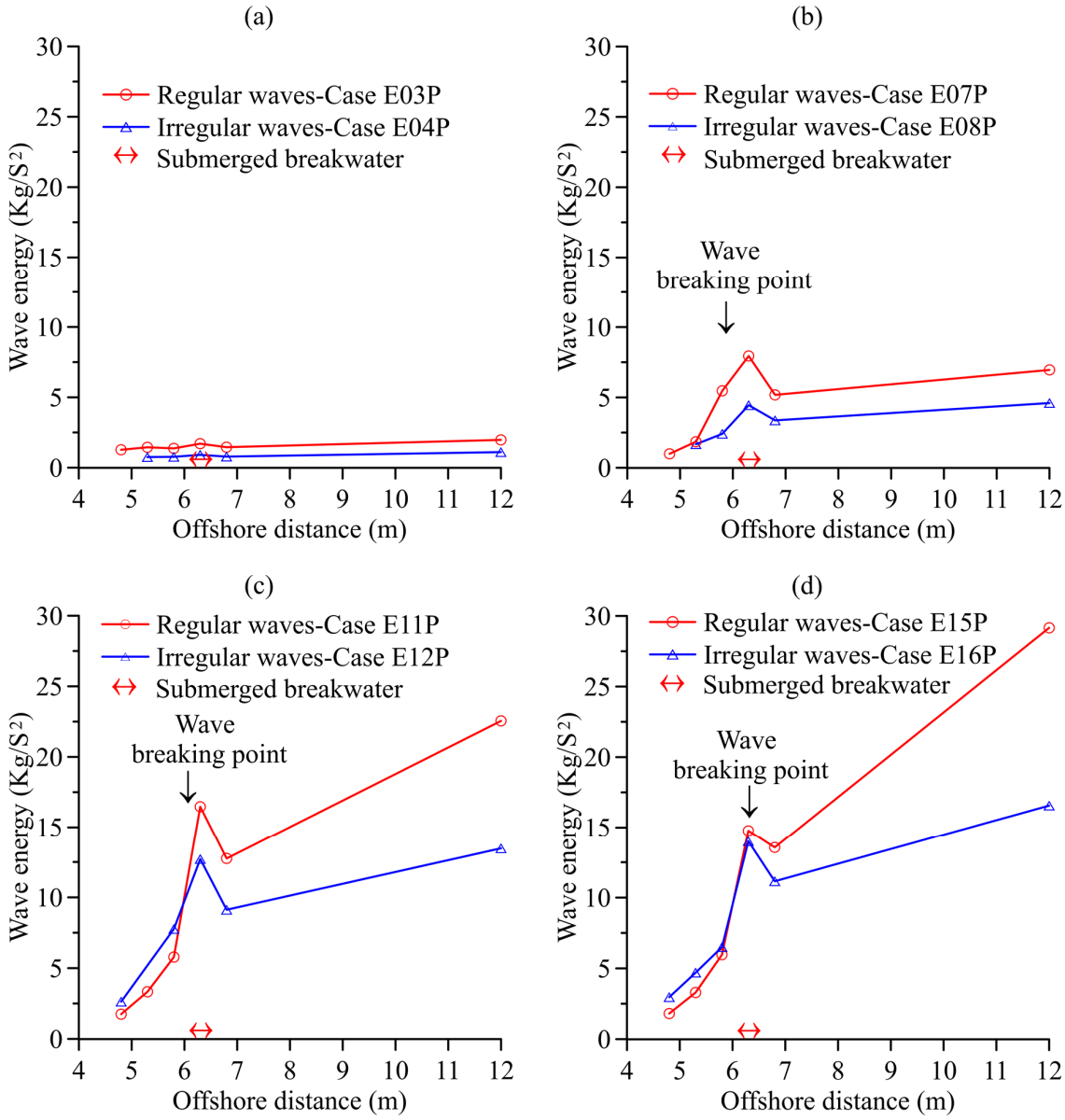

Fig. 4.9 Wave energy distribution along the beach profile of regular and irregular waves at mean water level.

The wave breaking points of irregular waves distributed in a long distance over the perched beach. In addition, for the equivalent wave height, the wave energy of irregular waves was less than that of regular waves. The sediment at the places near submerged breakwater received less energy. Therefore, the less sediment was transported over submerged breakwater caused less volume loss.

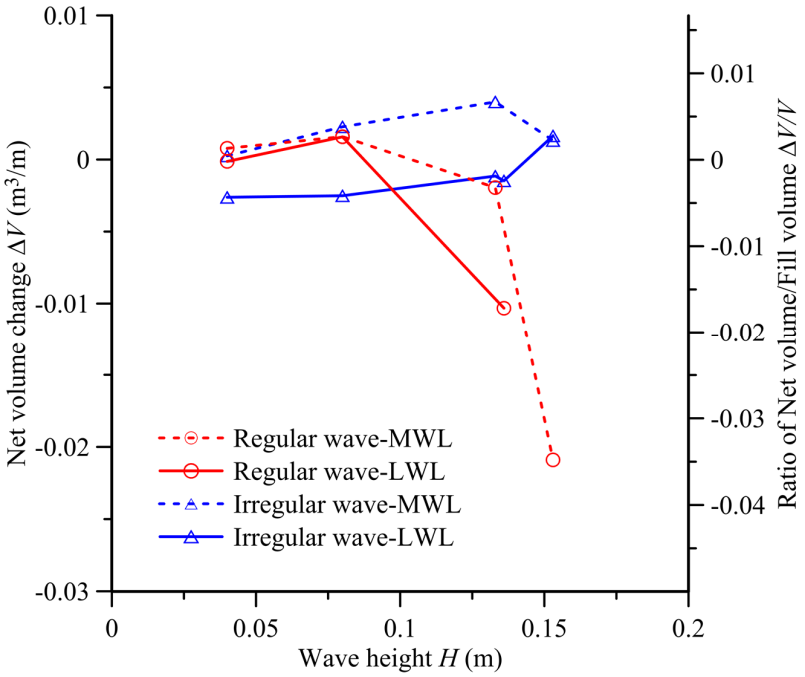

Fig. 4.10 Net volume loss for different wave conditions and water levels after 60mins of wave generation.

The wave energy fluxed over the submerged breakwater will transmitted to the perched beach. The wave spectral density of the irregular waves that was measured at the wave gauge No. 4 above the submerged breakwater were shown in Fig. 4.11. The peak of wave spectrum was slightly shifted to low frequency in the cases of perched beach nourishment. In addition, the wave spectral density in low frequency region 0-0.3Hz that gave an opportunity for accretion of sediment in the foreshore area tends to increase in the irregular wave cases E06P, E08P, E10P, E12P, E14P, E16P and E18P (Fig. 4.11b, c, d, e). Above all, some of high waves of irregular waves were broken at the seaward of the submerged breakwater. Thus, the energy was dissipated before approaching the perched beach. Hence, the wave spectra density transmitted over the submerge breakwater decreased. With all the reasons above, the accretion at the foreshore area of perched beach may results. The submerged breakwater and the nourished beach gradually absorbed the wave energy, changed the wave conditions i.e. significant wave height and wave period. It can be concluded that the irregular waves under the experimental conditions decreased the deformation and increased the accretion at the foreshore area of the perched beach may result.

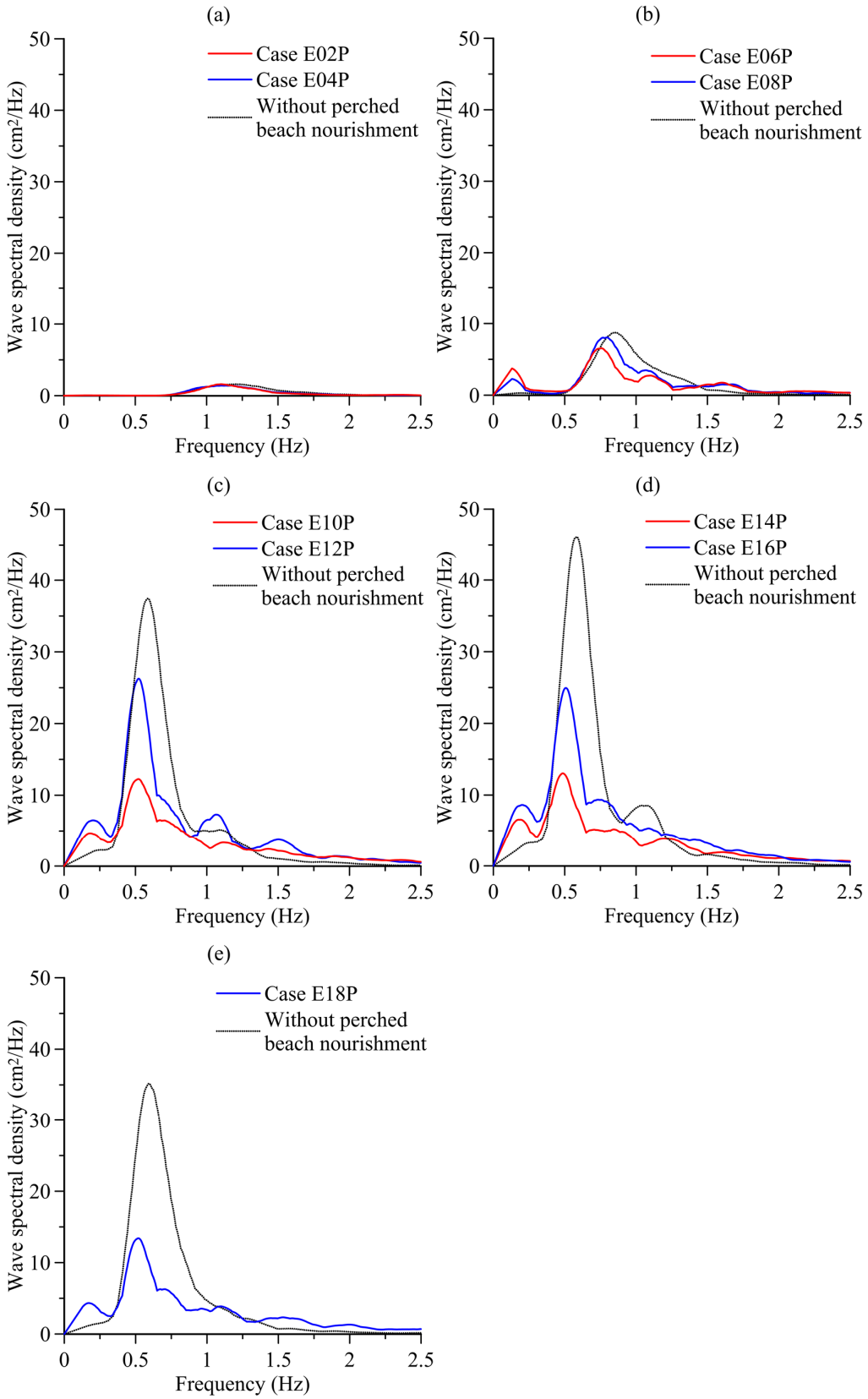

Fig. 4.11 Wave spectrum of the irregular wave cases at wave gauge 4th in low and mean water levels.

4.2.2 Effect of Water Levels on Response of Perched Beach Profile

To identify the different responses of perched beach profiles in different water levels, the results of three pair cases of experiment E17P and E18P, E19P and E20P, E21P and E22P were discussed (Table 4.1). The water levels of three pair cases were low water level *LWL*=0.067 m, high water level *HWL*=0.124 m and highest high water level *HHWL*=0.190 m, respectively. The significant wave height and wave period of irregular waves were set equivalently to wave height and wave period of regular waves.

In the same irregular erosive waves, with the different water levels, the perched beach profiles were deformed very much near the submerged breakwater and slightly at the foreshore area (Fig. 4.12). Although, in erosive waves, the perched beach profile of the case E18P with low water level was accreted at foreshore area. The amount of sediment at the nearshore area was transported onshore, thus a small berm was formed. Fig. 4.13 showed the wave energy measured at the submerged breakwater by the wave gauge No. 4. The peak of wave spectrum slightly shifted to low frequency in the cases with perched beach nourishment. Whereas, in high water levels, the high waves of the cases E20P and E22P could pass over the submerged breakwater and approached to the perched beach, in low water level, some of the high waves of the case E18P were broken seaward or at the submerged breakwater. Thus, the wave energy approaching to the perched beach greatly reduced. As the water level decreases, less energy was transmitted over submerged breakwater to the perched beach. In addition, there were some long period waves 0-0.3 Hz were observed when it passed over submerged breakwater. Therefore, in the experiment in the low water level, the erosive waves were changed to accretive waves once it transmitted over submerge breakwater to the perched beach. Hence the perched beach slightly accreted at the foreshore area.

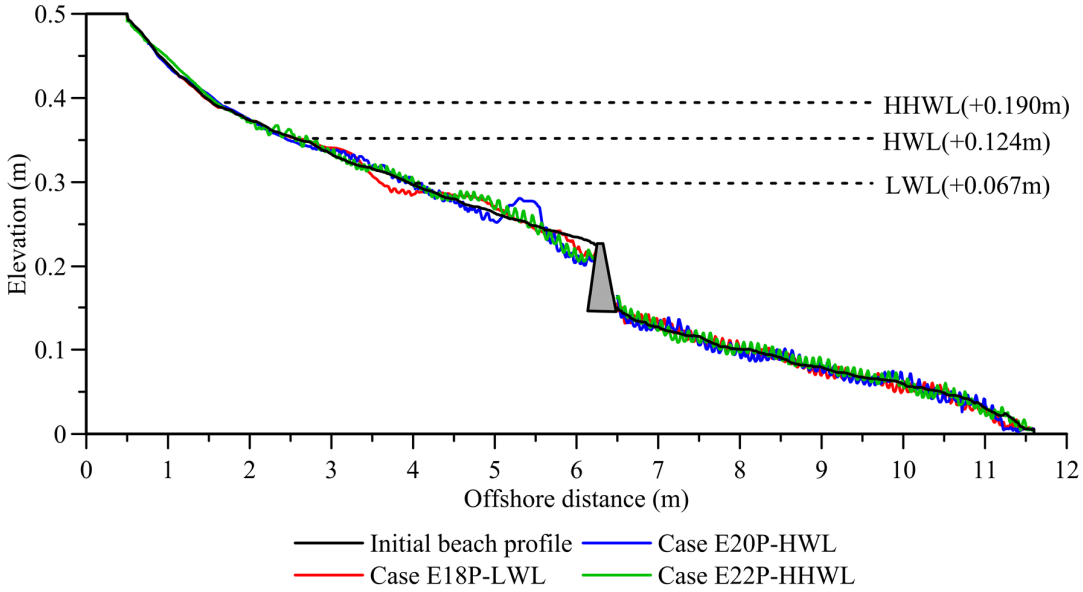

Fig. 4.12 Beach profile in irregular waves at different water levels after 60mins of wave generation.

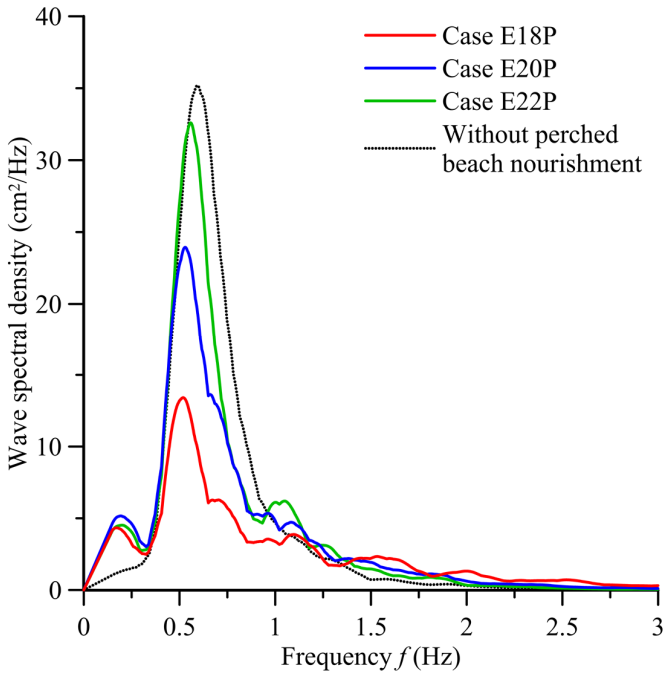

Fig. 4.13 Wave spectrum of the same irregular wave conditions over the submerge breakwater (the wave gauge 4th) in different water levels.

The regular waves with the same wave height and wave period as the significant wave height H_s and wave period T_s of the irregular waves yielded greater deformation of perched beach profile at the breaker zone (Fig. 4.14). In the low and high water levels, the scour depth of perched beach by regular waves were greater than that of irregular waves (Fig. 4.15). In the case of the highest high water level, the scour depth in regular waves was much larger than that in irregular waves. The intensity and positions of the deformation of perched beach tend to increase and move further onshore as the water level increased. Gonzalez[11] studied the equilibrium beach profile model for the perched beach and showed that if $d/h_e > 0.1$, where d is the water depth above submerged breakwater and h_e is the water depth at the toe of structure, i.e. the higher water level the scour depth is larger. In the high water levels, the high waves could pass over the submerged breakwater and transmitted to the perched beach. In the low water level, however, the high waves break seaward or at the submerged breakwater. Thus, the wave energy fluxed over the perched beach significantly decreased. In addition, whereas the regular waves transmitted the perched beach, the energy quickly decreased in the short distance on the perched beach (Fig. 4.16), in the irregular wave cases, the wave energy was dissipated in a long distance after passing the submerged breakwater. Moreover, the energy of regular waves was larger than that of irregular waves in equivalent wave height. Therefore, the scour depth by the regular waves was higher than that by the irregular waves.

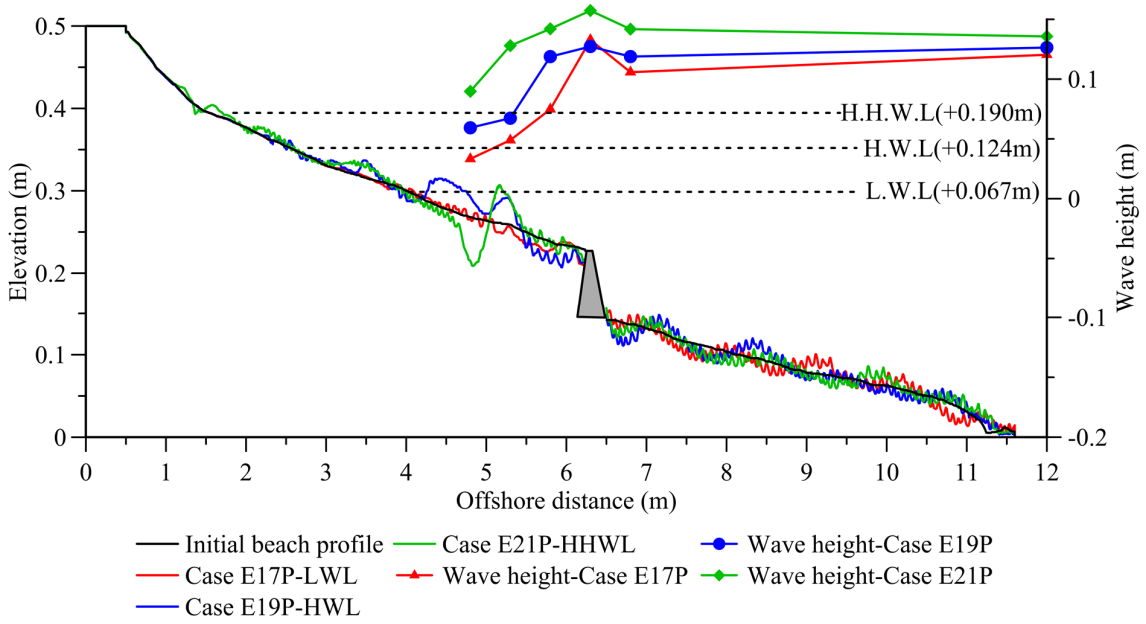

Fig. 4.14 Beach profile in regular waves at different water levels after 60mins of wave generation.

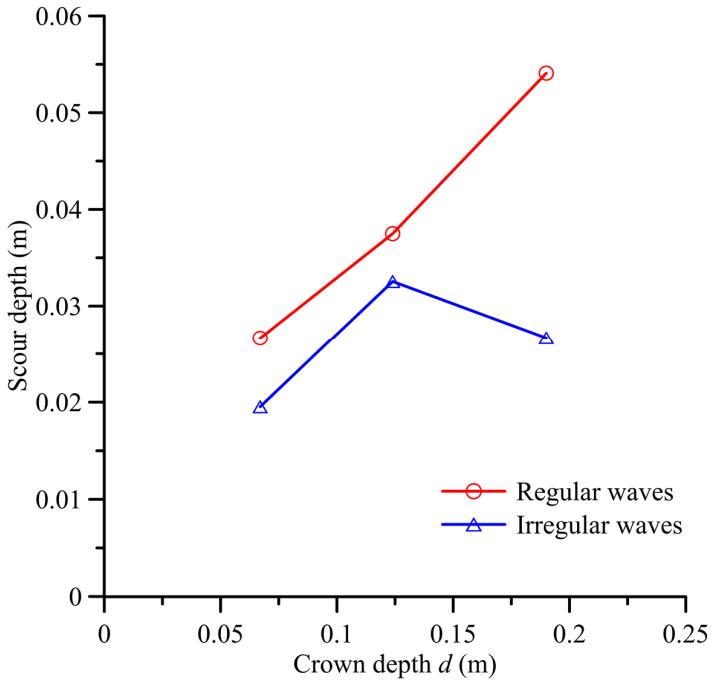

Fig. 4.15 Scour depth in different water levels after 60mins of erosive wave generation.

The volume loss of sediment in irregular waves was insignificantly affected by the water level. in the regular waves, however, the volume loss increased as the water level decreased (Fig. 4.17). In the irregular wave cases, the wave energy on the perched beach was smaller than that in regular wave cases (Fig. 4.16). In the higher water level, although the larger energy entered on the perched beach. The

energy was dissipated in a long distance on the perched beach. Thus, the volume loss insignificantly changed as the water level increased. In the regular wave cases, Fig. 4.14 shows that the wave breaking position in low water level the case E17P was very close to the submerged breakwater. As the water level increased, the wave breaking positions moved further onshore from the submerged breakwater. Most of the energy of the regular waves in low water level was dissipated immediately behind the submerged breakwater (Fig. 4.16a). As the waves broke and dissipated the energy, the mobility of sediment at the breaking area was very high. It caused suspended sediment in this area to be easily transported offshore over submerged breakwater. In the higher water level cases, the high wave energy transmitted onto the perched beach, which caused large deformation in the onshore side, and a big volume of sediment was transported offshore. However, because the breaking points were far from the submerged breakwater, the sediment transported offshore may be still inside the perched beach. It can be concluded that in regular waves, in the cases in which the location of the wave breaking point was close to the submerged breakwater, i.e. low water level in the experiment, large volume loss may result.

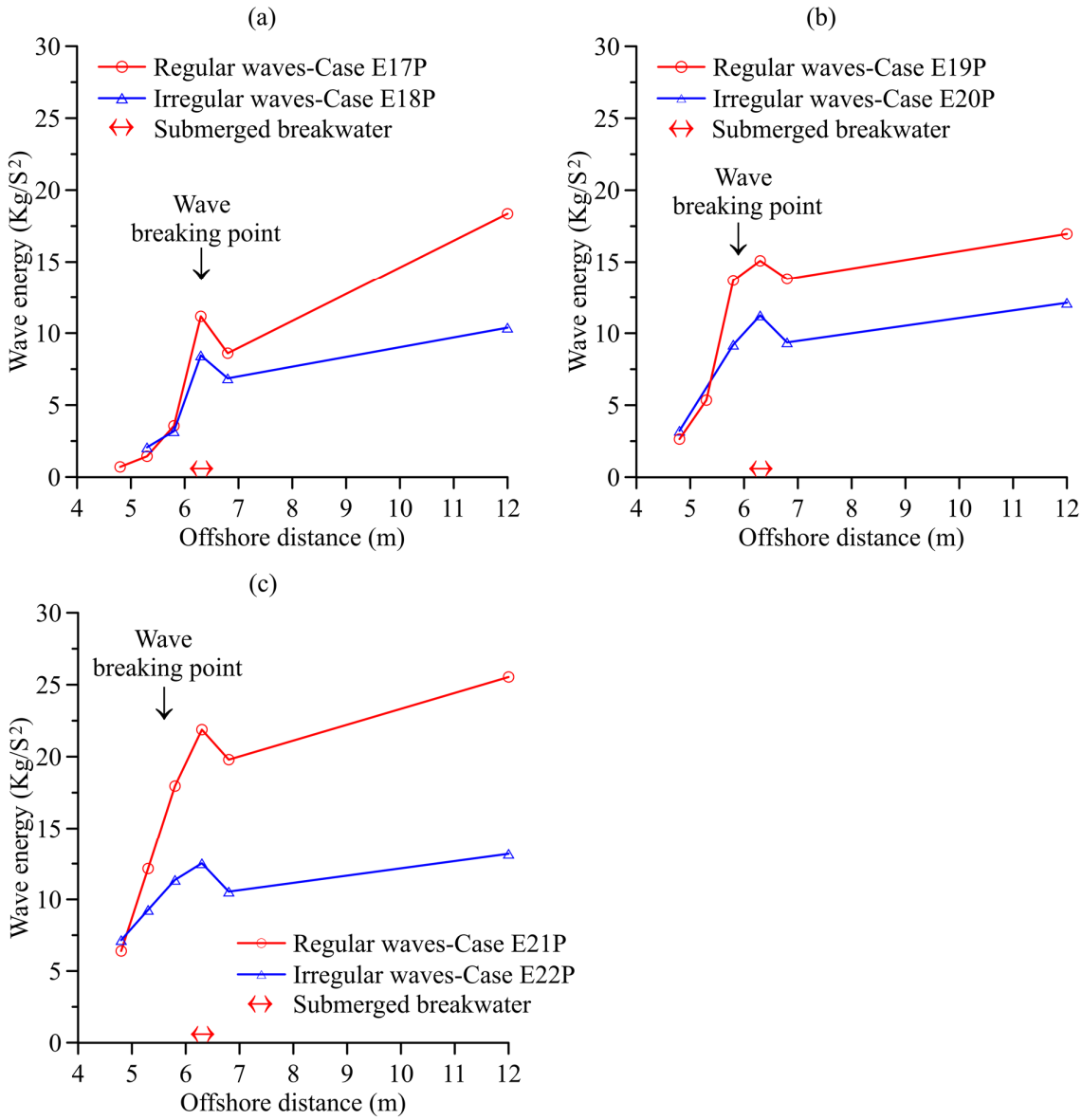

Fig. 4.16 wave energy distribution along the beach profile of regular and irregular waves in different water levels.

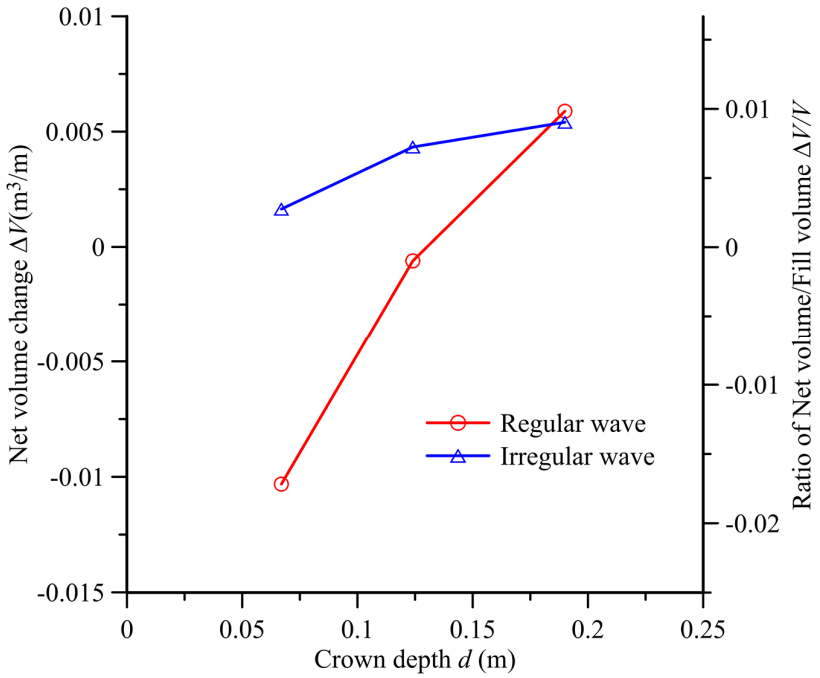

Fig. 4.17 Net volume in different water levels after 60mins of erosive wave generation.

4.3 Equivalent Wave Energy of Regular and Irregular Waves

In this section, the wave heights of regular and irregular waves were adjusted in order to make the energy of these two equivalent. For two pair cases of irregular and regular waves E12P and E24P, E16P and E25P of experiments, respectively. To get the equivalent wave energy, the wave height of each pair cases need to satisfy the Equation 4.7. The beach profiles of the two pair cases E12P and E24P, E26p and E25P were shown in Fig. 4.18 and Fig. 4.19, respectively. Despite the similar wave energy, the scour depth of perched beaches in regular and irregular waves were very different (Fig. 4.20). On the other hand, the location of deformation of the perched beach profile in regular and irregular waves were both in the places near submerged breakwater. In addition, at the foreshore area, the sediment was transported slightly onshore and a berm was formed in all cases. The volume loss of each pair case of regular and irregular waves were similar and insignificant (Fig. 4.21). The wave energy distribution in each pair case were also similar (Fig. 4.22).

Although there was a difference in scour depth, the perched beaches in regular and irregular waves were both accreted. In addition, the difference of volume loss and wave energy distribution of these two were also very small. It can be concluded that in the equivalent wave energy the responses of perched beach profiles in regular and irregular waves were similar.

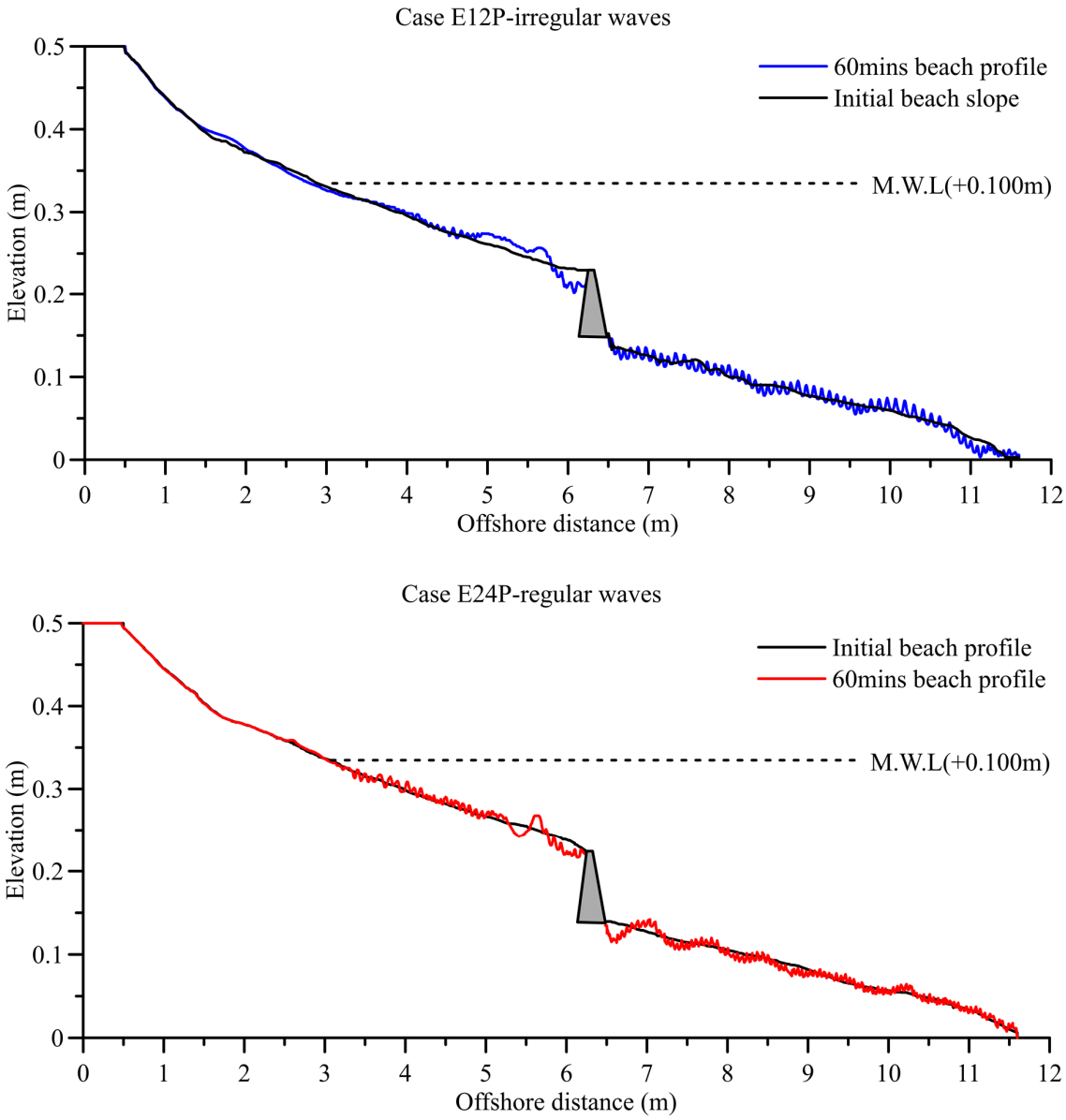

Fig. 4.18 Beach profiles in the same wave energy of irregular/regular erosive wave condition 3 and 6 after 60mins of wave generation, respectively.

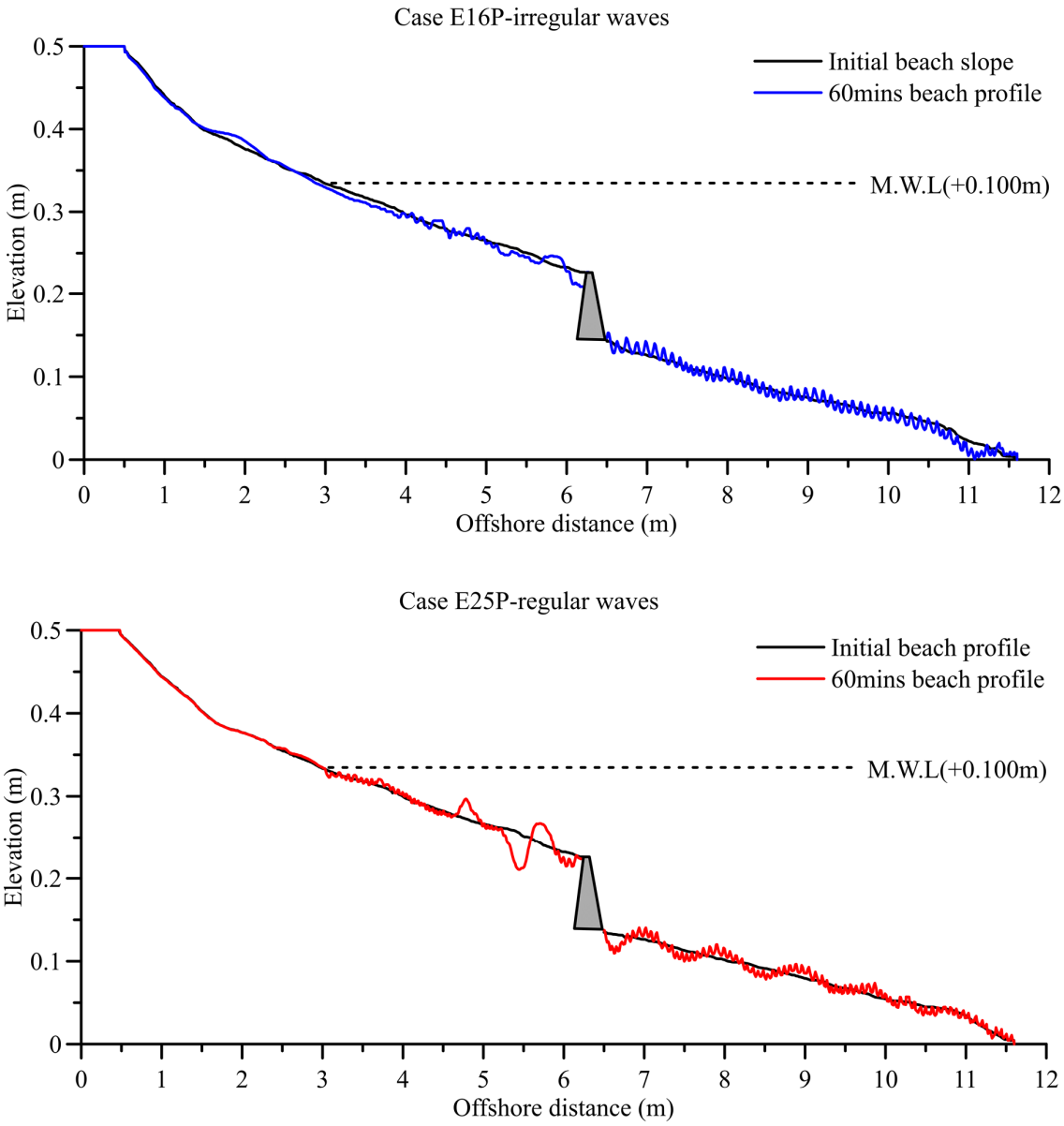

Fig. 4.19 Beach profiles in the same wave energy of irregular/regular erosive wave condition 5 and 6 after 60mins of wave generation, respectively.

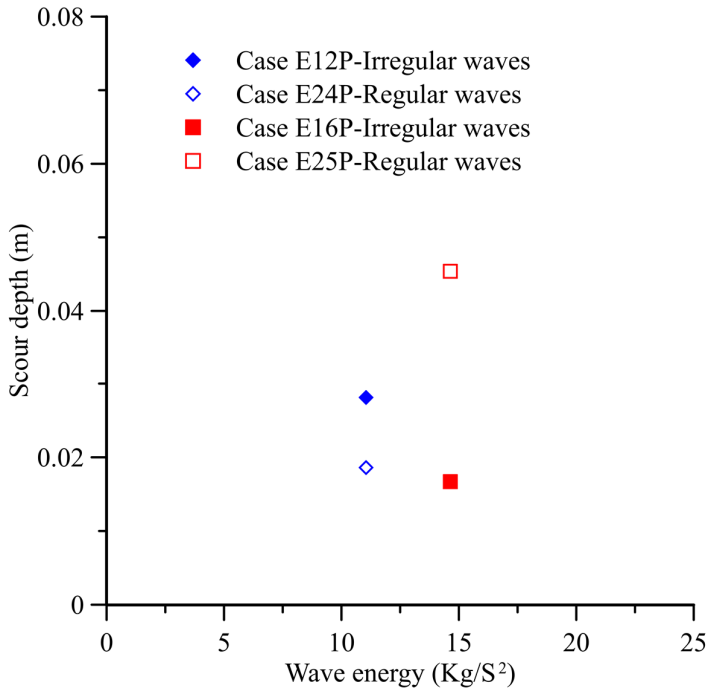

Fig. 4.20 Scour depth of the cases in similar wave energy after 60mins of wave generation.

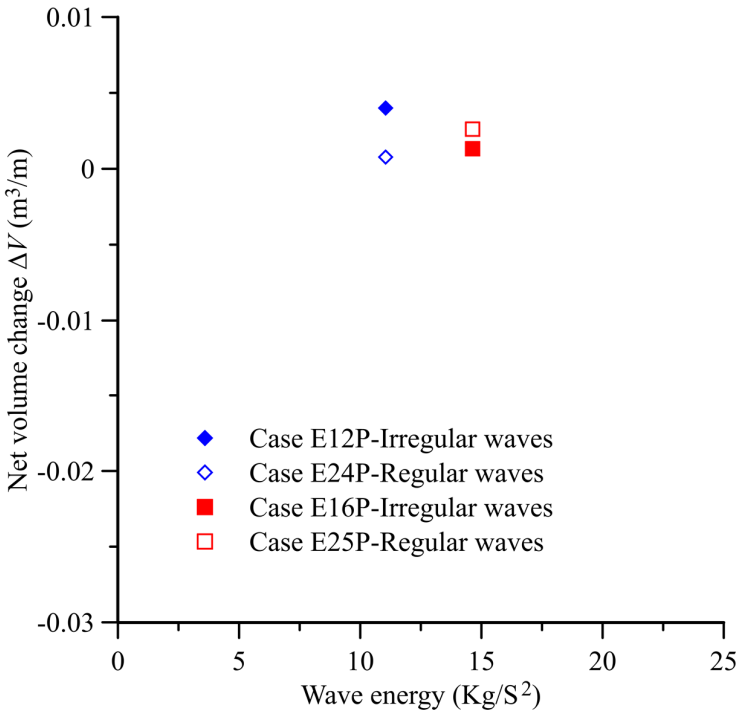

Fig. 4.21 Net volume of the cases in similar wave energy after 60mins of wave generation.

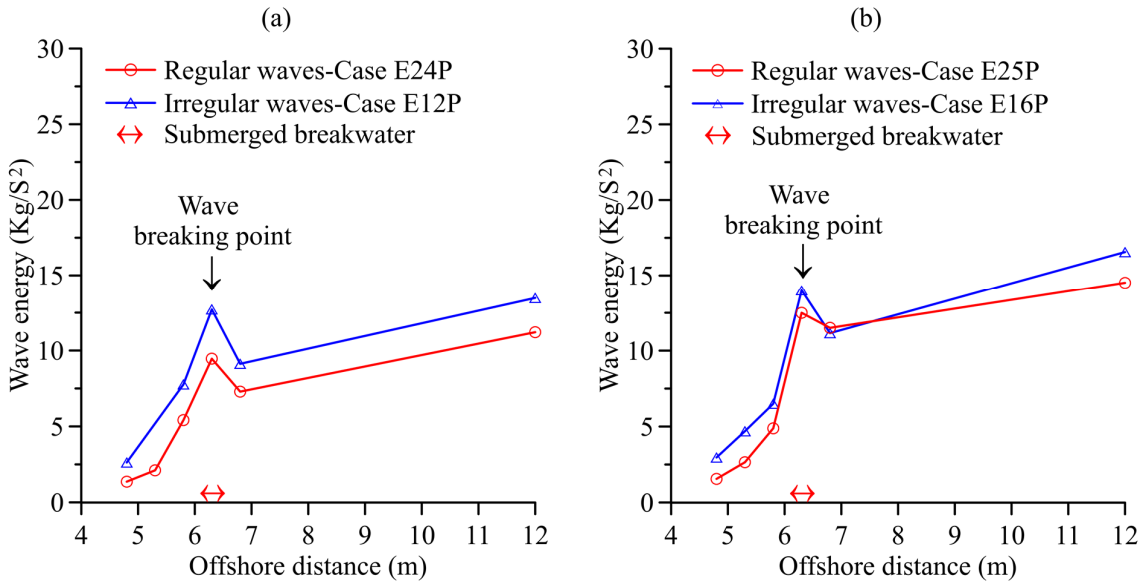

Fig. 4.22 Wave energy distribution along the beach profile of regular and irregular waves with similar wave energy.

Larson and Kraus[7] studied the response of normal beach profile in regular waves and classified it into erosion and accretion profiles based on the wave conditions and grain size of the sediments. In the section 4.2, whereas the results with the equivalent wave height showed that the responses of the perched beach profile in regular and irregular waves were different. In the equivalent wave energy, however, the responses were in good agreement. Thus, the classification of the perched beach profiles in irregular waves should be based on the equivalent wave energy instead of wave height. Once the transmitted wave energy over submerged breakwater was known, the type of perched beach was identified. The equivalent incident wave energy over submerged breakwater of regular and irregular waves should be written as Equation 4.8. The wave energy of irregular waves was measured above the submerged breakwater. It was a function of transmitted significant wave height H_{st} and independent from transmitted significant wave period T_{st}. The transmitted wave energy of irregular waves was written as

$$E_I = \rho g \int_0^{+\infty} 0.257 H_{st}^2 x^{-5} e^{-1.05x^{-4}} dx \tag{4.9}$$

in which $x=T_{st}f$, H_{st} is the transmitted significant wave height (m), T_{st} is the transmitted significant wave period (s), f is wave frequency (Hz).

Using linear wave theory, the transmitted wave energy of regular waves was written as

$$E_R = \frac{1}{8}\rho g H_t^{\,2} \tag{4.10}$$

in which ρ is density of water (kg/m^3), H_t is transmitted wave height (m).

The relationship between H_t and H_{st} was given as

$$H_{st} = \frac{H_t}{\sqrt{2}} \tag{4.11}$$

Larson and Kraus[7] suggested that the equation classifying the type of normal beach profile in regular waves as shown in Equation 4.12. By combining Equation 4.11 and 4.12 the classification of perched beach profile type in irregular waves was given by Equation 4.13. The graph expressed the criterion for classifying profile type in irregular waves was shown in Fig. 4.23.

$$\frac{H_t}{L_t} = 0.0007\left(\frac{H_t w}{T_t}\right)^3 \tag{4.12}$$

$$\frac{H_{st}}{L_{st}} = 0.00035\left(\frac{H_{st} w}{T_{st}}\right)^3 \tag{4.13}$$

in which w is sediment settling velocity (m/s), L_t is wave length (m). The Fig. 4.23 showed that in the regular waves, the response of perched beach profile was agreement with equation of Larson and Kraus[7], however in the irregular waves, the response follows the modified Equation 4.13. Although, there was no datum in the “erosion” side of the solid line, the classification of the perched beach in irregular waves was considered to be reliable because the solid line was modified from the Equation 4.12 based on the energy equivalence.

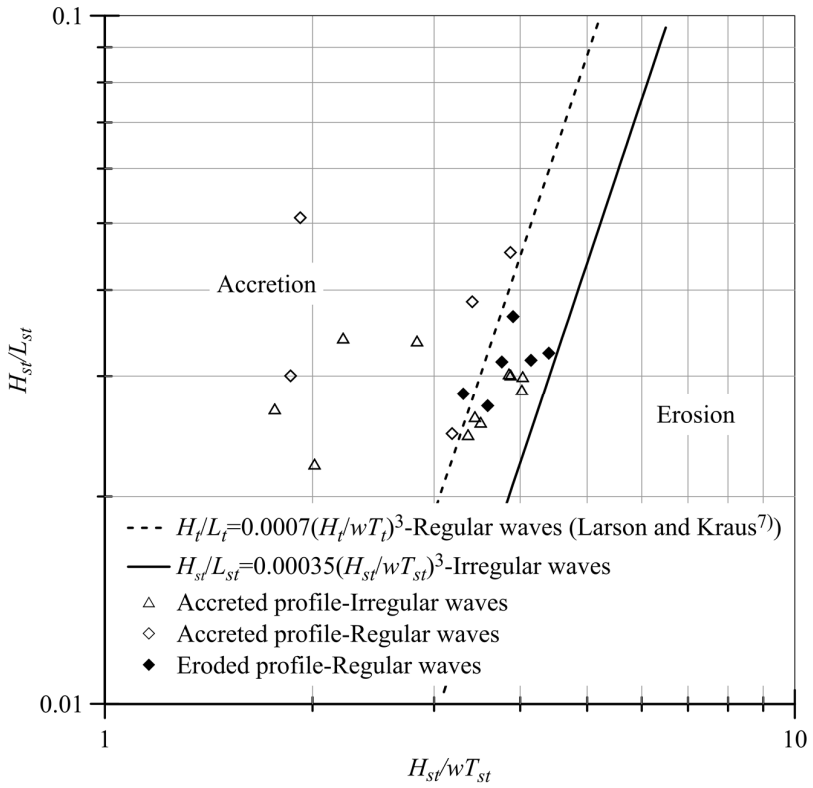

Fig. 4.23 Criterion for distinguishing profile type of irregular waves regarding to experimental data.

4.4 Discussions

Chatham[6] and Sorensen and Beil[2] studied the effectiveness of perched beach nourishment by conducting experiment in regular and irregular storm waves, respectively. The storm waves were generated to get the equilibrium perched beach. Whereas, the period of storm waves generation of their experiment was very long 3-42 hours, the real time scale of storm is only 3-5 hours. Thus, the deformation and volume loss in their experiments were comparatively large with those of the perched beach in the real storm. In this study, the period of storm wave generation of the experiments was 1 hour. It was compatible with the time scale of the real storm. Therefore, the scour depth and volume loss of the experiments were reasonable for evaluation of the effectiveness of perched beach in storm waves.

In the equivalent wave height, the results of experiment showed that in normal waves, the response of perched beach profile in regular and irregular waves were similar. However, in storm waves, it was significantly different. The scour depth and volume loss in regular waves were significantly larger than those in irregular waves (Fig. 4.8 and Fig. 4.10). The energy of regular waves was double the energy of irregular waves (Fig. 4.2). On the perched beach, whereas the energy of irregular waves was dissipated in a long distance, the regular wave energy was dissipated in a short distance (Fig. 4.9 and Fig. 4.16). Consequently, in the regular waves, the sediment near the wave breaking area receive more

energy than that in irregular waves. Thus, the mobility of the sediment was very high and easily transport offshore over submerged breakwater. On the other hand, in the equivalent wave energy, the volume loss and scour depth of perched beach profile in regular and irregular waves were similar (Fig. 4.18, Fig. 4.19 and Fig. 4.21). Therefore, the comparison of experiment in regular and irregular waves, the equivalent of wave energy of those should be assured.

In the wave trains of irregular waves there were long period waves and short period waves. As the irregular waves transmit over a submerged breakwater, the wave height and wave period could be changed by the submerged breakwater. The peak of wave spectral density shifted slightly to lower frequency (Fig. 4.11b, c, d, e). Furthermore, the low frequency 0-0.25 Hz waves were formed due to submerged breakwater. Thus, some of the irregular storm waves after transmission over submerged breakwater were transformed to accretive waves. Consequently, the perched beach was likely to form accretion at the foreshore area (Fig. 4.4 and Fig. 4.6).

In regular storm waves, the scour depth of the perched beach and volume loss were very large. However, the regular storm waves were not real. Thus, the experimental results in regular waves could not represent for the perched beach at the real field. The irregular waves in the experiments were modelled nearly similar to waves in the field. In addition, in all cases of the irregular storm waves, both of the scour depth and the volume loss was insignificant. Therefore, the results of experiments in irregular waves were exactly expressed the response of perched beach in storm waves at the fields.

4.5 Conclusions

The perched beach nourishment advances shoreline, does not change the beach landscape, reduces an amount of nourished sediment. All above, the results of the physical experiments showed that the irregular wave energy was significantly reduced by the submerged breakwater as the wave transmitted onto the perched beach. The submerge breakwater of perched beach can protect the shore against storm waves. Therefore, the perched beach nourishment is a practical method for protecting the coast under the global climate change.

The responses of perched beach profiles in regular and irregular waves are similar when their energies are equivalent. Therefore, when conducting the experiment in both cases of regular and irregular waves, the equivalent wave energy should be taken into account. Based on the results of the experiments and the type of beach profile classification in regular waves by Larson and Kraus[7)], a new classification of beach profile type in irregular waves is proposed.

References

1) Ruig J, Roelse P. A feasibilty study of a perched beach concept in the Netherlands. NY: Proceedings, 23rd International Conference on Coastal Engineering, ASCE. 1992. 2581-2598.

2) Sorensen R, Beil N. Perched beach profile response to wave action. Proceedings 21st Coastal Engineering Conference, ASCE. 1988. 1: 482-492.

3) Risio MD, Lisi I, Beltrami G, Girolamo PD. Physical modeling of the cross-shore short-term evolution of protected and unprotected beach nourishments. Ocean Engineering. 2010. 37: 777-789.

4) Musumeci R, Cavallaro L, Foti E. Performance of perched beach nourishments. Santander, Spain: Proceedings of 33rd Conference on Coastal Engineering. 2012. 1: 112-125.

5) Faraci C, Scandura P, Foti E. Evolution of a perched nourished beach: Comparison between field data and numerical results. Seoul, Korea: Proceedings of 34th Conference on Coastal Engineering. 2014.

6) Chatham CE. Movable bed model studies of perched beach concept. Proc. 13th International Conference on Coastal Engineering. 1972. 1197-1215.

7) Larson M, Kraus NC. Sbeach: Numerical model for simulating storm-induced beach change. Report 1: Empirical foundation and model development. Coastal Engineering Research Center, Waterways Experiment Station, Corps of Engineers. 1989. 129-137.

8) Bretschneider CL. Significant waves and wave spectrum. Ocean Industry. 1968. 40-46.

9) Mitsuyasu H. On the growth of spectrum of wind-generated waves (2)-Spectral shape of wind waves at finite fetch. 17th Japanese Conf. Coastal Engineering. 1970. 1-7 (in Japanese).

10) William HP, Saul AT, William TV, Brian PF. Numerical recipes in Fortran: the art of scientific computing, second edition. Cambridge University Press. 1992.

11) Gonzalez M. Equilibrium beach profile model for perched beaches. Coastal Engineering. 1999. 36: 343-357.

Chapter 5 Conclusions

The argument of the study is that under the global climate change, the amount of offshore sediment transport is higher than that of onshore sediment transport. Under the global climate change, coastal zones have been threatened by natural hazards, for instance, sea level rise, increment of storm wave height, increment of wind velocity, etc. By storm waves, sediment at the foreshore is dragged offshore and deposited at offshore bar, hence the shoreline is retreated. After the storm, this amount of sediment is transported back onshore under accretive wave conditions and the shoreline is recovered. Because of the global climate change, in some areas frequency of tremendous storm increases, thus a huge amount of sediment is transported offshore. The result is that the recovery rate of post-storm beach becomes very slow. If the post-storm beach recovery occurs in a long time scale, the amount of onshore sediment transport is smaller than that of offshore sediment transport, i.e. the shoreline is incompletely recovered in that period. Thus the global climate change causes unbalance in on/offshore sediment transport rate, hence coastal erosion. Under the effects of global climate change on beach erosion, shore protection works by coastal structures such as detached breakwaters and groins has recently shown some limitations causing various environmental problems. In addition, with the increment of world population and enlargement of coastal cities, the demand of leisure activities in coastal zone have been quick increased. Therefore, the protection of coastal zone while retain some features of the natural shorelines are essential for the coastal conservation. The beach nourishment has been verified as a good solution for this issues. However, the huge volume of nourished sediment is necessary. In this study, a new concept of shore protection in the management of on/offshore sediment transport was proposed and discussed. Two practical countermeasures for shore protection were suggested to verify the new concept. The applicability of two methods are examined through a series of the hydraulic experiments.

Two practical countermeasures for shore protection under severe storm conditions while preserving the features of natural beaches as well as reducing the volume of nourished sediment are proposed. The first countermeasure is “shore-face nourishment” which is based on the new idea that the post-storm beach recovery rate is accelerated by dredging some amount of sand at offshore bar and nourishing it on shore-face of the beach. This countermeasure includes two processes i.e. the sand dredging at the offshore bar and the beach nourishment at the shore-face. The procedure of sand dredging at the offshore bar may cause the negative effects to the coastal erosion. Therefore, the effects of the sand dredging at the bar on the shoreline change were quantified through a series of 2D and 3D hydraulic experiments, theoretical analysis and numerical simulations. To evaluate the effectiveness of the shore-face nourishment on the post-storm beach recovery rate, a series of experiments were conducted in 2D hydraulic wave flume. The second countermeasure is “perched beach nourishment” which is based on the viewpoint of protection of sediment lost over submerged breakwater under storm

waves. The effectiveness of the perched beach nourishment was identified through a series of hydraulic experiments in 2D wave flume.

Sand dredging at the offshore bar under the erosive wave conditions caused quick retreat of the shoreline at the lee of dredged hole and vicinity areas. The shoreline retreat caused by the sand dredging was quantified with a simple relationship between the volume of sand dredging and the shoreline position of the equilibrium profile. This study found that the quantity of the shoreline retreat was almost proportional to the dredged volume. Sand dredging in the nearshore zone is an activity that takes sediment away from the littoral cell. In the beaches which the long shore sediment supply is limited, taking the sediment out of the littoral cell should be prohibited.

The offshore bar was also dredged periodically and under the calm wave conditions. The final magnitude of retreat of shoreline under periodic sand dredging and under the calm wave conditions is similar to that of the case of one-time sand dredging in erosive wave condition, however, the speed of shoreline retreat is delayed. To mitigate or delay the effects of offshore bar sand dredging on the shoreline retreat, it is suggested to dredge sand periodically in the calm wave seasons.

After a big or successive storms, the recovery rate of post-storm beach is very slow. To accelerate the recovery rate, some amount of sand dredged at the bar can be nourished on the shore-face of the beach. This amount of sediment is transported onshore under the accretive wave conditions. The results of the investigation of offshore bar sand dredging showed that offshore bar should be dredged in the calm wave seasons to mitigate the negative effects of offshore bar sand dredging on the change of shoreline. The “shore-face nourishment” enhances the onshore sediment transport rate, therefore the recovery rate of post-storm beach is able to significantly accelerate.

The “shore-face nourishment” method is tested in various methods of sand dredging under different conditions of waves and sea levels. The sand volume of nourishment, the wave condition and the sea level are predominant parameters that showed the significant effects on the post-storm beach recovery rate. In addition, the location of the nourishment is also an important factor affects to the recovery. In the test cases of without “shore-face nourishment”, the recovery rate of the beach is comparatively high in a short period at the beginning of calm wave condition, however, it quickly decreases. To enhance the effectiveness of acceleration of post-storm beach recovery rate, a sufficient volume of sand should be dredged and nourished as soon as possible after storm in calm wave season.

The response of perched beach profile under storm waves were discussed in terms of perched beach deformation and sediment volume that is lost offshore over a submerged breakwater. A significant amount of energy of incident waves is dramatically dissipated by a submerged breakwater before transmitted to the perched beach. In addition, the transmitted energy of irregular waves is dissipated in a long distance on the perched beach profile. Therefore, under irregular storm waves, both

the beach deformation and the volume loss are insignificant, which indicates the “perched beach nourishment” has high potential for shore protection.

The effects of irregularity of the waves are highlighted by comparing the beach deformation and sediment volume loss between regular and irregular wave cases. The different response between regular and irregular waves were discussed in equivalent wave height and equivalent wave energy. The deformation of the perched beach profile and volume loss under regular waves are always greater than those under irregular waves in the cases of equivalent wave height, whereas in the cases of equivalent wave energy, the response of perched beach under regular and irregular waves are nearly similar, except for the scour depth. In the conduction of physical experiment for future researches, the regular and irregular waves should be considered in equivalent wave energy instead of equivalent wave height.

As a consequences of experimental conditions, insufficient data and lack of field data, this study encountered a number of limitations which need to be considered. In the classification of the types of perched beach profile in irregular waves, the number of physical experiment data is insufficient for classifying the eroded types of perched beach profile due to the limitation of wave generator. In the hydraulic experiments of this study, the current flow is not included. In addition, well-sorted sediment grain size is used. On the other hand, in the actual field site the current flow and poor-sorted grain size play as important factors for sediment transport. The results of this study can be applied to the beaches wherein the on/offshore sediment transport is dominant and the longshore sediment transport is minor or in balance.

Based on the limitations and results of the study, some recommendations for the future research are suggested. The “shore-face nourishment” method was tested by a number of physical experiments. It is a potential method for accelerating post-storm beach recovery rate. However, the application needs to get verification and further assessment by field case studies. Although in equivalent wave energy, the deformation of perched beach profile under regular and irregular waves are different. This is caused by the difference of dissipation of wave energy along the beach profile. Therefore, the response of beach profiles may give a different result. The classification of normal type of beach profiles in irregular waves should be carried out.